UNIVERSITE DE YAOUNDE I

FACULTE DES SCIENCES

CENTRE DE RECHERCHE ET DE FORMATION DOCTORALE EN SCIENCES, TECHNOLOGIE ET GEOSCIENCES

UNITE DE RECHERCHE ET DE FORMATION DOCTORALE CHIMIE ET APPLICATIONS

UNIVERSITY OF YAOUNDE I

FACULTY OF SCIENCE

POSTGRADUATE SCHOOL OF SCIENCES, TECHNOLOGY AND GEOSCIENCES

RESEARCH AND POSTGRADUATE TRAINING UNIT IN CHEMISTRY AND APPLICATIONS

DEPARTMENT OF INORGANIC CHEMISTRY
DEPARTEMENT DE CHIMIE INORGANIQUE

LABORATORY OF APPLIED INORGANIC CHEMISTRY
LABORATOIRE DE CHIMIE INORGANIQUE APPLIQUEE

Design and characterisation of flame retardant polymer nanocomposites with low ecological impact

Thesis

Submitted and defended in partial fulfillment of the requirements for the degree of Doctor of Philosophy in Chemistry

Specialty: Inorganic Chemistry

Option: Macromolecular Chemistry

BIBLIOTHEQUE UNIVERSITAIRE UYI

by

KANEMOTO ALLONG Stanley Olivier
Registration No.: 07T178
MSc in Chemistry

Under the co-supervision of:

NDIKONTAR Maurice KOR
Professor

NGOMO Horace MANGA
Professor

Year 2023

UNIVERSITY OF YAOUNDE I
UNIVERSITE DE YAOUNDE I

FACULTY OF SCIENCE
FACULTE DES SCIENCES

DEPARTMENT OF INORGANIC CHEMISTRY
DEPARTEMENT DE CHIMIE INORGANIQUE

ATTESTATION OF THESIS CORRECTION
ATTESTATION DE CORRECTION DE THESE

We the undersigned NDI Julius NSAMI (Associate Professor, Examiner), NDIKONTAR Maurice KOR (Professor, Supervisor) and DJOUFAC WOUMFO Emmanuel (Professor, President), attest that this PhD thesis defended on the 3rd July 2023 in the Pedagogic Block, Multimedia hall of the Faculty of Science, University of Yaoundé I, by KANEMOTO ALLONG Stanley Olivier on the topic **"Design and characterisation of flame-retardant polymer nanocomposites with low ecological impact"**, for the award of a PhD in Inorganic Chemistry, has been corrected in conformity with the recommendations of the defence jury.

In testimony whereof, this attestation is issued.

Yaoundé, 4th September 2023

Examiner	**Supervisor**	**President**
NDI Julius NSAMI	NDIKONTAR Maurice KOR	DJOUFAC WOUMFO Emmanuel
Associate Professor	*Professor*	*Professor*

Dedication

To my parents, MonÂme and Bénéficiando, with everlasting love.

&

To my sisters, Jud'Emé, TEstFleur, BénéMar, and Tif'Ida, in appreciation and love.

"Any obstacle reinforces determination.

Whoever has set a goal for himself does not change it."

Leonardo da Vinci

Acknowledgements

This work would have been impossible without the generous financial support of Third World Academy of Sciences (TWAS) Italy and the Council of Science and Industrial Research, India (CSIR) through 2016 TWAS-CSIR sandwich postgraduate fellowship award FR number: 3240293589. I warmly acknowledge them. I also extend my thanks for the providing appropriate testing services and computing equipment to the University of Yaoundé I.

I express my sincere gratitude to Prof. Ndi Julius Nsami, Head of Department of Inorganic Chemistry, for his availability and help.

I wish to express my deep gratitude to Prof. Ndikontar Maurice Kor for giving me the chance to join his research group and grow as a scientist. I am really grateful to him for his continuous involvement which made this work much more satisfying.

I am greatly thankful to my co-supervisor Prof. Ngomo Horace Manga, for his supervision, I thoroughly enjoyed his guidance.

My sincere thanks go to my host supervisor Dr. Suguna Lakshmi (CSIR-CLRI, India) for her professional guidance, valuable advice, support and encouragement, not only on this thesis but also in my personal life. She was as a mother to me. May our paths cross again.

I thank the staff members from the Department of Inorganic Chemistry who have been a source of inspiration. Particularly, I sincerely thank Prof. Cheumani Yona Arnaud for his critical views and suggestions which kept me focused and helped enrich my work.

My deep gratitude goes to Dr. Bangaru Chandrasekaran, former director of the CSIR-CLRI (Chennai, India), for receiving me in the Institute and giving me the opportunity to join the Polymer Science and Technology Division. Also, I want to thank Dr. Kalarical Janardhanan Sreeram, director of the CSIR-CLRI, for providing all the facilities available in CSIR-CLRI to carry out the research. Special thanks go to Dr. Siddan Gouthaman for teaching me about the synthesis in chemistry and NMR analysis data.

My special thanks go to all my friends from around the world and other doctoral students of the same batch, who shared in my work and my life. In particular, I am very much grateful

to Venkatesh Madhu, Dr. Periyamuthu Ramar and Dr. Murugan Vinayagam, whose views and thoughts on polymer science helped me throughout this work.

I thank all the PhD students and members of the Macromolecular Chemistry research team who helped me regroup my thoughts during the writing of this dissertation.

Finally, I am beyond words for the constant encouragement and tireless support along my education from Kanemoto family.

Table of contents

List of figures

List of tables

List of abbreviations

AFM:	Atomic Force Microscopy
ASTM:	American Standard for Testing and Materials
DGEBA:	Diglycidylether of Bisphenol A
DMF:	Dimethyl Formamide
DSC:	Differential Scanning Calorimetry
DTG:	Differential Thermogravimetric
FT-IR:	Fourier Transform Infrared spectroscopy
IPDT:	Integral Procedural Decomposition Temperature
LOI:	Limiting Oxygen Index
NMR:	Nuclear Magnetic Resonance spectroscopy
PU:	Polyurethane
SEM:	Scanning Electron Microscopy
TEA:	Triethylamine
TETA:	Triethylenetetramine
TGA:	Thermogravimetric Analysis
THF:	Tetrahydrofuran
UL-94:	Underwriters laboratories test standard
XRD:	X-ray Diffraction spectroscopy

Abstract

This thesis aims to design phosphorus- and nitrogen-based polyurethane and epoxy polymers and study their physico-chemical and mechanical properties. The modification of polymeric materials by reactive organic-inorganic hybrid polymer precursors was investigated to improve their thermal stability and flame retardation properties, while reducing their ecological impact. Different phosphorus and phosphorus-nitrogen polyols and epoxy monomers were synthesised and used in the preparation of polyurethanes and epoxy products. Phosphorus-containing polyols, tris-(5-hydroxypentyl) phosphate, tris-(4-hydroxybutyl) phosphate and tris-(3-hydroxypropyl) phosphate were successfully prepared by reacting phosphoryl chloride with three different aliphatic diols: 1,5-pentanediol, 1,4-butanediol, or 1,3-propanediol. The compressive properties of phosphorus-based polyurethane foams were proportional to their relative density, and the elastic region of deformation was found to be similar. The foams were classified as slow-burning materials according to the Limiting Oxygen Index tests. Phosphorus-functionalised epoxy resins were synthesised by glycidylation reaction of tris-(5-hydroxypentyl) phosphate, tris-(4-hydroxybutyl) phosphate, and tris-(3-hydroxypropyl) phosphate. The ensuing glycidylated phosphorus-triol compounds were then blended with diglycidylether of bisphenol A, and the hybrid epoxy formulations were cured with triethylenetetramine for the protection of leather against fire. In addition, triethanolaminodiethyl phosphate (PN-OH) was synthesised by the reaction of diethylchlorophosphate and triethanolamine, and used for the preparation of polyurethane with polyethylene glycol and hydroxylated polydimethylsiloxane. Effective construction of polyurethane foam was achieved between PN-OH and toluene-2,4-diisocyanate with inclusion of polyethylene glycol (PEG) and polydimethylsiloxane (PDMS). The polyurethanes were characterised by TGA, DSC, AFM, and XRD analyses. These analyses indicated that the foams were mainly amorphous, but the reduction of PEG/PN-OH (wt/wt) ratio slightly changed the microphase separation. The polyurethane systems were found to be “slow-burning” with a level of UL-94 V-0, and their ignition delay time was estimated at 8 s. These polyurethane systems can be also used in specific applications for energy-saving measures in buildings.

Keywords: Polymer composites; reactive flame retardants; polyurethane foams; epoxy resins; flame retardation properties; eco-design

Résumé

Cette thèse vise à concevoir des polymères polyuréthanes et époxy à base de phosphore et d'azote et à étudier leurs propriétés physico-chimiques et mécaniques. La modification des matériaux polymères par voie réactive avec des précurseurs polymères hybrides organiques-inorganiques a été étudiée afin d'améliorer leur stabilité thermique et leurs propriétés ignifuges, tout en réduisant leur impact écologique. Différents polyols et monomères époxy phosphorés et phospho-azotés ont été synthétisés, puis utilisés dans la préparation de polyuréthanes et de produits époxy. Des polyols contenant du phosphore, le phosphate de tris-(5-hydroxypentyle), le phosphate de tris-(4-hydroxybutyle) et le phosphate de tris-(3-hydroxypropyle) ont été préparés avec succès en faisant réagir le chlorure de phosphore avec trois diols aliphatiques différents : 1,5-pentanediol, 1,4-butanediol ou 1,3-propanediol. Les propriétés de compression des mousses de polyuréthane à base de phosphore étaient proportionnelles à leur densité relative, et la région élastique de déformation s'est avérée similaire. Les mousses ont été classées comme matériaux à combustion lente selon les tests de l'indice limite d'oxygène. Des résines époxy fonctionnalisées au phosphore ont été synthétisées par réaction de glycidylation du phosphate de tris-(5-hydroxypentyle), du phosphate de tris-(4-hydroxybutyle) et du phosphate de tris-(3-hydroxypropyle). Les composés phosphore-triol glycidylés ainsi obtenus ont ensuite été mélangés au diglycidyléther de bisphénol A, et les formulations époxy hybrides ont été durcies avec le triéthylènetétramine pour protéger la surface du cuir du feu. En outre, le phosphate de triéthanolaminodiéthyle (PN-OH) a été synthétisé par la réaction du diéthylchlorophosphate et de la triéthanolamine, et utilisé pour la préparation de polyuréthane avec du polyéthylène glycol et du polydiméthylsiloxane hydroxylé. Une construction efficace de mousse de polyuréthane a été réalisée entre le PN-OH et le toluène-2,4-diisocyanate avec l'inclusion de polyéthylène glycol (PEG) et de polydiméthylsiloxane (PDMS). Les polyuréthanes ont été caractérisés par des analyses TGA, DSC, AFM et XRD. Ces analyses ont indiqué que les mousses étaient principalement amorphes, mais que la réduction du rapport PEG/PN-OH (wt/wt) modifiait légèrement la séparation des microphases. Les systèmes de polyuréthane se sont avérés être "à combustion lente" avec un niveau UL-94 V-0, et leur délai d'inflammation a été estimé à 8 s. Ces systèmes de polyuréthane peuvent aussi être utilisés dans des applications spécifiques pour des mesures d'économie d'énergie dans les bâtiments.

Mots-clés : Polymères composites ; retardateurs de flamme par voie réactive ; mousses de polyuréthane ; résines époxy ; propriétés ignifuges ; écodesign

General Introduction

Polymeric materials, are increasingly employed in various industrial sectors including packaging, building construction, automotive, and leather processing. Thermoplastic polymers such as polyethylene and polypropylene are good alternatives to wood and metals in the production of windows, doors, and pipes because of their versatility, lightweight, and the myriad of possibilities offered in the design and processability (Saldivar and Vivaldo, 2013). Thermoset products such as polyurethanes, phenol-formaldehyde resins, and epoxy resins, are commonly used in coatings, adhesives, and electrical and thermal insulation (Li and Strachan, 2015). Polyurethanes are polymers containing, in their backbone, the aliphatic and aromatic portions linked though carbamates. They are considered one of the most versatile groups of polymers available. The total polyurethane market value was evaluated at USD 70.67 billion in 2020 (Kahlerras *et al.*, 2020), against USD 27.5 billion for the epoxy resins (Karak, 2021). Epoxy resins are macromolecular chemical systems in which each molecule contains two or more reactive oxirane rings. The oxirane ring can react with amine and carboxylic acid so-called hardener to form a three-dimensional thermoset system. Epoxy resin is known to be one of the most attractive synthetic thermosetting polymers due to its superior properties namely, great chemical resistance, good thermal stability, high moisture and solvent resistance (Cui *et al*., 2001). In Cameroon, polyurethanes are largely commercialised as cheap mattress; various types with different flexibility ranges are available (Kanemoto *et al*., 2021). These resins are mostly found in the system of two pack adhesives. The demand of such versatile products is expected to significantly increase in Cameroon and other developing countries due to population growth and the need for modern infrastructure to improve the standard of living. The legislation and standard on the use of materials in particular applications are becoming more and more stringent worldwide regarding the mechanical, physical and fire performances and environmental risks (Yang *et al.*, 2016). Polymeric materials in their virgin state are generally highly flammable and easily ignited in the presence of a heat source and oxygen (Xu *et al*., 2017). This can cause severe material and equipment damage through the loss of material properties (Campo, 2008). In addition, smoke and toxic gases formed during combustion could affect human health and cause death. Because of this, fire hazards associated with the use of polymeric materials have caused the introduction of legislation and safety standards concerning

flammability and extensive research has been made in the area of flame retardants for polymeric materials (Höhne *et al.*, 2018).

In the scenario of fire, flame retardants can lower the contribution of the polymeric materials to the expansion of fire and to smoke production, at least in the primary period to allow inhabitants to escape from the burning zone.

In order to overcome the problem of flammability of polyurethane foam and leather, three routes were developed to improve the fire resistance of these polymeric materials (Salmeia *et al*., 2015). The first one is to synthesise intrinsically fire retardant polymers or to graft active functions onto the backbone of existing polymers. The second one is to add fire retardant compounds to the polymer matrix. Finally, a protective coating can be applied at the surface of the material to act as a barrier for the heat and mass transfer responsible for combustion. Due to toxic effects and not being environmentally friendly, many flame-retardant additive molecules, such as the halogen-based flame-retardant compounds, have been banned (Lu and Hamerton, 2002; Hull *et al.*, 2014; Gu *et al.*, 2015). These halogen-based flame retardant compounds, upon incorporation into the polymer matrix, release gases which are toxic to human beings as well as the environment when the polymeric materials are burned. Inevitably, compounds based on phosphorus, nitrogen, silicon, and boron elements have gradually replaced halogenated flame retardants (Wang *et al*., 2017a). Among these, environmentally friendly flame retardants made from nitrogen and phosphorus are much exploited (Nguyen *et al*., 2012; Marosi *et al*., 2014; Yuan *et al*., 2016).

This work aims to design a series of phosphorus-based polyols and epoxy precursors for developing new three-dimensional polymeric networks, specifically polyurethane and epoxy products with improved thermal stability and fire retardancy. In order to provide protection in various fire scenarios, different concepts have been elaborated to improve flame retardancy or flame resistance of polyurethane foams and epoxy resins.

The strategy and results collected in the present work have been reported and organised into three chapters. The first chapter deals with the general information about polymer chemistry and flame retardancy, including a brief overview of polyurethane and epoxy resin. It also gives detailed information on the preparation, applications, and improving flame retardation properties of polyurethanes and epoxy.

The second chapter details the materials and experimental procedures used. It describes the conditions employed to characterise flame retardants and final materials.

The third chapter shows the results collected from the experimental section and the discussion of these results. It is divided into four parts.

(i) The first part reports the results of the study focusing on the preparation and characterisation of phosphorus-based polyurethane foams from three different phosphorus-containing polyols, tris-(5-hydroxypentyl) phosphate, tris-(4-hydroxybutyl) phosphate, and tris-(3-hydroxypropyl) phosphate.

(ii) The second part discusses the results focused on the preparation and characterisation of a series of phosphorus- and nitrogen-based polyurethanes using triethanolaminodiethyl phosphate as a potential reactive flame retardant.

(iii) The third part reports the results of the preparation, thermal stability, and effect of nano-clays on properties of phosphorus-based epoxy resins from glycidylated phosphorus-containing polyols.

(iv) The fourth part presents the specific details concerning the evaluation of the ecological impact of all the materials obtained, from the synthesis stage of the flame retardant to the flammability test of the polymer material.

Chapter 1: Literature Review

This chapter provides general information about the chemistry and modification of polymers, and the preparation and applications of polyurethanes and epoxy resins. In addition, the available literature on the flame retardancy of these polymers is reviewed, followed by research strategies and objectives.

1.1 | Introduction to polymer concept

1.1.1 | Definition and main types of polymers

Polymers are systems of macromolecules which are formed by assembling many smaller molecules through covalent bonds. Polymers are synthesised from monomers by several chemical mechanisms in different polymerisation reactions such as radical, cationic, and anionic polycondensation (Hosier *et al.*, 2004). Given the versatility of polymers, they can be classified following different criteria (Saldivar and Vivaldo, 2013). For instance, depending on their applications and value in use, some of the main types of polymers can be identified as plastics, elastomers, fibres, and liquid resins. Polymers can also be classified either thermoplastics or thermosets depending on their thermal behaviour. Figure 1.1 summarises the classes of polymers based on synthesis mechanism, chain topology, origin and thermal behaviour.

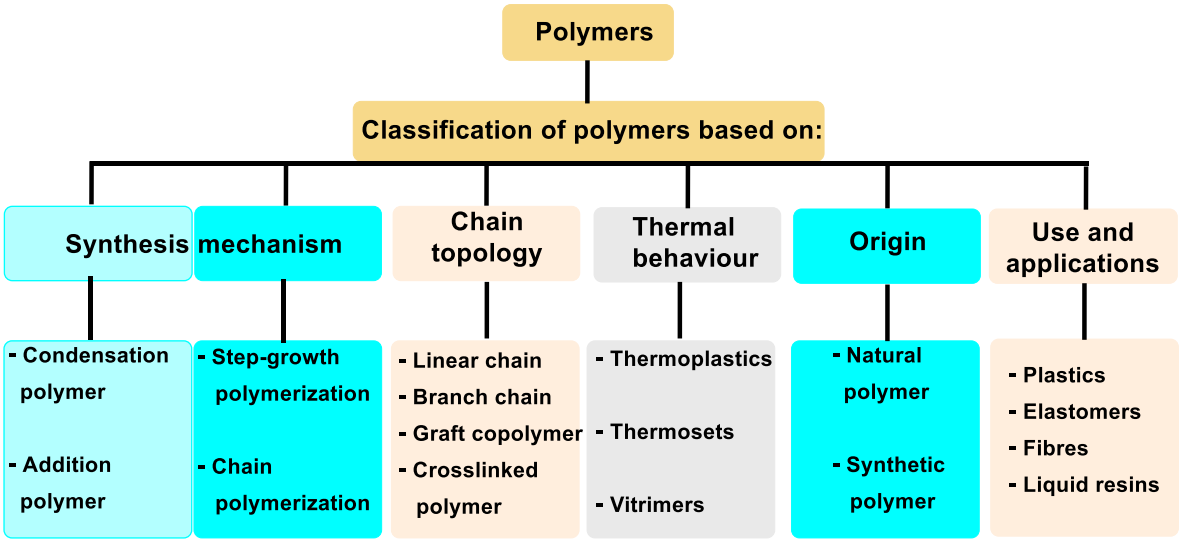

Figure 1.1 Typical classification of polymers

1.1.1.1 | Classification based on synthesis mechanism

The classification based on synthesis reaction of polymers is one of the oldest and most important. It splits polymers into two major types: addition and condensation polymers. The modern accepted criterion determines that a condensation polymer is that which satisfies any of the following conditions.

(i) Some atoms of the monomer are lost as a small molecule during their synthesis.

(ii) They contain functional groups as part of the main polymer chain, such as ester, urethane, amide, or ether (Saldivar and Vivaldo, 2013).

If a polymer does not satisfy any of these criteria, then it is an addition polymer.

However, classification based on mechanism is based on the kinetic mechanism of the polymerisation reaction. It classifies polymerisations into two categories such as step-growth polymerisation and chain polymerisation.

Step-growth polymerisation

The fundamental scheme of this polymerisation is made by reacting a di-functional monomer A-B, which contains functional groups A and B in the molecule. Another schematic route involves the chemical reaction between two di-functional monomers of the type A-A and B-B. In this mechanism, the size of the chains increases gradually and relatively slowly. Some examples of polymers synthesised by this mechanism are polyurethane, polyamide, and polyester.

Chain polymerisation

It requires a generator of active centers, which are usually an initiator for free radicals, anions, or cations. The propagation of the active center means the chain growth by chain reaction between the active center and the monomer (Hosier *et al.*, 2004). In this mechanism, the monomer only reacts with active centers and is present throughout the reaction. Some of common polymers resulting from chain polymerisation are polyethylene, poly(vinyl chloride), and polypropylene.

Although sometimes the classifications of polymers produced by condensation and step-growth polymerisation are interchangeable, in like manner those of polymers from addition and chain-growth polymerisation, one must be conscious that the classification of polymers only by structure or only by mechanism may lead to ambiguities (Saldivar and Vivaldo, 2013). In order to avoid this problem, classification of polymers can be done depending on both structure and mechanism.

1.1.1.2 | Classification based on chain topology

Two polymers having the same chemical composition but different chain topologies can exhibit profound differences in crystallinity, physical properties, rheological behaviour, and so on. Figure 1.2 illustrates schematically the different polymers based on the chain topologies.

- Linear chain polymers are those with no branches.
- Branched chain polymers have at least one branch along the backbone chain. These branches are classified as short (usually less than 10 repeating units) or long. Branches can also be classified as tri-functional or tetra-functional, depending on the number of paths departing from the branching point.
- Graft copolymers are the polymers that have the branches formed by repeating units (monomers) different from those forming the main chain.
- Crosslinked polymers are those forming a three-dimensional network. They are insoluble and have very restricted chain-segment mobility; therefore, they do not flow.

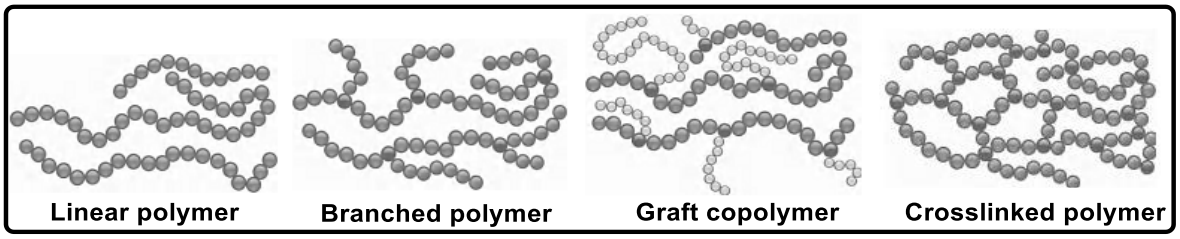

Figure 1.2 Different polymer chain topologies

1.1.1.3 | Classification based on structure thermal behaviour

Traditionally, synthetic polymer materials are classified into two major groups: thermoplastics and thermosets.

Thermoplastics

Thermoplastics can be melted and solidified many times, allowing the polymer to re-mouldable. Thermoplastics can be shaped under heating. Once they are heated above a suitable temperature, the thermoplastics flow as very viscous liquids and can adopt the shape of mould; once they are cooled down again, they keep the new moulded shape (Saldivar and Vivaldo, 2013). They can be moulded through injection or extrusion with the application of heat or solution process. Thermoplastics are synthesised in polymerisation plants and are then transformed in processing equipment to form a myriad of objects useful as packaging or utensils (Brandsch and Piringer, 2008). Some of the most familiar thermoplastics are

polyethylene, polypropylene, polystyrene, polyvinyl chloride, and polycarbonate. The polymers are linear or slightly branching.

Thermosets

Thermoset polymers are three-dimensional or highly reticulated systems formed reticulation reactions between a pre-polymer and a hardener. Once the polymer is hardened, it cannot be melted anymore because its melting temperature is too high compared to the degradation temperature. The pre-polymer and the hardener are mixed directly into a mould or just before the application. Once the precursors react, a crosslinked network is created and it cannot flow anymore under heating (Li and Strachan, 2015). Most thermosets must be polymerised in the mould to set the desired shape since they generally lack the ability to be re-processed after curing. Therefore, reaction and moulding into the final shape usually take place at the same time. Thermosets have excellent mechanical properties, solvent resistance, abrasion resistance, and load-bearing capacity, due to their covalently crosslinked structure. Examples of some thermosets are phenoplast and aminoplast resins, epoxy resins, and polyurethanes.

Meanwhile, another class of materials so-called vitrimers form a bridge between thermoplastics and thermosets. They are strong, durable and resistant like thermosets, yet mouldable, recyclable and malleable like thermoplastics (Brandsch and Piringer, 2008). These materials form a new class of chemically crosslinked polymers in which thermally stimulated exchange reactions permit the change of the network topology while keeping the number of bonds and crosslinks constant (Karak, 2021).

1.1.1.4 | Classification based on use and applications

The most common way of classifying polymers regarding the use and further applications is outlined in Figure 1.1 in which they are separated as follows: plastics composed of thermoplastics and thermosets, elastomers, fibres, and liquid resins.

Elastomers

Elastomers or rubbers are flexible materials that can stretch for more than 500% of their length and recover to their original shape after complete release of the applied force (Bhuvaneswari *et al*., 2017). They are amorphous linear polymers slightly crosslinked used above their glass transition temperature (Bandzierz *et al*., 2016). For some of their applications, they must be faintly crosslinked once they are elaborated into the suitable shape to provide them dimensional stability, since otherwise they tend to slowly flow. Mainly used in tyres, hoses, and seals; elastomers find others applications as adhesives (Salmeia *et al*.,

2015), and as impact modifiers of thermoplastics (Brandsch and Piringer, 2008; Bhuvaneswari *et al*., 2017). Some examples of common elastomers are natural rubber, polybutadiene, copolymer of acrylonitrile and butadiene, copolymer of styrene and butadiene, and copolymer of ethylene, propylene and norbornene.

Fibres

Fibres include the category of polymers with very high resistance to deformation, high toughness and very high modulus (Hearle, 2009). They elongate very little. Commonly used in clothing and textile, fibres are all partly crystalline, partially oriented, and linear polymers (Saldivar and Vivaldo, 2013). The main synthetic polymer fibres are polyamide (nylon), polyacrylonitrile (acrylic fibre), polyolefin, and polyesters (Campo, 2008).

Liquid resins

They are products available in the liquid form. This includes adhesives and coatings. The polymer is the binding agent. The liquid resin is eventually mixed with a hardener and cured by chemical reaction with the hardener, moisture, or oxygen in the air, or just by evaporation of the solvent. The polymer can be used to protect the surface of the substrates on which the paint or coating is applied or to glue two materials (Mohanty *et al*., 2021). Some examples of polymers used as paint are copolymer of styrene–butyl acrylate or copolymer of acrylic monomer–vinyl acetate. In the product, the polymer is either finely dissolved in a solvent (oil-based paints) or dispersed in water forming a latex (water-borne) (Du *et al*., 2016).

1.1.1.5 | Classification based on origin

Classification of polymeric materials can be based on the origin of the material or the repeating units. In this sense, they can be natural and synthetic polymers. Of course, natural polymers occur in nature and are of great importance. For instance, cellulose produced by plants, and chitin forming the shell of animals are the most abundant natural polymers (Hearle, 2009).

The synthetic polymers are synthesised in a chemical laboratory. Depending on the presence or absence of carbon atoms in the polymer chain backbone, they are divided into two families: organic and inorganic polymers (Ebnesajjad, 2016). Synthetic organic polymers are by far the most studied and utilised polymeric substances of the two categories, mainly because of the availability of organic monomers coming from the petrochemical industry (Brandsch and Piringer, 2008). On the other hand, inorganic polymers have long been known, and

recently, increasing research is being done in this field (Balani *et al.*, 2015). Typical inorganic polymers contain oxygen, silicon, nitrogen, or phosphorus in their backbones.

1.1.2 | Glass transition and melting point of polymers

Structure of polymers can be either amorphous or semi-crystalline. By definition, a material is amorphous if its atoms or molecules are not arranged on a lattice that repeats identically in space (Ebnesajjad, 2016). There are two important thermal properties that define the state of a polymer: these are the glass transition temperature and the melting temperature.

1.1.2.1 | Glass transition

Glass transition is a reversible and important phenomenon that is very useful to understand how external conditions affect physical properties of polymers. Below the glass transition temperature, the amorphous regions of a polymer are in a glassy state showing practically no chain motions (Campo, 2008). The glassy state of materials corresponds to a non-equilibrium solid state, in which the molecules composing the material are haphazardly arranged covering a volume greater than that of the crystalline state but having a similar composition. Above the glass transition temperature, the polymer behaves as a viscous liquid reflecting motions of the polymer chains or chain segments (Saldivar and Vivaldo, 2013). Also, at the glass transition temperature, many of the physico-chemical properties of the polymer change in a relatively abrupt way. The glass transition temperature of a non-crystalline material as glass or plastic, represents the crucial temperature at which its behaviour changes from being glassy to being rubbery (Ebnesajjad, 2016). In this context, glassy means hard, brittle and so relatively easy to break, while rubbery means elastic and flexible. Techniques such as differential thermal analysis, differential scanning calorimetry and dynamic mechanical analysis are widely used to measure the glass transition temperatures. These methods show the changes in specific heat of the polymer at the glass to rubber transition.

1.1.2.2 | Melting temperature

Melting temperature is a property exhibited by the crystalline regions of a polymer. It is the temperature above which the crystalline regions melt and become disordered or amorphous (Balani *et al.*, 2015). Melting point separates the solid and liquid phases. For any polymer whose melting temperature is higher than glass transition temperature, above the melting point, the polymer will flow as a viscous liquid (Ebnesajjad, 2016).

Amorphous polymers exhibit only a glass transition temperature, while semi-crystalline polymers exhibit both, a glass transition temperature and a melting temperature (Campo, 2008).

1.1.3 | Polymer additives

Additives are essential components of polymer formulations used for many different purposes. They can modify the mechanical behaviour of the polymer products (plasticisers), improve the UV light resistance (light stabilisers), reaction-to-heat fire (heat stabilisers, flame retardants), or natural degradation (biocides, antioxydants). Figure 1.3 shows an estimation of the main polymer additives market size in the world. Generally, the additives are incorporated in polymers not with the aim of influencing the polymer itself but to protect final goods. They embrace a wide area of different chemical structures. They can be classified into additives to maintain polymer properties and those to extend polymer properties.

First category of additives comprises the compounds able to transform the materials into the desired shape and to protect the materials from degradation by oxidation, heat, as well as chemical and mechanical attack mainly during processing (Ambrogi *et al*., 2017). Therefore, they keep the polymer chain and the polymer molecular weight basically unchanged (Pfaendner, 2013). Typical examples of the additives with polymer properties retention are antioxidants (secondary aromatic amines, phosphites, phosphonites, and sulfides) (Pfaendner, 2013), plasticisers (phthalates and isosorbide esters) (Yin and Hakkarainen, 2011), heat stabilisers (metallic salts and organometallic compounds) (Klampfl and Himmelsbach, 2016), processing aids (fluoropolymers and polydimethylsiloxanes) (Ambrogi *et al*., 2017), and lubricants (hydrocarbons) (Martín-Alfonso *et al*., 2007).

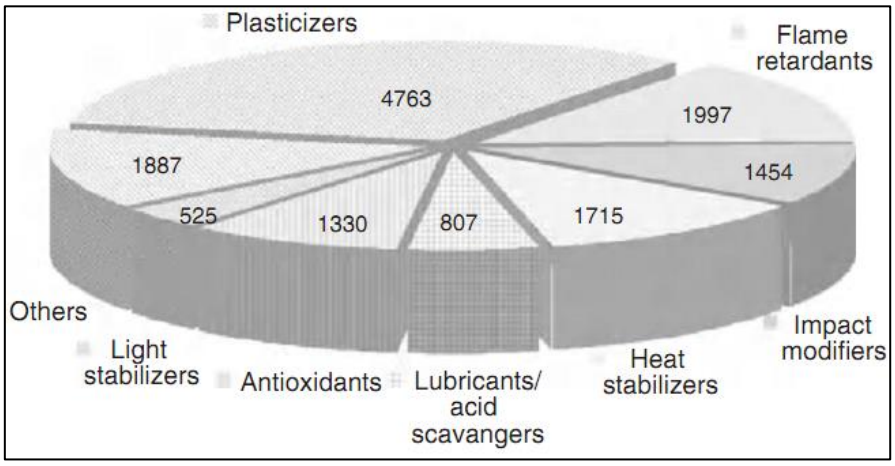

Figure 1.3 Turnover of additives in million dollars (Pfaendner, 2013)

Additives to extend polymer properties are useful in prolonging the service life of polymeric materials and allowing the use of the polymers in additional applications. By using these additives, the molecular weight of polymer and polymer chain remain unchanged for an extended period, under specific use conditions (Pfaendner, 2013). Examples of these additives are antimicrobials (Hosier *et al*., 2004), UV light stabilisers (Klampfl and Himmelsbach, 2016), and flame retardants (Kausar *et al*., 2016).

1.1.4 | Flame retardancy

1.1.4.1 | Mode of action of flame retardants

The combustion process of polymers is divided into four main steps: heating, decomposition, ignition and flame spread. If the energy given to the polymer is sufficient for its degradation, products from the decomposition of polymer are released in the gas phase. Then, these flammable gases are mixed with oxygen from the air and ignition occurs when the system of gases reaches a critical level of concentration. Part of the energy of the flame is given back to the polymer, so that the combustion process continues without contribution of external energy. As long as oxygen remains in sufficient amount, there is an auto-fed flame which can spread to its surroundings. This combustion involves the formation of free radicals in the flame. Schemes 1.1 - 1.5 describe the major reactions occurring in the flame during the combustion of polymers.

Initiation: $RH + O_2 \longrightarrow HO^* + RO^*$ Scheme 1.1

Propagation: $RH + HO^* \longrightarrow H_2O + R^*$ Scheme 1.2

Branching: $R^* + O_2 \longrightarrow RO^* + O^{**}$ Scheme 1.3

$O^{**} + H_2 \longrightarrow HO^* + H^*$ Scheme 1.4

Termination: $H^* + HO^* \longrightarrow H_2O$ Scheme 1.5

Generally, flame or fire retardants are added to polymer formulations to reduce the risk of fire, for instance, for electric, electronic or construction applications (Dasari *et al*., 2013). They do not transform the polymer into a non-burning material but delay the incineration. A flame retardant may be viewed as a substance built-in, or treatment applied to a material that suppresses or delays combustion thereof under specific conditions (Salmeia *et al*., 2015). It works by breaking the combustion cycle in one of three manners:

(a) modifying the thermal degradation process;

(b) quenching the flame; or

(c) reducing the supply of heat from the flame back to the polymer surface.

Their mechanism of activity can be described via physical and chemical actions. By physical action, the combustion process can be restrained in several ways, namely:

(i) cooling: observed when the endothermic reactions cool the polymeric material;

(ii) isolation by forming protective layer: during this phenomenon, a protective char layer can be formed, isolating the material beneath from heating source, oxygen and flames and preventing the volatile compounds to be transported to the flame; or

(iii) fuel dilution: release of inert gases may dilute the volatile flammable compounds in the flame.

The chemical action of flame retardant occurs either in the gas phase or the condensed phase.

Gas-phase additives

These additives act chemically in the gas phase to scavenge free radicals generated as a product of thermo-oxidative decomposition of polymer (Dasari *et al*., 2013). Burning polymeric materials form many species able to react with atmospheric oxygen. As a result, the propagation of combustion occurs mostly through the following reactions (schemes 1.6 – 1.8).

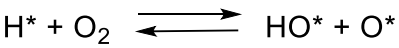

Scheme 1.6

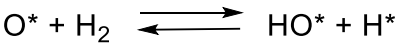

Scheme 1.7

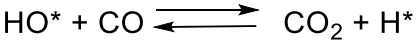

Scheme 1.8

However, the reaction linked to scheme 1.8 is the main exothermic reaction and provides the most energy to maintain the flame. The hindering of the chain-branching reactions related in schemes 1.6 and 1.7 can slow down or completely stop the combustion. Some additives can also demonstrate a physical mode of action in the gas phase that either generates a considerable amount of non-combustible gases that dilute the flammable gases or those which endothermically dissociate by reducing the flame temperature (Salmeia *et al*., 2015).

Condensed-phase additives

These additives display the role of charring and barrier promotors. They act either by chemical interaction with a polymer or by physically constraining and therefore reducing polymer volatilisation (Kausar *et al*., 2016; Ambrogi *et al*., 2017). Flame retardants or their thermal decomposition products catalyse dehydration and condensation reactions that lead to

crosslinking, forming a char layer over the polymer surface (Dasari *et al*., 2013). This solid residue protects the polymer by isolating the non-burned material from the heat, oxygen and flames. It hinders the volatile products from reaching the flame and feed it. Intumescent systems are preferably used where a porous carbonaceous material barrier is generated which hinders thermal transfer to material as well as blocking the oxygen supply, hence, extinguishing the flame (Alongi *et al*., 2015).

There is no doubt that the best flame retardant additives work in more than one way in more than one phase.

1.1.4.2 | Classification of flame retardants

The different fire retardant systems comprise mainly inorganic flame retardants, halogenated flame retardants, phosphorous- and nitrogen-containing flame retardants. A typical classification flow chart for flame retardant is presented in Figure 1.4.

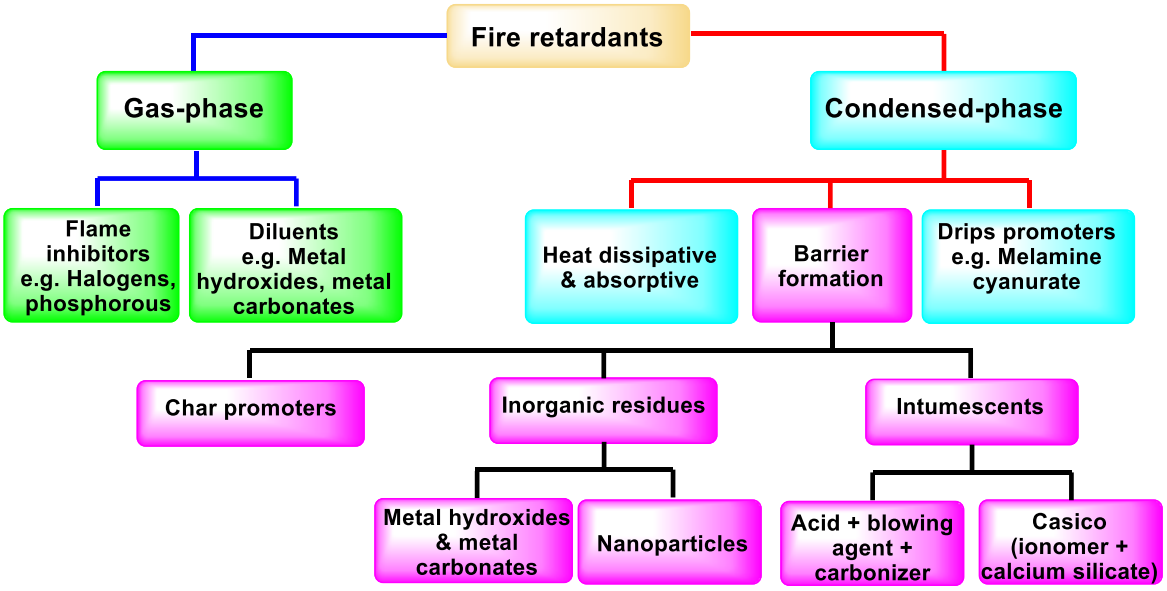

Figure 1.4 Typical classification of flame retardants

Inorganic flame retardants

Inorganic flame retardants go through endothermic dissociation in condensed phase generating non-combustible residues or simply act through the physical mode by creating a tortuous path limiting volatilisation (Kausar *et al*., 2016; Dasari *et al*., 2013). Most common metal hydroxides used as flame retardants for polymers are aluminum trihydroxide, aluminum oxyhydroxide (boehmite), and magnesium dihydroxide. These metal hydroxides decompose at elevated temperatures endothermically with the formation of water which further cools down

the pyrolysis zone (Wang *et al.*, 2017b). Therefore, they act in the condensed phase by removing heat and diluting the burning gases. On the other hand, layered silicates and carbon nanotubes have found an interest as flame-retardant additives (Lee *et al*., 2010). They act through barrier formation at the surface and thus insulating the polymer from the flame source (Pack *et al*., 2009).

Halogenated flame retardants

Halogen-based flame retardants are chlorine-based and bromine-based compounds that can form halogen radicals (X*) close to or at the polymer decomposition temperatures. Halogenated compounds may act in the condensed phase, but detailed research indicates that they are primarily vapour-phase flame retardants, interfering with the free radical reactions involved in flame propagation (schemes 1.9 and 1.10) (Lewin and Weil, 2001).

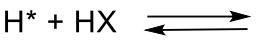

Scheme 1.9

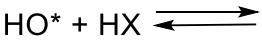

Scheme 1.10

Halogen radicals extract hydrogen from polymer chains to form hydrogen halide that volatilises. Thus, creating the radical site in polymer chain. Halogen radical recombines to become the relatively stable halogen molecule.

Hydrogen halide acts as a catalyst to self-propel the reactions (Dasari *et al*., 2013). The gaseous hydrogen halide acts as radical scavengers for hydroxyl radicals and gas-phase hydrogen formed because of combustion (Salmeia *et al.*, 2015). Except for a few chlorinated products such as chlorinated paraffins, these flame retardants usually contain molecules with several bromine atoms. For instance, the bromine compounds are mainly active during combustion process in the gas phase, whereas bromic acid (HBr) reacts with hydroxyl (OH*) and hydrogen (H*) radicals to form less reactive halogen radicals (Lewin and Weil, 2001).

The addition of halogenated compounds has the disadvantage to increase the quantities of smoke and toxic decomposition products which are released during the combustion of the polymer. Moreover, halogenated compounds also lead to additional risk of formation of strong acid gases, such as HBr and HCl, which are released during combustion. Therefore, halogenated compounds represent an environmental pollution problem, which has been considered especially in recent years (Covaci *et al.*, 2011; Witkowski *et al*., 2016). The concept of sustainable development requires the use of flame retardant technologies with minimal impact on the environment.

Phosphorus-based flame retardants

Phosphorus-based flame retardants are most widely used alternatives to halogen-based flame retardants (Nguyen *et al.*, 2012; Marosi *et al.*, 2014; Gu *et al.*, 2015). Their reactivity in the condensed phase leads to the production of phosphoric acid as a product of thermal dissociation of the flame retardants, which, through rejection of water, produces phosphates. The water release dilutes the combustible gases (Lewin and Weil, 2001). They can further act in the condensed phase by catalysing char formation (Lu and Hamerton, 2002). Phosphorous can take many oxidation states (phosphine oxides, phosphines, phosphonium compounds, phosphonates, phosphates, phosphites and elemental red phosphorus), showing many modes of action of phosphorus-based flame retardant compounds (Dasari *et al.*, 2013). Some phosphorus based-flame retardants form volatile active radicals in gas phase like PO_2*, PO*, HPO* that readily scavenge hydroxyl radicals (OH*) or hydrogen radicals (H*) from the gas phase to inhibit combustion (Lewin and Weil, 2001). The mechanism of radical scavenging by the phosphorous can be resumed in schemes 1.11 – 1.13 (Kausar *et al*., 2016). The most abundant phosphorous radicals and compounds in the flame are HPO_2*, HPO*, PO_2 and PO.

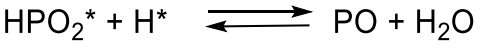

Scheme 1.11

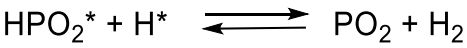

Scheme 1.12

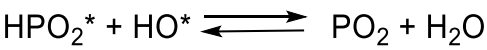

Scheme 1.13

Nitrogen based-flame retardants

Nitrogen-containing flame retardants can be used as blowing agents (Gao *et al.*, 2013). They can decompose to incombustible gases such as nitrogen oxide or ammonia without smoke (Salmeia *et al.*, 2015). Nitrogen-based flame retardants act by providing both a heat sink and inert diluents for the burnable gases in the flame (Lewin and Weil, 2001). For instance, melamine and melamine derivatives, such as melamine cyanurate and melamine polyphosphate, are industrially representatives of nitrogen-containing flame retardants (Yang *et al*., 2016; Sut *et al.*, 2019).

Most high-efficiency flame retardant can be prepared by integrating multiple elements in a single flame retardant system (Gu *et al*., 2015; Wang *et al*., 2017a; Sun *et al*., 2018). So, the flame retardancy of nitrogen-based flame retardants can be significantly enhanced with the synergistic effect of other elements such as phosphorus and silicon (Zhang *et al*., 2020).

1.2 | Overview on polyurethanes

1.2.1 | Definition and presentation of polyurethanes

Polyurethanes are one of the most versatile groups of polymers. Figure 1.5 shows their general structure. They are highly used in a wide range of applications such as construction, medical devices and electronic equipment. By that way, the total polyurethane market size was evaluated at USD 70.67 billions in 2020 and is expected to average 3.8% of annual growth rate from 2021 to 2028 (Kahlerras *et al*., 2020). Polyurethane is regarded as the fifth most common synthetic polymers after polyethylene, polyvinyl chloride, polypropylene, and polystyrene (Oertel and Abele, 1994; Jeong *et al*., 2016).

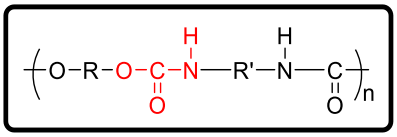

Figure 1.5 Illustration of linear chain polyurethane

1.2.2 | Classification of polyurethanes

Polyurethanes have high tunable molecular structures through the selection of reactants from a wide variety of available polyols and isocyanates between the reactants i.e., isocyanate groups and hydroxyl groups ratio, reaction sequence control, and the use of different synthetic process conditions.

Polyurethanes can be found in liquids resins (coatings and adhesives), elastomers, rigid insulation foam, soft flexible foams, elastic fibres (Ashida, 2006; Engels *et al*., 2013; Akindoyo *et al*., 2016). Their estimated global production with different types of polyurethane is given in Figure 1.6.

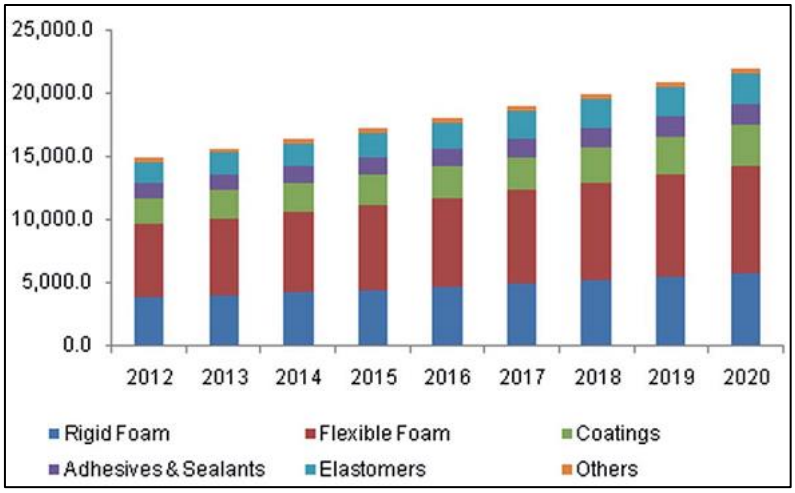

Figure 1.6 Estimated polyurethane production (Akindoyo *et al*., 2016)

1.2.2.1 | Rigid polyurethane foams

Rigid polyurethane foams are one of the most used materials for insulation, energy-saving, and sealants. Rigid polyurethane foams consist of a high percentage of cells with a closed-cell structure and have a low density approximately 25–150 kg m^{-3} (Nikje *et al*., 2011; Kirpluks *et al*., 2014). They account for over 25% of the overall polyurethane market (Lochner *et al*., 2022). Their demand is increasing substantially because of their wide range of applications as heat insulator in refrigerators (freezers), building construction and transportation materials, floatation and padding materials, encapsulates to isolate and support thermally sensitive components within weapon systems, and shock absorbers in industry (Marzec *et al*., 2017). They are used in building construction inside the walls and roofs, and for packaging. The use of these foams can considerably reduce energy costs, as well can make residential and commercial appliances much more comfortable (Kirpluks *et al*., 2014; Kahlerras *et al*., 2020). Foam properties are affected by the choice of raw materials and can be altered by modifiers. Depending on the properties, different technologies are used to produce rigid polyurethane foams, with the most often employed at large scale being the moulding, and slabstock (Ashida, 2006).

1.2.2.2 | Flexible polyurethane foams

Flexible polyurethane foams are polymers characterised by cellular structures that allow some degree of compression and resilience. The flexible foams are composed of block copolymers whose elasticity depend on the phase separations between the soft and hard segments (Rao *et al*., 2018a). Thus, they can be adjusted by simply changing the compositional ratios of these segments. Their synthesis involves two major processing technologies, the blowing and then gelling (Ashida, 2006). Flexible polyurethane foams have a virtually completely open-cell structure with typical densities of 20–45 kg m^{-3} (Nikje *et al*., 2011). They occupy the greatest portion of overall polyurethane market with approximately 31%, and find application as cushion materials for a wide range of consumer and commercial products, including carpet underlays, furniture, seats, bedding, automotive interior parts, and packaging (Höhne *et al*., 2018).

1.2.2.3 | Thermoplastic polyurethanes

Thermoplastic polyurethanes are relatively expensive materials that reveal vast arrangements of both physical properties and processing applications. Generally, they are flexible, soft and elastic with interesting mechanical properties, such as good resistance to

abrasion, impact and weather (Engels *et al*., 2013). The several property combinations of thermoplastic polyurethanes make them suitable for wide use in many applications requiring toughness and high resistance to abrasion, lubricating and fuel oils, combined with a wide range of operating temperatures such as in automotive, footwear, construction, biomedical, hose and cable sheathing (Akindoyo *et al.*, 2016). Thermoplastic polyurethanes can be fabricated using extrusion, blowing, compression and injection-moulding (Claeys *et al*., 2015). Some examples of objects made of thermoplastic polyurethanes are keyboard protector for laptop, outer cases of mobile electronic devices, drive belts, caster wheels, inflatable rafts, and sporting goods (Ashida, 2006; Sut *et al.*, 2019).

1.2.2.4 | Polyurethane ionomers

Polyurethane ionomers have ionic groups in the polyurethane backbone chain. For instance, polyurethane-based cationomers can be prepared by ternisation of a sulfur atom or quaternisation of a nitrogen atom (Zhang *et al.*, 2014). Polyurethane ionomers have many benefits, such as excellent dispersion in common polar solvents by because of their enhanced hydrophobicity and upgraded thermo-mechanical properties (Jaudouin *et al.*, 2012). In particular, the shape memory feature provides the materials with the properties required for use in biomedical devices (Raasch *et al*., 2015). Shape memory polyurethanes possess a thermo-responsive shape memory behaviour, and consequently present different mechanical properties from the other polyurethanes. From the temporary shape, the permanent shape of materials can be recovered after heating above a switch temperature. Another important feature of polyurethane ionomers is their biocompatibility (Zhang *et al.*, 2014). The successful end-use of these materials is found in different medical applications for artificial hearts, connector tubing for heart pacemakers and hemodialysis tubes (Jaudouin *et al.*, 2012; Engels *et al.*, 2013).

1.2.2.5 | Coatings, adhesives, and sealants

As can be seen in the markets, a wide and growing field of applications directly derives from the use of liquid polyurethanes resins in coatings, adhesives, sealants or binders. They together account about 9-10% of the overall polyurethane market (Lochner *et al*., 2022).

Polyurethane adhesives can offer good bonding properties, whereas very tight seals may be obtained from polyurethane sealants. For a polyurethane to be suitable for coating applications, it needs to possess high chemical resistivity, good adhesive properties, low temperature flexibility, excellent drying and adequate scratch resistance (Mohanty *et al*., 2021). Sometimes, different types of nanoparticles, such as, silicon dioxide and titanium oxide may be employed

for high-performance coating applications (Zuber *et al*., 2013). These additives impart the material resistance to corrosion. Adhesives and coatings are prepared systems of which the polyurethane may represent the most significant volume, but sometimes it plays the role of binder for the other components add into the solution system. The additives are solvent, solid fillers, pigments, dyes, antioxidants, toughеners, surfactants, coupling agents, moisture scavengers, plasticisers, coalescing agents, defoamers, and numerous hybridising polymers (Wu *et al*., 2019).

Polyurethane binders are frequently used to bond natural or synthetic fibres and other materials together. Binders made from polyurethane help to provide a constant gluing effect between organic materials and oriented strand boards, long-strand lumbers, laminated veneer lumber, particle boards medium, density fibre boards, and also straw boards (Lei *et al*., 2015). As a binding material, the ratio of the hard/soft segments of polyurethanes should be high and good thermal stability is required. The major areas of application are in elastomeric or rubbery flooring surfaces, ink-jet printing, wood panel manufacturing, foundry industries and sand casting (Lei *et al*., 2014). Among these, the major application of polyurethane binders is in the fabrication of oriented strand board. Polyurethane, due to its good binding properties, is a convenient alternative to organic solvent-based binders.

Polyurethanes are interestingly used in the preparation of water-borne dispersion coatings that can substitute solvent-borne coatings. Water is used in these systems as a solvent instead of volatile and toxic organic solvents (Lei *et al*., 2010). Polyurethane dispersions offer a unique advantage for viscosity of the dispersion, because the viscosity is not dependent on the polymer molecular weight. Therefore, high solid-content water-borne polyurethanes can be prepared by the drying process only. The dispersion is a two-phase colloidal system, which includes the polyurethane particles and the water medium (Gu *et al*., 2015). The polyurethane coatings are prepared with several pendent acid or tertiary nitrogen groups which are neutralised to form salts which are at the origin of the water dispersibility of the product (Wu *et al*., 2019).

1.2.3 | Preparation of polyurethane

Polyurethanes are produced through different routes (Akindoyo *et al*., 2016). Regarding the reagents, the polyurethane can be prepared by two different ways, namely isocyanate-based polyurethane, and non-isocyanate polyurethane.

1.2.3.1 | Isocyanate-based polyurethane

Polyurethanes are generally obtained by the step-wise polyaddition reaction between a polyol and a di- or poly-isocyanate component which form urethane groups (–NH–CO–O–) as

shown in Figure 1.7 (Oertel and Abele, 1994). Generally, the reaction occurs in presence of a suitable catalyst, chain extender, and other additives (Kahlerras *et al*., 2020). The polymers can contain in their backbone structure aliphatic and aromatic portions, R and R'. Polyurethanes can also contain urea linkages resulting from reaction of isocyanate groups with water or/and amine groups. The resulting molecular structure of polyurethane is a typical block polymer in which the macromolecular chains are mainly composed of alternating soft and hard chain segments (Engels *et al*., 2013). The soft segment comprised of the macromolecule polyol confers the flexible properties and presents a random curl, while the rigid segment proceeding from urethane group comprised of the isocyanate and chain extender-like small molecule, has a reasonably large energy of cohesion and can be easily combined, aggregated as well as stretched into a rod aspect (Lu *et al*., 2021). These segments are incompatible. Therefore, there is micro-phase separation in polyurethane, which affects the physical properties of polyurethane materials.

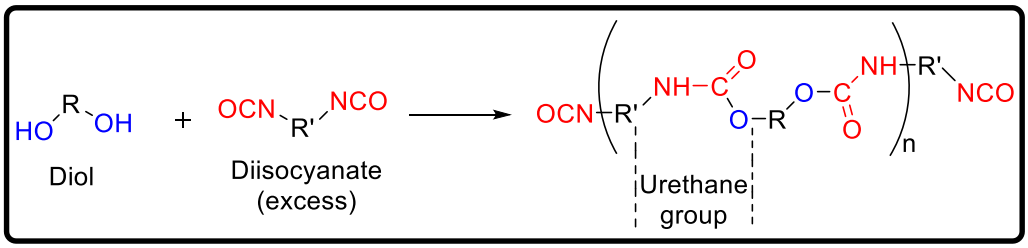

Figure 1.7 Schematic diagram of the polyurethane synthesis mechanism

Isocyanates

Isocyanates are essential components for polyurethane preparation. They are di-functional or poly-functional isocyanates bearing at least two isocyanate –N=C=O groups per molecule. They can be categorised as aromatic, aliphatic, cyclo-aliphatic, or polycyclic in nature. The structures of some common isocyanates are presented in Figure 1.8.

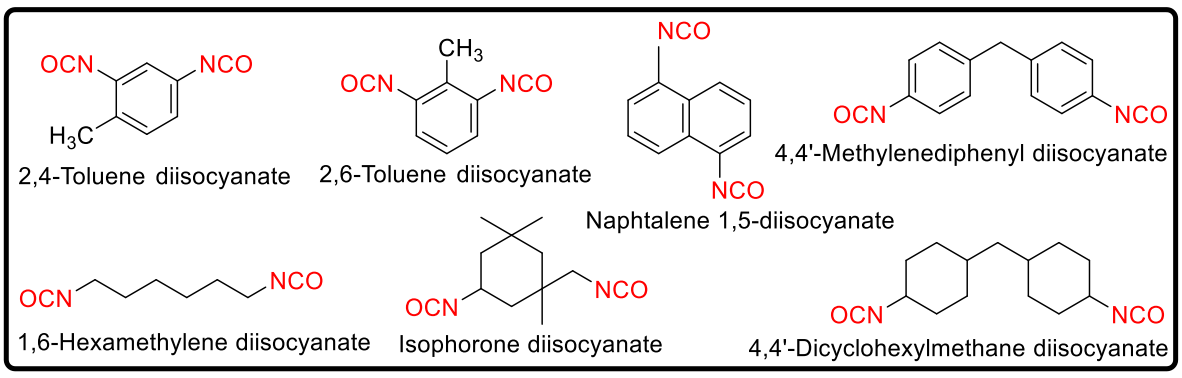

Figure 1.8 Common isocyanates

The reactivity of isocyanate (*R*–N=C=O) is conducted by the electropositive character of the carbon atom, which can be attacked by nucleophiles (electron donors), and nitrogen and oxygen by electrophiles (electron acceptors). If the radical *R* is an aromatic system, the negative charge gets strongly delocalised into *R*; thus, the aromatic-containing isocyanates are more reactive than cyclo-aliphatic and aliphatic isocyanates. In the case of aromatic-containing isocyanates, the chemical structure of the substituent additionally determines the reactivity. So, electron-attracting tendency of substituents in the ortho- or para-position increase the reactivity, and electron-donating substituents diminish the reactivity of isocyanate groups. Among the several available options, methylenediphenyl diisocyanate and toluene diisocyanate are cheaper and more reactive than other isocyanates (Sharmin and Zafar, 2012). Industrial grade, they are usually used for producing flexible foams, rigid foams, and elastomers.

Polyols

Polyols are substances containing two or more reactive hydroxyl groups per molecule (Figure 1.9). The polyol components can range from simple molecules such as glycerin, ethylene glycol, diethylene glycol to polymeric polyethylene glycol of various mean molecular weight (e.g. 400, 1000, 4000 g mol^{-1}) and very complex polyols containing other functionalities like amide, acrylic, ester, metalloid and metal, along with hydroxyl groups. Relatively high molecular-weight polyol components are generally preferred to reduce the amount of the isocyanate component (most expensive component) required to produce a polyurethane with acceptable properties.

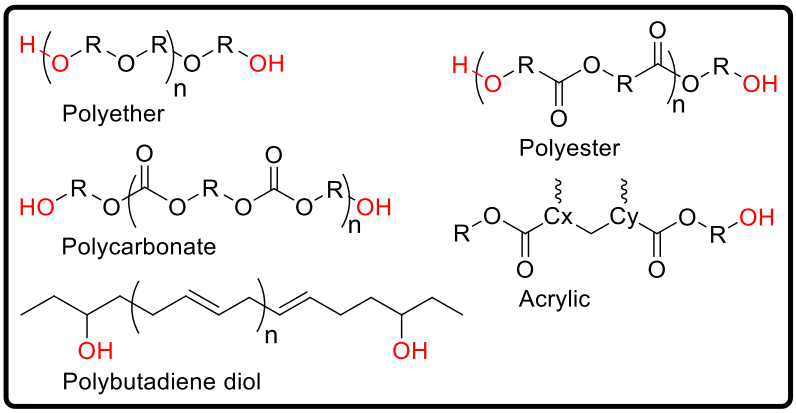

Figure 1.9 Some examples of polyol

Polyester polyols consist of ester and hydroxyl groups in their backbone. They are made from the reaction between an active hydrogen-containing compound and an epoxide. They are synthesised by the condensation polymerisation between glycols, like ethylene glycol, 1,4-butanediol, or 1,6-hexanediol, and an anhydride or dicarboxylic acid (Oertel and Abele, 1994;

Sharmin and Zafar, 2012). The properties of a polyurethane also depend upon the degree of crosslinking as well as the molecular weight of the starting polyester polyols. While highly branched polyester polyols are much more useful for the preparation of rigid polyurethanes with good chemical and thermal resistance, less branched polyester polyols result in polyurethanes with low chemical resistance and good flexibility at low temperature (Sundararajan *et al*., 2017a).

Similarly, low molecular-weight polyols produce rigid polyurethanes, while high molecular-weight long-chain polyols yield flexible polyurethanes (Das and Mahanwar, 2020). Polyester polyols can be easily hydrolysed because of the presence of ester groups, which hydrolysis also reduce the mechanical properties of resultant polyurethane. This difficulty can be avoided by the addition of a small amount of carbodiimide (Sharmin and Zafar, 2012). However, polyester polyols are progressively replaced by polyether due to several advantages, such as ease of handling, low cost, and improved hydrolytic stability over the former (Das and Mahanwar, 2020).

Polyether polyols are generally formed by the addition reaction of ethylene oxide or propylene oxide with alcohol or amine initiators in the presence of a variety of acidic or basic catalysts. Polyurethanes developed from polyether polyols show low glass transition temperature and high moisture permeability (Rao *et al*., 2018a).

Acrylated polyol, another example of polyols, is a result from free radical polymerisation reaction of methacrylate or hydroxylethyl acrylate with other acrylics. Acrylated polyols improve the thermal stability of polyurethane and also impart specific characteristics of acrylics (Mohanty *et al*., 2021).

Polysiloxane polyols are very meaningfully used to construct a building block based on the oligo-polyol structure with multiple terminal hydroxyl groups. They give polyurethanes which conserve their mechanical properties (Wu *et al.*, 2019). Polysiloxane chains display a system of interesting properties, namely very low glass transition temperature, low surface energy, high gas permeability, hydrophobicity, biocompatibility, UV and oxidative stability, good electrical properties and physiological inertness (Sharmin and Zafar, 2012; Das and Mahanwar, 2020).

Metal-containing polyols are formed by modifying polyols (polyester and polyether polyols) with metal salts such as metal carboxylates, acetates, chlorides. Polyurethanes obtained from these hybrid polyols exhibit good anti-microbial behaviour, gloss, and thermal stability (Zhang *et al*., 2014). A category of polyols commonly called specialty polyols is required to manufacture elastomers, adhesives, and sealants that need high qualities to

withstand environmental and chemical factors (Zuber *et al*., 2013). Some examples of these polyols are polysulfide polyols, polycaprolactone polyols, polybutadiene polyols, and polycarbonate polyols (Wang *et al*., 2017; Ousaka and Endo, 2021).

Catalysts

Catalysts are used in polyurethane manufacturing to promote the reaction between polyol and isocyanate by enhancing the reaction rates, deblocking the blocked isocyanates, and decreasing the deblocking, curing times and temperatures. Some amine compounds (tertiary amines), organometallic compounds, and alkali metal salts of carboxylic acids are employed as catalysts. Table 1.1 shows typical catalysts used in polyurethane preparation and their most important applications.

Table 1.I Some catalysts used in polyurethane manufacturing

Chemical name	**Chemical family**	**Applications**
Bis-(2-dimethylaminoethyl) ether	Aliphatic amine	Rigid foam, semi-rigid foam, flexible foam
Triethylenediamine	Cyclic amine	Rigid foam, semi-rigid foam, flexible foam, elastomers, coatings, adhesives, sealants
N,N-Dimethylcyclohexylamine	Alicyclic amine	Rigid foam
2-Hydroxypropyl trimethylammonium formate	Quaternary ammonium	Semi-rigid foam
4-[2-(Dimethylamino)ethyl] morpholine	Cyclic amine	Flexible moulded foam
2,4,6-Tris(dimethylaminomethyl) phenol	Aromatic compound	Semi-rigid foam
Dibutyltin dilaurate Stannous octoate Dibutyltindiacetate Zirconium chelates	Organometallic compound	All Flexible slabstock foam Flexible moulded foam Water-borne systems
Potassium octoate Potassium acetate	Alkali metal salt	Rigid foam

With tertiary amines, the catalytic activity is estimated by their structure as well as their basicity. Their catalytic action consists in forming a complex between amine and isocyanate and donating the present electrons on the nitrogen atom of tertiary amine to the positively charged carbon atom of the isocyanate (Muuronen *et al*., 2019). Catalytic activity enhances with increased basicity, but the steric hindrance around the nitrogen atom of amine decreases

the catalytic activity (Sharmin and Zafar, 2012). For the basic catalyst, the following mechanism has been proposed in Figure 1.10.

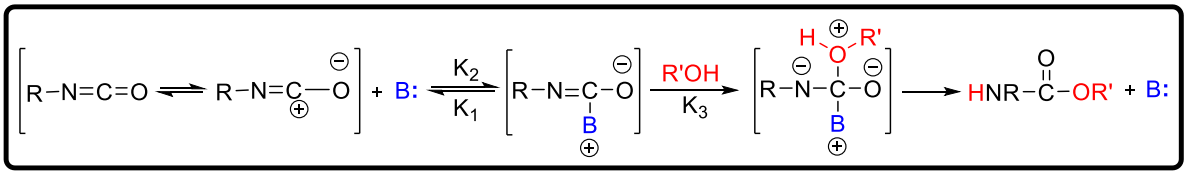

Figure 1.10 Basic catalysis mechanism

Organometallic catalysts, and especially organotin compounds, are the most widely used due to their strong gelation activity. They are much more efficient than the amines, particularly for the reaction between the alcohol group and isocyanate (Silva and Bordado, 2004). Organotin compounds allow the chain of polyol-isocyanate to extend at a sufficient rate, increase viscosity rapidly to a state where gas is effectively trapped, as well as to develop enough gel strength to prevent any cell structure from collapsing after gas evolution has ceased.

Additives

Along with an isocyanate and a polyol, some additives may also be required during polyurethane production, essentially to control the reaction, change the reaction conditions, modify the processing conditions, and finish the final product. These consist of chain extenders, moisture scavengers, crosslinkers, fillers, blowing agent and colorants.

Low molecular-weight diols such as 1,4-butanediol, 1,6-hexanediol, ethylene glycol, and cyclohexane dimethanol are used as chain extenders (Zhang *et al.*, 2010; Lei *et al.*, 2014). As there are ideally two end groups per chain, a linear molecular weight increase is possible. Amine such as ethylenediamine, diethanolamine, and triethanolamine are also used to extend the chain of initial polyurethane products. The reaction between the amine and isocyanate groups forms a urea bond (–NH–CO–NH–). Therefore, a poly(urea-urethane), commonly referred to as polyurethane, is formed (Ashida, 2006).

Crosslinking results in a three-dimensional network and depends on the functionality and additive concentration. In polyurethane preparation, the low molecular-weight polyols with functionality three and more are used as crosslinkers (Bai *et al.*, 2008). Since isocyanates are very sensitive to moisture and water even in trace amounts, moisture scavengers, namely oxazolidine derivatives and zeolite type molecular sieves, are incorporated to eliminate the substantial involvement of water during polyurethane preparation (Pfaendner, 2013; Ambrogi *et al.*, 2017). They are more reactive with water molecules than an isocyanate.

1.2.3.2 | Non-isocyanate polyurethane

Despite the importance of diisocyanates, environmental challenges have led researchers to investigate possible route avoiding their use, especially to reduce the environmental problems and other diisocyanate-related toxicity issues. Non-isocyanate polyurethanes are formed by reacting the polycyclic carbonate oligomers and aliphatic polyamines containing primary amino groups (Figure 1.11) (Khatoon *et al.*, 2021). For this, environmental renewable resources like lignin, terpenes, and vegetable oils are successfully used as an intermediate for synthesising cyclic carbonates, which are further reacted with amine group acting as a curing agent (Ousaka and Endo, 2021). The pioneering work for preparing polyurethanes without isocyanates was conducted from ethylene carbonate (Khatoon *et al.*, 2021). The two broad methods for the synthesis of non-isocyanate polyurethanes are as follows.

(i) Polycondensation reactions as illustrated in Figure 1.11(a) (Wolfgang *et al.*, 2021).

(ii) Polyaddition reactions as presented in Figure 1.11(b) (Ousaka and Endo, 2021).

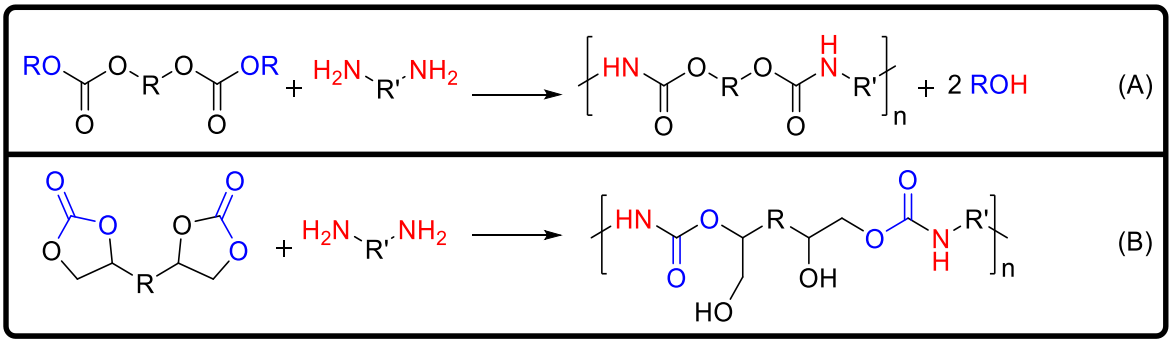

Figure 1.11 Synthetic schemes for non-isocyanate polyurethane

Non-isocyanate polyurethanes do not proceed through toxic isocyanates, this way is relatively safe for both the environment and humans compared to the conventional polyurethanes, hence significantly gaining fame as green polyurethanes.

1.2.4 | Polyurethane systems

The preparation of isocyanate-based foams is a simultaneous occurrence of polymer formation and gas generation. Foams are prepared by mixing component A (diisocyanate) and component B (a blend of polyol, surfactant, chain extender, and catalyst) at room temperature. No heating is necessary. Foaming systems can be classified into three different systems: the one-shot or one-step system, the quasi-prepolymer system, and the full-prepolymer system.

1.2.4.1 | One-shot or one-step system

With the one-step system known as the one-shot process, all reactive chemicals are brought simultaneously to the reaction, which slowly or quickly progresses exothermally. In the single-step system, the entire reaction occurs when all three basic components, such as polyol, diisocyanate, and chain extender, plus catalysts and pigments are mixed (Ashida, 2006). Polyurethane foams are obtained with or without using a solvent. Schematic diagram of the one-shot system is shown in Figure 1.12.

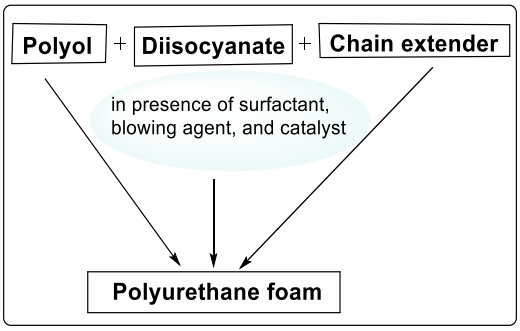

Figure 1.12 One-shot process for polyurethane foam preparation

1.2.4.2 | Two-step system

In the case of the two-step process, part of the polyol reacts with a surplus of the pre-polymer isocyanate, and this reacts, still fluid, with the component.

Quasi-prepolymer or semi-prepolymer system

Quasi-prepolymer systems are a version of the two-step process in which a part of the polyol component reacts with an excess of the diisocyanate component. The pre-polymer formed further reacts with the remaining polyols, containing chain extender and suitable catalysts, to obtain a high molecular-weight polymer (Sharmin and Zafar, 2012). The schematic diagram of such a system is presented in Figure 1.13(a). Its advantage is that the exothermic energy is spread between the preparation of the quasi-prepolymer and the final polyurethane.

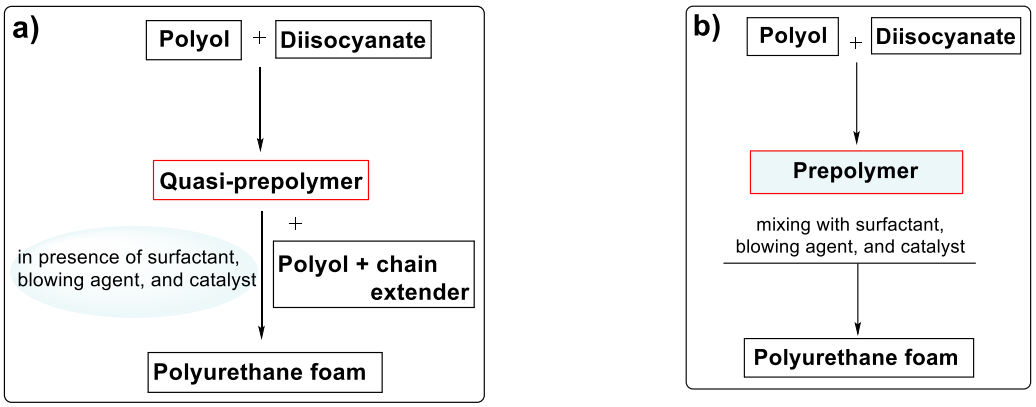

Figure 1.13 Quasi-prepolymer (a) and full-prepolymer (b) systems for the formation of a polyurethane foam

The one-step and the quasi-prepolymer systems are currently used in the urethane foam industry, in which the one-step process has become the major process for both flexible and rigid foams. However, bio-based polyurethane is mostly prepared by the pre-polymerisation procedure.

Full-prepolymer system

The full-prepolymer process was used only in the early years of the polyurethane foam industry and is now used only for unconventional foam manufacturing such as amide and imide foams (Ashida, 2006). The usual route of chemical formation for the polyurethanes by a full-prepolymer system is illustrated in Figure 1.13(b). In this case, the final polyurethane foam is formed in two separate stages. Initially, the diisocyanate and polyol components are mixed to form an intermediate polymer of low molecular-weight, which is called a pre-polymer and is often a low-melting-point solid of low strength or thick viscous liquid (Szycher, 2012). The pre-polymer is then turned into the final high molecular-weight polymer by further reaction with a chain extender (diamine or diol); this step is usually referred to as the chain extension stage in which the catalyst is used.

1.2.5 | Flame retardancy of polyurethane

The flammability of polyurethane is a great safety hazard, threatening lives and goods (Lu *et al*., 2021). Considering this, the fire resistance of polyurethanes can be improved upon in different ways. Depending on the classes and applications of polymers, fire retardation could be achieved using flame retardants or changing the polymer structure. Currently, the principal methods of flame retardancy of polyurethane are blending and addition (Pfaendner, 2013; Zuber *et al.*, 2013), nanocomposites (Kausar *et al*., 2016; Marzec *et al*., 2017), and reaction grafting (Rao *et al*., 2018a). Flame retardancy of polyurethane foams reduces the flammability and toxic smoke level of material.

1.2.5.1 | Mechanism of polyurethane flame retardancy

Additive flame-retardant polyurethane

As described earlier, this method consists of incorporating flame retardants into the polyurethane resin by physically compounding at any stage of production and processing. It is the most commercially used method due to its low cost and easy applicability. Commonly used additive flame retardants include inorganic flame retardants or organic compounds containing halogens, phosphorus, and nitrogen (Lewin and Weil, 2001). Their use has some disadvantages: they can be removed easily with detergents, water, or solvents and can migrate,

while at the same time altering the physical and chemical properties of the final material. In addition, there is a phase separation due to loss of homogeneity, high loads, and high viscosity of compositions (Salmeia *et al.*, 2015). The systems obtained by mixing of many flame retardants have proven to be efficient (Wang *et al.*, 2017; Sut *et al.*, 2019). Several additive flame retardants which can impart good flame retardancy to polyurethanes are nowadays available in the market, such as aluminum and magnesium hydroxide, ammonium polyphosphate, tris(2-chloroethyl) phosphite, decabromodiphenyl ether, melamine, and melamine pyrophosphate (Lu *et al.*, 2021).

Reactive flame-retardant polyurethane

Reactive flame retardancy is also known as intrinsic flame retardancy. It can be achieved by several approaches, which are summed up basically in modifying already-existing polymers by chemically grafting some active functional segments onto the polymer backbone or by readjusting the raw material with potentially active functions as fire retardants before polymerisation (Davesne *et al.*, 2015). Flame retardancy of polyurethane via this method consists of introducing isocyanates, chain extenders, or polyols-containing flame-retardant elements such as halogens, phosphorus, nitrogen, silicon, or boron into the polyurethane molecular chain through chemical bonding (Gu *et al.*, 2015; Yuan *et al.*, 2016). Reactive flame retardants have the advantage to be permanently bonded to the main chain. In fact, a relatively low amount of reactive flame retardants can have a similar effect to that achieved with relatively high loads of additive flame retardants (Singh and Jain, 2009). On the contrary, preparation of reactive systems is more expensive and time-consuming, because it requires the development of a novel polymer with specific chemical and physical properties (Lu and Hamerton, 2002). Based on the differences of flame retardant elements (Yuan *et al.*, 2016), reactive flame retardant polyurethane can be divided into halogen-containing, nitrogen-containing, phosphorus-containing, and phosphorus-nitrogen flame retardant polyurethane.

1.2.5.2 | Eco-friendly flame retardancy

As presented earlier, polyurethane materials need to be flame and fire retardant for safe use. Usually, halogen-based compounds are added to serve this purpose. These compounds are toxic and not environmentally friendly. Furthermore, besides the toxicological effects of using halogen-related compounds or additive-type fillers for their flame retardation properties, they can also reduce the mechanical properties of polyurethane. The growing number of recommendations and restrictions from the international community has promoted the

sustainable development of safe and ecological non-halogen-containing flame retardant polymers (Hull *et al*., 2014). To improve the efficiency of halogen-free flame retardant, some techniques, such as crystallisation, nanotechnology, and catalysis, are receiving increased attention. Therefore, reactive-type fillers for flame retardation properties are preferred to the additive-type. Inevitably, compounds based on phosphorus, nitrogen, silicon, and boron elements gradually replaced the use of halogenated flame retardants. Among these, environmentally friendly raw materials made from nitrogen and phosphorus are much more being exploited (Marosi *et al*., 2014). They are also known as intumescent flame retardants and were considered an effective way to improve the fire behaviour of polyurethane foams (Gu *et al*., 2015; Yuan *et al*., 2016). For instance, phosphoryltrimethanol was synthesised and employed as a crosslinking agent to prepare flame-retardant flexible polyurethane foams with good char formation during combustion (Chen *et al.*, 2014). The polyol of N, N-Bis (2-hydroxyethyl)-aminomethylphosphonic acid diethylester was synthesised and used to form a flame retardant polyurethane quasi-prepolymer for toughening phenolic foam (Ding *et al*., 2015). With the same approach, Çelebi *et al.* (2004) adopted bis(4-aminophenoxy)phenyl phosphine oxide as a chain extender for the synthesis of water-dispersed flame retardant polyurethane resins. Nitrogen- and phosphorus-containing compounds have great potential due to their synergistic performance in polymeric materials (Yuan *et al*., 2016). In addition, some studies shown that polyurethanes produced from phosphorus- and nitrogen-based materials offer the benefit of protecting the environment as well as improving mechanical properties (Singh and Jain, 2009; Hull *et al*., 2014; Marosi *et al*., 2014; Yuan *et al.*, 2016).

1.3 | Epoxy resins

1.3.1 | Definition and classification of epoxy resins

Epoxy resins are systems composed of molecules containing each two or more reactive epoxide groups (oxirane ring) (Elizalde *et al*., 2013). A common epoxy resin is diglycidyl ether of bisphenol-A (DGEBA) which is synthesised by the reaction of Bisphenol-A with epichlorohydrin in the presence of sodium hydroxide (Maso *et al*., 2002). Figure 1.14 shows the links between a general structure of DGEBA and the material properties. With increasing the number of repeat units "n" in the epoxy pre-polymer, the physical state of epoxy resin could be transformed from liquid to solid. The main parameters that control the polymer structure are the functionality, which is the number of reactive sites per monomer, and the molar ratio between co-reactive sites.

Depending on their molecular structure and applications, epoxy resins can be classified into two families: the glycidyl epoxy and non-glycidyl epoxy.

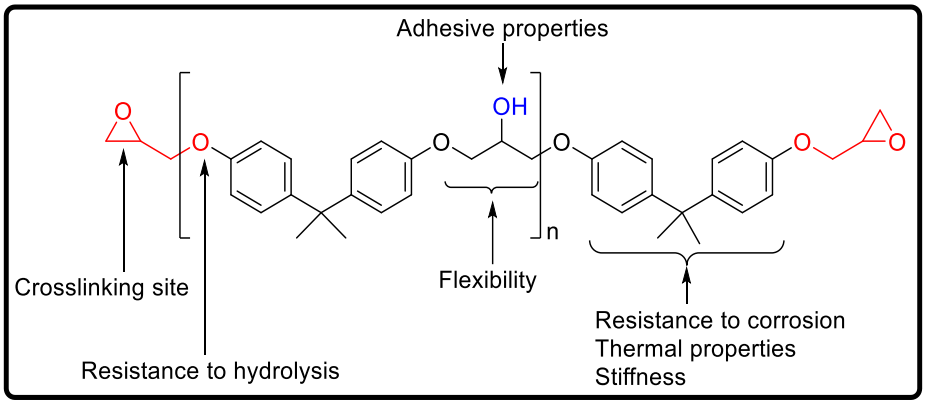

Figure 1.14 Correlation between a DGEBA epoxy pre-polymer and material properties

1.3.1.1 | Glycidyl epoxies

They are produced by a condensation reaction of the appropriate dibasic acid, dihydroxy compound or diamine, and epichlorohydrin. They can be divided into three types on the basis of their structure: glycidyl ether, glycidyl ester, and glycidyl amine.

Glycidyl ether

Glycidyl ether of epoxy resin is the most common class of epoxy resins. This is the first commercial high molecular-weight epoxy resin and is most widely used known as DGEBA (Figure 1.15). It is available in a range of molecular weights 900 – 3000 g mol^{-1}.

Glycidyl ester

Compared to DGEBA, glycidyl ester of epoxy resin is usually less viscous, highly reactive, highly adhesive, and has good-using processability. Some specific examples are: o-Phthalic acid diglycidyl ester, m-Phthalic acid diglycidyl ester, and tetrahydrophthalic acid diglycidyl ether (Figure 1.15).

Glycidyl amine

Glycidyl amine resins can be prepared by reacting epichlorohydrin with an amine. They are generally highly viscous liquids and behave like semisolids at room temperature. Though such resins are multifunctional, they have high epoxy value, and high crosslinking density. The most important resin in this class is tetraglycidyl methylene dianiline (Figure 1.15). These resins are more expensive than the DGEBA.

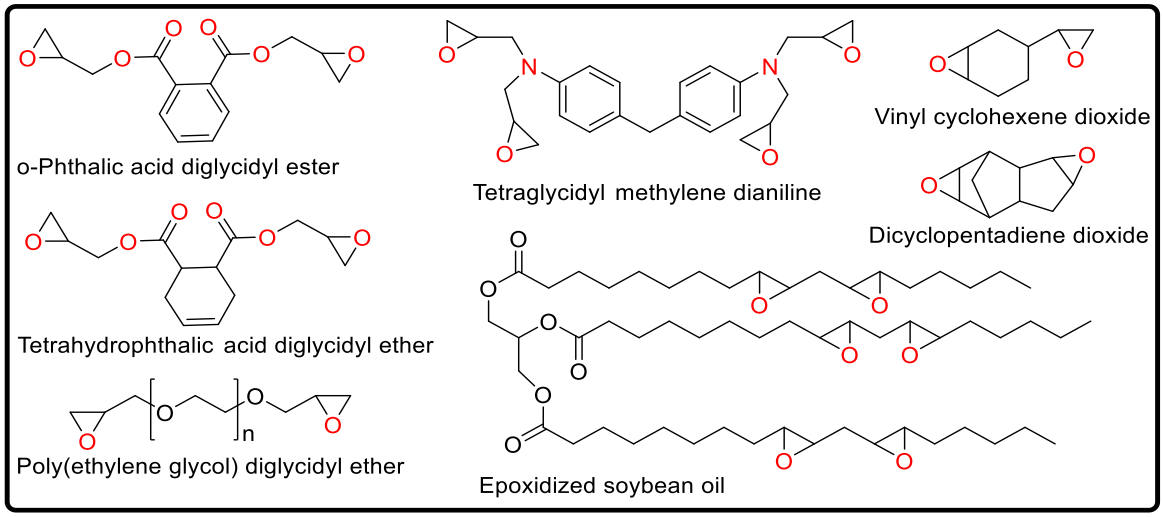

Figure 1.15 Some examples of epoxy resins

1.3.1.2 | Non-glycidyl epoxies

Non-glycidyl ether epoxides are of two types: cyclic aliphatic resins and acyclic aliphatic epoxy resins.

Cyclic aliphatic resins

They are closed in structure with epoxide group in the molecule. Vinyl cyclohexene dioxide, and dicyclopentadiene dioxide, are some examples of the commercially available cyclic aliphatic epoxy resins (Figure 1.15).

Acyclic aliphatic epoxy resins

These have a linear structure to which epoxide groups are attached. Three different categories of resins can be identified among acyclic aliphatic epoxy resins: epoxidised diene polymers, polyglycol diepoxides, and epoxidised oils (Figure 1.15). Commercially epoxy resins are marketed under the trade names Araldite, DER, Epi-Cure, Epi-Res, Epikote, Epon, Epotuf, and so on.

1.3.2 | Mechanism for the synthesis of epoxy resin

Nowadays, 80-90% of commercial epoxy resins are petroleum-based. Figure 1.16 summarises the preparation of DGEBA by reacting bisphenol-A and epichlorohydrin. The grafting of epoxy groups on a compound having active hydrogen (AR–OH) takes place through the reactions illustrated in Figure 1.17 (Joost *et al.*, 1990).

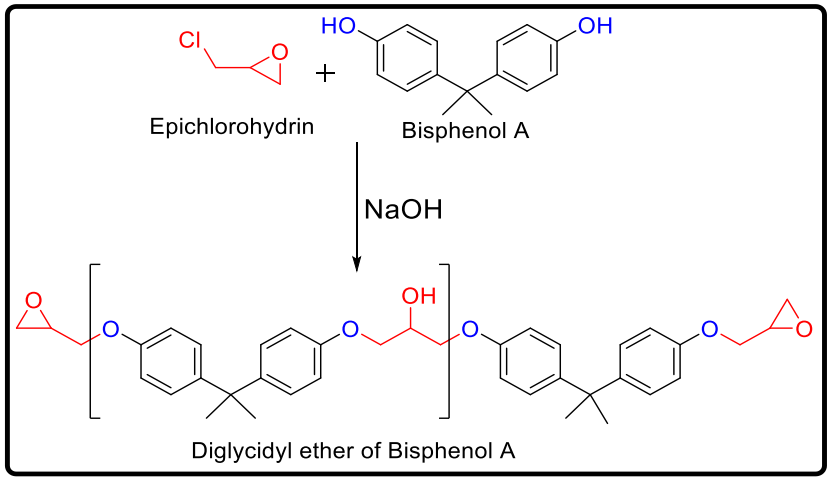

Figure 1.16 Schematic synthesis reaction of DGEBA

Sodium hydroxide catalyses the reaction to by opening the epoxy ring; the intermediate product being chlorohydrin. It also acts as the dehydrohalogenating agent, neutralising the hydrochloric acid formed in the reaction (Saldivar and Vivaldo, 2013). to give a new epoxy as shown in Figure 1.17. Varying the ratio of reactants produces different relative amounts of the high molecular-weight products in addition to the monomeric unit. The epoxy formed is a viscous liquid or a brittle high-melting solid depending on the molecular weight. Considering both the chemistry of epoxy resins and all the reactants required to synthesise it, catalyst, unreacted starting raw materials, impurities, and other monomeric substances may be expected to be present in the resin in low levels (less than 100 ppm). The effective factors such as reaction conditions (temperature and time), and quantities of water present in the mixture influence the final properties of low molecular-weight epoxy resin (Lakshmi and Reddy, 2002).

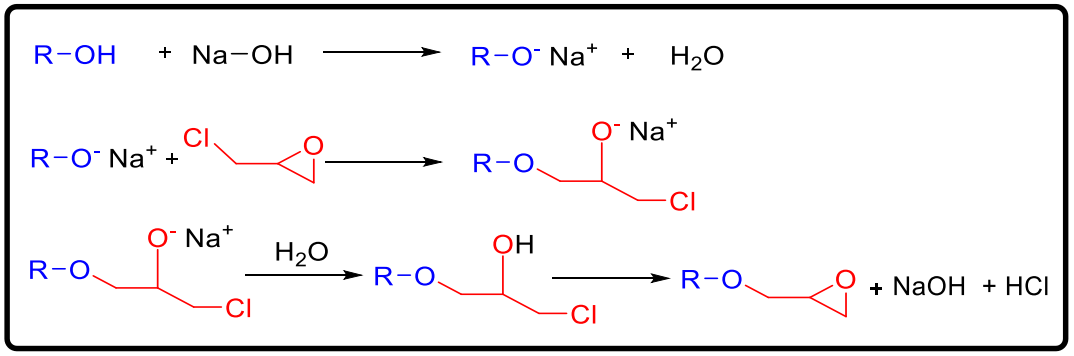

Figure 1.17 Major reaction schemes in epoxy resin synthesis from active hydrogen compound

Besides the main reaction for the production of epoxy resins, some side reactions can take place and may influence the properties of resulting epoxy resins (Yan *et al.*, 2021). Some side reactions are shown below.

i. Hydrolysis of epoxy groups

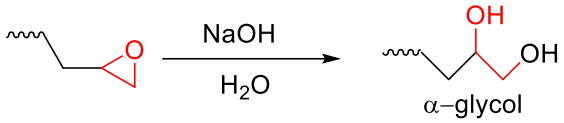

Scheme 1.14

ii. Formation of bound chlorine

- by reacting epichlorohydrin with secondary alcohol

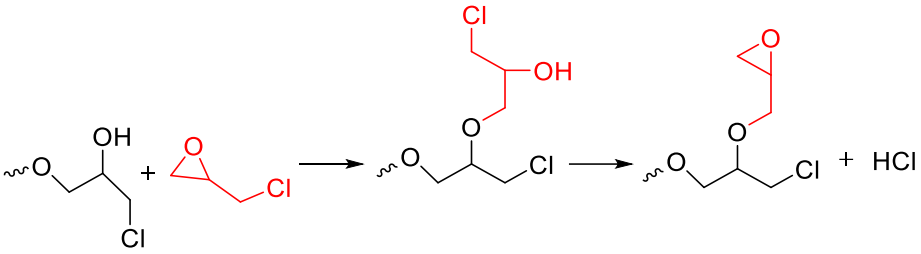

Scheme 1.15

- by abnormal addition of phenolic hydroxyl

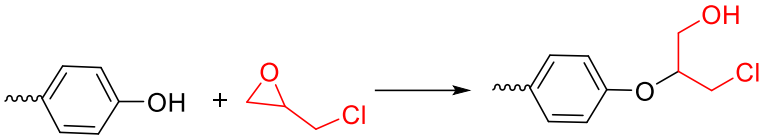

Scheme 1.16

iii. Incomplete dehydrochlorination

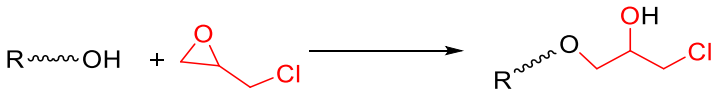

Scheme 1.17

Sometimes, quaternary ammonium salts and phosphonium salts can be used a catalyst to promote the condensation reaction of bisphenol A with epichlorohydrin (Elizalde *et al.*, 2013).

1.3.3 | Curing or crosslinking agents for epoxy resins

The useful properties of epoxy resins appear only after curing. The curing step transforms the epoxy from a low molecular-weight material to a highly crosslinked three-dimensional network. The network is composed of segments involving both the epoxy monomer and the crosslinking agent. The crosslinking of epoxy resins may be carried out either by way of the epoxy groups or through the hydroxyl groups. For linking epoxide resin molecules together, the different types of curing agents can be recognised as either direct participant in the crosslinked network or those which promote crosslinking catalytically.

1.3.3.1 | Catalytic self-curing

Epoxy resins have a strong tendency to form three-dimensional structure by reacting with itself in the presence of an anionic and cationic catalyst. In catalytic crosslinking, an ionic

complex is formed, which may open up a new epoxy group and generate another ion, thus the crosslinking proceeds. The curing reaction can also involve homo-polymerisation catalysed by Lewis acids or tertiary amines (Karak, 2021). The reaction occurs at a high temperature, and leads to creation of polyether networks with great chemical and thermal resistance (Brocas *et al*., 2013). However, the network is very brittle. In most cases, Lewis acid-based catalytic reactions are too fast for practical systems, whereas reactions in the presence of tertiary amines as catalysts are too slow and require of very high temperatures. Imidazoles are an example of types of anionic polymerising curing agents for epoxy resins (Saldivar and Vivaldo, 2013).

1.3.3.2 | Polyfunctional crosslinking agents

A multitude of different curing agents are available for epoxy resins depending on the process and properties required. The most widely used curing agents for epoxides include amines, polyamides, phenolic resins, anhydrides, isocyanates and polymercaptans (Elizalde *et al*., 2013). The choice of resins and hardeners depend on the properties desired, the process selected and the application fields. The general reaction of the epoxy group with other functional groups to give linear, branched, or crosslinked products is summarised in Scheme 1.18. Some of the typical curing agents are illustrated in Figure 1.18.

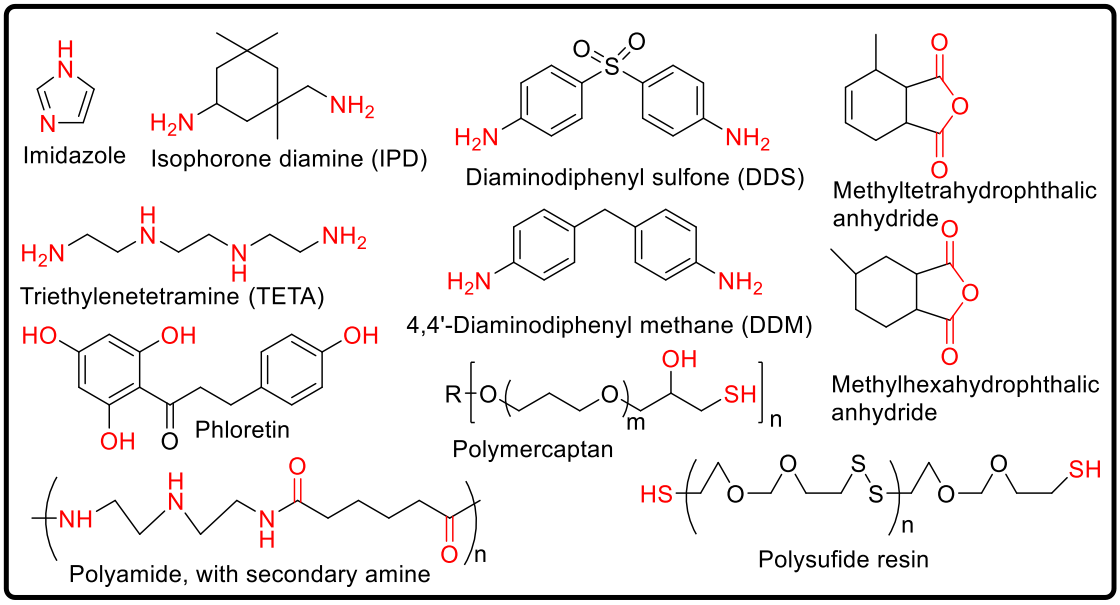

Figure 1.18 Some examples of curing agents

The curing temperature and the thermal stability of epoxy resins have been found to decrease with the type of curing agent in the order: acid anhydrides > phenol > aromatic amine > cyclo-aliphatic amine > aliphatic amine.

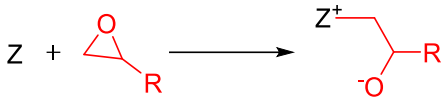

Scheme 1.18

In scheme 1.18, compound Z is a crosslinking agent (amine, phenol, thiol, carboxylic acid, acid anhydride, or amide).

Amines

Aliphatic amines are agents which are capable of curing epoxy resins at room temperature. The cured resin has outstanding properties. A primary amine can react in two steps via its two active hydrogens forming a secondary amine and then a tertiary amine (Figure 1.19). Under specific conditions, the tertiary amine generated can act as a catalyst for the self-polymerisation of epoxy groups. Tertiary amines are very important as accelerator especially for acid anhydrides but less used as curing agent. The cured amine end product has been found to be highly dependent on the type of epoxy resin, amount of hardener loaded, and the curing speed (Lakshmi and Reddy, 2002). The epoxy resins cured with aliphatic amine such as diethylenetriamine, and triethylenetetramine have good bonding properties and excellent resistance to water and some solvents (Kausar *et al.*, 2016).

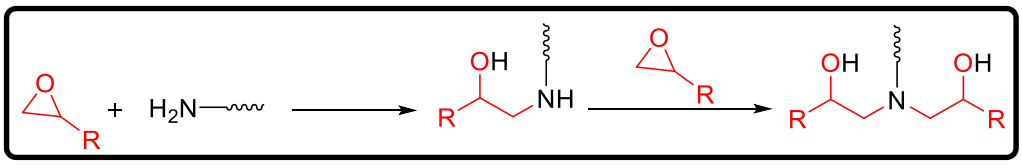

Figure 1.19 Attack of primary amine on epoxy group

Aromatic amines, due to steric hindrance by the aromatic ring, slowly cures at room temperature. It has weaker basicity than aliphatic amine. 4,4'- diaminodiphenyl methane and diaminodiphenyl sulfone are common aromatic amines used as curing agents. They provide good thermal stability, and mechanical and electrical properties with the diglycidyl derivative of bisphenol A (Srividhya *et al.*, 2005).

Anhydrides

They are generally used for their long pot life and comparatively well-balanced properties. Most of the commonly used anhydrides are alicyclic anhydrides. For instance, methyltetrahydrophthalic anhydride, tetrahydrophthalic anhydride, hexahydrophthalic anhydride, and methylhexahydrophthalic anhydride are known curing agents of the anhydride family (Barabanova *et al.*, 2019). Anhydrides from dicarboxylic acids produce linear structures with diepoxides, and crosslinking usually occurs due to esterification of the alcohol groups

(Figure 1.20). In addition, the studies have revealed that resins obtained from epoxidised vegetable oil and anhydrides can be a good alternative to petroleum-based epoxy resins (España *et al*., 2012).

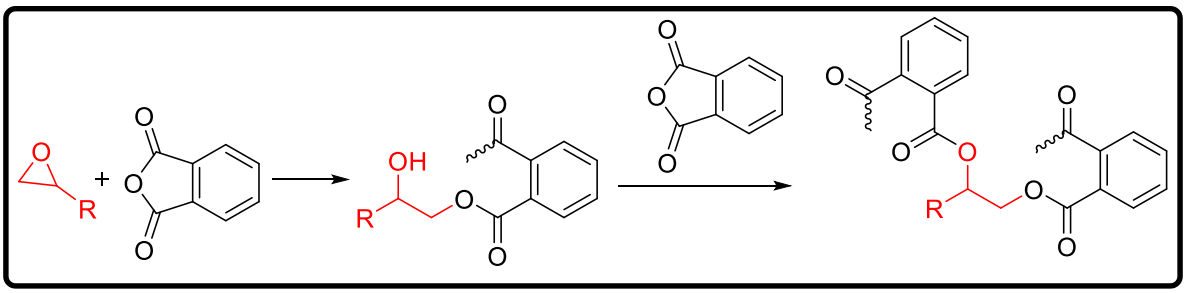

Figure 1.20 Schematic reaction of epoxy curing with anhydride

Alcohols

Aliphatic alcohols are reactive with epoxies; but they are not normally used as curing agents, whereas polyphenols are becoming more frequently used because they favor a high glass transition temperature of the cured epoxy (Figure 1.21).

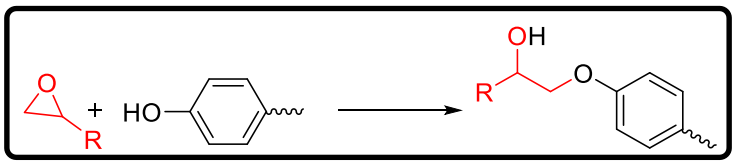

Figure 1.21 Epoxy resin curing reaction with phenolic compound

Polyamides

Polyamide resins obtained by the condensation reaction between acid and amine are widely used to cure epoxy resins. They contain reactive primary and secondary amines; polyamides are used to cure bisphenol A-type epoxy resin at normal temperatures or below with moderate heat generation. It cures so slowly that it has a long pot life (Pradhan *et al*., 2016). Polyamides are also used to cure epoxy resin in highly plasticised rigid thermosetting polymers, due to their high hydrocarbon moieties.

Polymercaptans

Liquid polymercaptans are known as polythiols. They are attracting interest as low temperature curing agents because they can cure epoxy resins at 0 to 20°C (Pradhan *et al*., 2016). However, the addition of a tertiary amine accelerators is required. Polysulfide resins have terminal mercaptan groups, and are used both as curing agents and flexibilisers. In addition, polysulfide resin can be used in the preparation of sealing agents, adhesives, and casting materials, due to its good resistance to water (Cui *et al*., 2001).

Generally, epoxy materials are unrecyclable thermosets, but the recent progress in vitrimers show that they can be made recyclable and reversible by suitable design and curing. Thus, epoxy vitrimers can present such behaviour if they contain imine-epoxy, transesterified epoxy, sulfur-epoxy, or siloxane-epoxy thermo-reversible linkages (Hayashi *et al*., 2020).

1.3.4 | Application of epoxy resins

Epoxy resins are the most attractive synthetic thermosetting polymers due to their typical properties such as dimensional stabilities and good thermal, excellent chemical resistance, high water and solvent resistances, good adhesion strength to other varieties of substrates, and superior electrical properties (Pradhan *et al*., 2016). In 2020, the market value of epoxies was approximately USD 27.5 billion (Karak, 2021). They are used for various ranges of applications in the modern world, which are summarised as follows.

Adhesives and bonding

Approximately 5% of the total production of epoxy resins is consumed in the adhesive field (Elizalde *et al*., 2013). Modern adhesive technologies have developed many epoxy-based adhesive systems with different specifications to cover all uses. Epoxy-based adhesives are produced in several forms including heat-curing liquids, room temperature-curing two-component liquids, powders, hot-melt adhesives, tapes and films (Bhuvaneswari *et al*., 2017). The bonding properties of epoxy resins are linked to the low shrinkage of epoxy resins during the curing, which causes low internal stress in adhesive joints.

Surface (protective) coatings

The large quantity of epoxy resin, around 60% of the global production, is used in the coatings industry. They are mostly consumed in baking varnishes and powder coatings. They are also used both in thermal and ambient cure applications in industries such as aerospace, civil engineering. and automotive. Amine curatives have been suggested to be the best way for epoxy resins in coating applications (Pradhan *et al*., 2016). The epoxy-resin coating systems are available in various forms such as solid resins (fusion-bonded epoxy coating), liquid resins, radiation curable resins, and high molecular-weight thermoplastic resins (Liu *et al*., 2018).

Electrical and electronic applications

Epoxy resins are commonly used in electrical applications for potting, casting, impregnation, encapsulation, coating, sealing, and moulding. The wide application of epoxy

resins in the electrical industry is attributed to its fast curing at room temperature, excellent insulation property, and high chemical and moisture resistance (Elizalde *et al.*, 2013).

Composites and reinforced resins

Epoxy resin is also used as a polymer matrix in fibre reinforced plastics in which the stiffness and strength of epoxy resins are significantly improved with the reinforcing fibres. The resulting material can be used in building construction, electrical insulation, aerospace and marine industries (Yasmin *et al.*, 2006). Composite and laminate industry uses approximately 28% of epoxy resins produced (Liu *et al.*, 2018).

Other applications

Epoxy resins are also used as polymer stabilisers, plasticisers and plastics for pipes (Pradhan *et al.*, 2016).

1.3.5 | Flame retardancy of epoxy resins

As polyurethane and other polymers, epoxy resins are flammable and produce a large amount of smoke and heat during combustion. In this sense, flame retardancy analysis has been recognised as an inescapable test and undeniable requirement for growing novel generations of highly efficient epoxy-based materials. A vast portion of the literature on epoxy-based composites has been primarily devoted to the use of flame retardant epoxy (Kausar *et al.*, 2016). Some recent methods of halogen-free flame retardancy of epoxy resins by additive and reactive flame retardants are described in this section. Nowadays, halogen-free flame retardants have aroused great interest from the perspective of environmental protection due to its non-toxic constituents.

1.3.5.1 | Additive flame-retardant epoxy resins

The first type of flame retardant epoxy resins is by physical blending, in which synthetic compounds, inorganic materials or modified biomass resources are added directly during the curing process. Some examples are listed below.

Synthetic-based flame retardants

These are the products of synthesis reaction. Examples are melamine (Shen *et al.*, 2017), 9,10-dihydro-9-oxa-10-phosphaphenanthrene-10-oxide (Tang *et al.*, 2017), and organic phosphorus such as phosphonates, phosphate esters, organic phosphorus salts and phosphorus heterocyclic compounds (Chen *et al.*, 2015).

Inorganic fillers

They are used to forming epoxy/nanocomposites. The incorporation of nanocomposites does not promote only the toughness and strength, but also provide barrier properties, heat resistance and flame retardancy to epoxy products. Among them, montmorillonite (Lee *et al*., 2010), carbon-based materials (such as carbon nanotubes, graphene, and expandable graphite) (Wang *et al*., 2017), silicon-based materials (silica (SiO_2), siloxane, and polyhedral oligomeric silsesquioxane) (Srividhya *et al*., 2005), boron nitride nanosheets (Kausar *et al*., 2016), and inorganic phosphorus (such as red phosphorus, ammonium polyphosphate and phosphates) have been extensively studied and developed (Lee *et al*., 2010; Dasari *et al*., 2013).

Metal-containing compounds

They are used in practice applications because, they are often inefficient when used alone. The added amount ranges from 50-70% of the flame-retardant materials to achieve the required flame-retardant level. Boehmite (AlO(OH)) (Lu and Hamerton, 2002), aluminium hydroxide ($Al(OH)_3$) (Kausar *et al*., 2016), and aluminium trihydrate (H_6AlO_3) (Dasari *et al*., 2013) are typical examples of metal-containing flame retardants for epoxy.

Bio-based flame retardants

The result of modification of biomass resources such as phytic acid, starch, castor oil, bamboo fiber, cardanol cellulose, and lignin have been successfully applied to epoxy resin with reasonable effectiveness (España *et al*., 2012; Ferdosian *et al*., 2016).

Currently, synergistic flame retardants for epoxy resins have become a new focus due to unusual flame retardancy and thermal stability. These are phosphorus/nitrogen-containing, and phosphorus/silicon-containing flame retardants (Kausar *et al*., 2016; Karak, 2021).

1.3.5.2 | Reactive flame-retardant epoxy resins

This method of preparation focuses on a chemical modification, in which desired functional groups or flame retardant elements are grafted onto raw material or hardener by chemical reactions before curing. For instance, bis-phenoxy (3-hydroxy) phenyl phosphine oxide has been synthesised and used as raw material to prepare epoxy resin (Ren *et al*., 2007). The results of analysis showed that the introduction of new resin imparts flame retardancy to the final epoxy. Likewise, Spontón *et al*. (2007) prepared flame retardant epoxy resins based on diglycidyl ether of (2,5-dihydroxyphenyl) diphenyl phosphine oxide and obtained a considerable improvement in flame retardant performance of resulting epoxy material.

1.4 | Objectives and strategies of this work

Due to the high flammability of polymeric materials, foams and leather, this thesis aims to design phosphorus- and nitrogen-based polyurethane and epoxy polymers and study their physico-chemical and mechanical properties and reactions with fire. To fulfill this objective, several stages will be considered and can be divided into three items:

- Synthesis and characterisation of reactive phosphorus-containing monomers. A nitrogen moiety will also be introduced to promote the synergistic effect between phosphorous and nitrogen actions on flame resistance.

- The use of the phosphorus-nitrogen based polyols for the preparation of flexible and semi-rigid polyurethane foams and characterisation of the products.

- Synthesis of epoxy hybrid products by blending the phosphorus compounds with commercial DGEBA, clays nanoparticles and curing with TETA. The epoxy products will be used as coatings for leather.

Chapter 2: Experimental Methods

This chapter presents detailed information on the materials used in this thesis, syntheses of different reactive organic-inorganic hybrid monomers, and the various formulations of polyurethane foams and epoxy nanocomposites. In addition, the equipment, conditions employed for characterisation of the materials and analysis of the flame retardant performances and final materials are also described. All the experiments described herein were carried out in the Polymer Science and Technology Laboratory of the CSIR-Central Leather Research Institute, Chennai, India.

2.1 | Materials

2,2′,2″nitrilotriethanol, diethylchlorophosphate, toluene-2,4-diisocyanate (TDI), dibutyltin dilaurate (DBTL), polyethylene glycol (PEG, MW = 400 g mol^{-1}), poly(dimethylsiloxane) hydroxy terminated (PDMS, average Mn ~ 550) were purchased from Sigma-Aldrich chemical company. 1,3-Propanediol (> 98%), 1,4-Butanediol (> 99%), 1,5-Pentanediol (> 97%), phosphoryl chloride (> 98%), epichlorohydrin (> 99%), and silicone surfactant were supplied by TCI Chemicals Pvt. Ltd., India. Nanoclay, Nanomer 1.34TCN (montmorillonite clay surface modified with 25-30 wt.% methyldihydroxyethyl hydrogenated tallow ammonium) was obtained from Aldrich Chemical Company whereas, solvents such as tetrahydrofuran (THF), diethyl ether, dimethyl formamide (DMF) and triethylamine (TEA) were purchased from Merck, Chennai, India. Diglycidylether of Bisphenol A resin (DGEBA, LY556, EEW 180-185, Density 1.23, Refractive Index 1.57 and viscosity 10000 cP) was supplied by Ciba Speciality Chemicals Pvt. Ltd., India. Triethylenetetramine (TETA, Aradur HY951 IN) was supplied by Huntsman International Pvt. Ltd., India.. The leather sheets were provided by the tannery division of CSIR-Central Leather Research Institute, Chennai, India, processed as per standard procedures (Thorstensen, 1993). All the reagents were used as received.

2.2 | Compound design and experimental procedures

2.2.1 | Phosphorus-based polyurethane foams

2.2.1.1 | Synthesis of reactive phosphorus-based polyols (P-OHs)

Tris-(5-hydroxypentyl) phosphate (P-Pen-OHs) was synthesised as follow: In a 100-mL round bottom flask equipped with a magnetic stirring bar and a nitrogen inlet, 0.1 mol of

phosphoryl chloride was dissolved in 20 mL of tetrahydrofuran (THF). The mixture was cooled in an ice bath, then 0.3 mol of pentanediol dispersed in 5 mL of tetrahydrofuran was added dropwise. The reaction mixture was stirred continuously and 0.3 mol of triethylamine were added slowly. The reaction was allowed to continue for 12 h to ensure complete conversion. The formation of the products was revealed by the precipitation of a solid. The precipitate was filtered using a Buckner funnel, washed and dried. The final compound tris-(5-hydroxypentyl) phosphate (P-Pen-OHs) was obtained with a yield of 86%.

Tris-(4-hydroxybutyl) phosphate (P-But-OHs) and tris-(3-hydroxypropyl) phosphate (P-Pro-OHs) were synthesised according to the same experimental procedure by reacting phosphoryl chloride with butanediol and propanediol, respectively. Their yields were 85%. Figure 2.1 summarises the synthetic route of the phosphorus-based polyols (P-OHs).

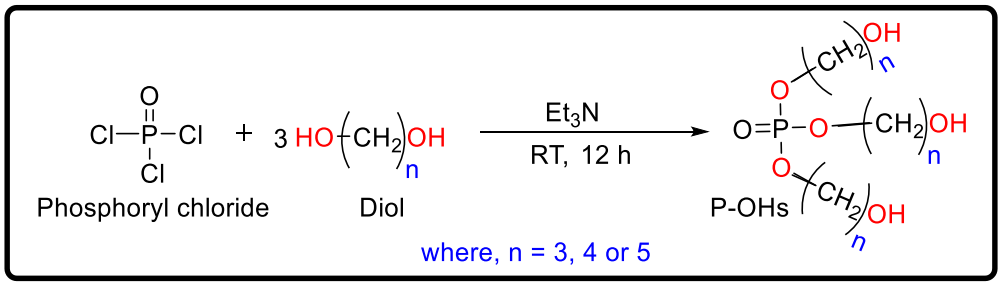

Figure 2.1 General synthetic route of precursors P-OHs

2.2.1.2 | Preparation of polyurethane foams from P-OHs and PEG

Phosphorus-based polyurethane foams were manufactured by the one-shot process. The P-OHs, polyethylene glycol, catalyst, surfactant, and distilled water were mixed (in the proportions given in Table 2.I) and vigorously stirred in a 500-mL conical flask with a mechanical stirrer at 2500 rpm for 1 min. The mixture was allowed to degas for 3-5 min. When the gas-foam at the surface of mixture was completely dissipated, toluene diisocyanate was added rapidly and stirring was continued for another 20 s at the same speed. The mixture was immediately poured into a wooden cylindrical mould lined with aluminum foil and the foam was allowed to rise and set at ambient conditions (28±5ºC). The polyurethane (PU) foam samples were removed from the mould and kept in a desiccator at room temperature for 24 h before testing. Table 2.I shows the formulations of polyurethane foam samples. The samples were cut to the dimensions required to characterize its physical, chemical, thermal, and mechanical properties.

Table 2.I Recipe for formulation of phosphorus-based polyurethane foams

Material	pph (parts per hundred of polyol by mass)
Polyethylene glycol	50
P-OHs*	100
Catalyst DBTL	0.4
Silicone surfactant	0.8
Water	4
Toluene diisocyanate	51.2

* Different polyols used were either P-Pen-OHs, P-But-OHs, or P-Pro-OHs

2.2.2 | Phosphorus- and nitrogen-based polyurethanes

2.2.2.1 | Preparation of triethanolaminodiethyl phosphate

Synthesis of triethanolaminodiethyl phosphate (PN-OH) was carried out as follows. To a solution of 30 g (0.2011 mol) of triethanolamine in 150 mL of dry THF, 20 g of triethylamine was added dropwise through a syringe. Then 34.7 g (0.2011 mol) of diethylchlorophosphate was added dropwise through a syringe and the mixture was stirred under nitrogen atmosphere. The triethylamine triggered an exothermic reaction. The addition was completed at 0°C with placing the mixture in an ice bath, and the reaction temperature rose to 50°C for 3 h. After this pre-defined time, the reaction mixture was cooled to room temperature. The solvent was removed using a rotary evaporator, 300 mL of diethyl ether was added, and the mixture stirred for 30 min, filtered, and washed again with ether. Then ether was removed on a rotary evaporator. The desired product triethanolaminodiethyl phosphate (PN-OH) was obtained as a white opaque solid at a yield of 84%. Figure 2.2 illustrates the synthesis of PN-OH.

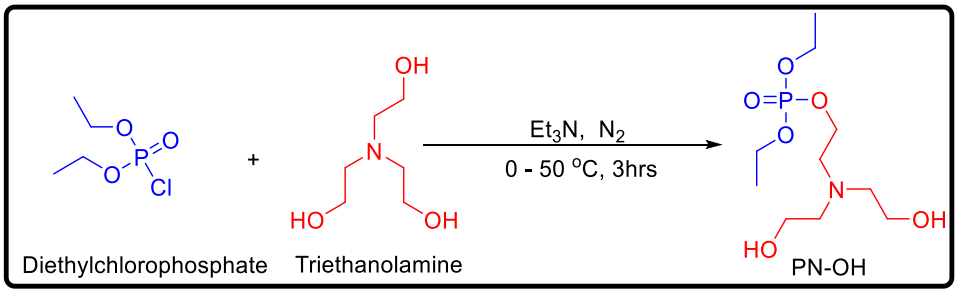

Figure 2.2 Synthesis route of triethanolaminodiethyl phosphate PN-OH

2.2.2.2 | Preparation of polyurethane from PN-OH, PEG and PDMS

A series of phosphorus and nitrogen-based polyurethane samples was synthesised by a two-step reactive process. The recipes for polyurethane preparation are given in Table 2.II. The procedure was as follow. In a 100-mL round bottom flask, 7.15 g (0.0264 mol) PN-OH was mixed with 3 mL of DMF at room temperature in N_2 atmosphere and stirred vigorously for 10

min. 8 mL of THF was added as a solvent and stirred briskly. A different mole ratio of PEG (40–100 pph) was added through a handy pipette and the mixture was stirred vigorously at a speed of 800 rpm at ambient temperature for 15 min. After this, the mixture was cooled down to 0°C using an ice bath. 4.6 g (0.0264 mol) toluene-2,4-diisocyanate was injected through the cannula into the suspension. Then 0.17 g of DBTL as a catalyst and the corresponding quantity of PDMS were added. After the addition was completed at 0°C, the reaction was allowed to attain room temperature and stirred for 24 h. The resulting mixture was a highly viscous liquid which was spread out in petri glass and allowed to dry for an hour. PEG was added as a chain extender and to increase the soft segments and elasticity of the materials. The materials appear to be more flexible than the samples previously prepared in section 2.2.1.2. PDMS can also contribute to the elasticity of a polymer material. The proposed structure of resulting polyurethane material is shown in Figure 2.3.

Table 2.II Recipe for formulation of phosphorus- and nitrogen-based polyurethane

Samples	TDI /pph	PN-OH /pph	PEG /pph	PDMS /pph	Catalyst /pph	Solvents	
						DMF	THF
PU1050	64.3	100	100	50	2.4	3 ml	8 ml
PU1025	64.3	100	100	25	2.4	3 ml	8 ml
PU0850	64.3	100	80	50	2.4	3 ml	8 ml
PU0825	64.3	100	80	25	2.4	3 ml	8 ml
PU0450	64.3	100	40	50	2.4	3 ml	8 ml
PU0425	64.3	100	40	25	2.4	3 ml	8 ml

pph stands for parts per hundred of polyol (PN-OH) by mass

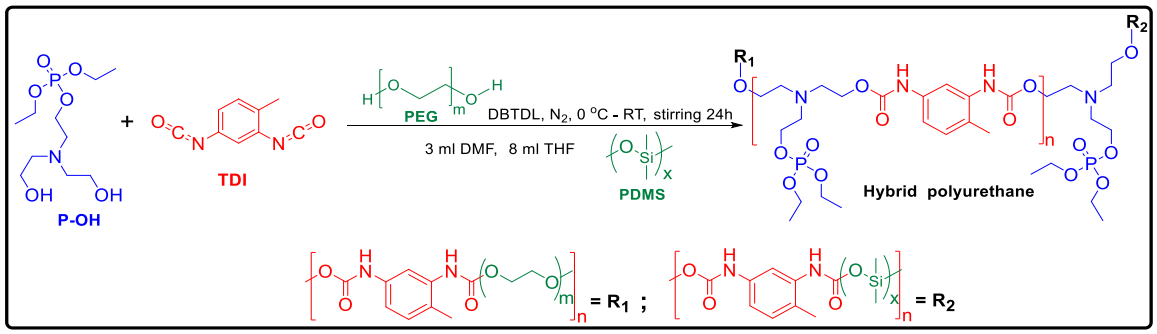

Figure 2.3 Schematic illustration of polyurethane formulation

2.2.3 | Phosphorus-based epoxy/clays nanocomposites

2.2.3.1 | Glycidylation of phosphorus-based polyols P-OHs

Functionalisation of tris-(5-hydroxypentyl) phosphate (P-Pen-OHs), tris-(4-hydroxybutyl) phosphate (P-But-OHs), and tris-(3-hydroxypropyl) phosphate (P-Pro-OHs) was carried out by glycidylation according to the procedure described as follows. In a 250-mL three necked round

bottom flask provided with stirrer and nitrogen inlets and a reflux condenser, 0.3 mol of epichlorohydrin and 0.1 mol of P-OHs were mixed, then stirred vigorously. The solution was refluxed for about 5 h at 50 °C then 0.1396 mol of NaOH was added slowly. The mixture was stirred further for a 3 h at the set temperature. The content was dissolved in benzene, and two phases were formed: an organic phase containing the epoxy resin and an aqueous phase containing sodium chloride by-product, sodium hydroxide catalysts and the remaining epichlorohydrin. The two phases were separated in a separating flask and the organic phase washed several times with distilled water to remove salts and unpolymerised components. This organic benzene layer was dried using a rota evaporator to get tris(pentyl glycidyl ether) phosphate (GEP-Pen-OHs), tris(butyl glycidyl ether) phosphate (GEP-But-OHs), or tris(propyl glycidyl ether) phosphate (GEP-Pro-OHs) depending on the precursor used as shown in Figure 2.4.

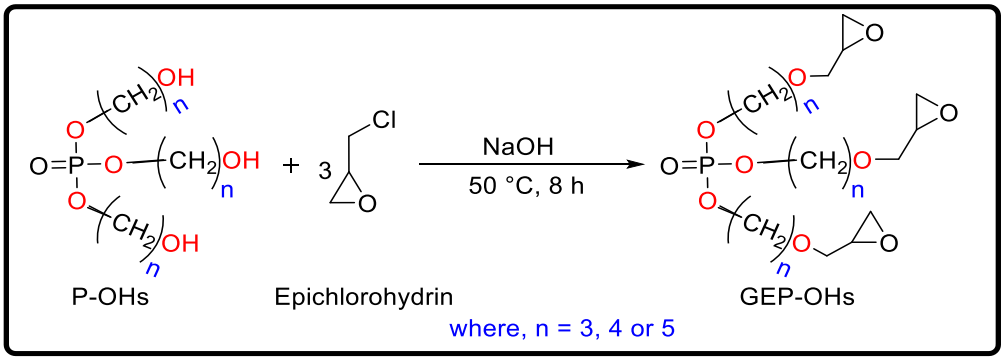

Figure 2.4 General synthetic route of the GEP-OHs pre-polymers

2.2.3.2 | Formulation and application of hybrid epoxy/clays nanocomposites

A series of epoxy formulations with or without nanoclays was formulated and then hardened with triethylenetetramine (TETA). Glycidylated hydroxyl precursors were blended with 10% wt. of DGEBA, 10% wt. of TETA to obtain their respective phosphorous-epoxy systems. The composition of the different samples is shown in Table 2.III. The epoxy formulations were cured at 70°C for 4 h.

Hybrid epoxy resins were also used as a finishing agent on the grain surface of leather. The phosphorous-epoxy hybrids were coated on the leather with a mass ratio of 1% based on the mass of leather.

Table 2.III Formulation and composition of different epoxy blends

Sample code	GEP-OHs pre-polymer	DGEBA/GEP-OHs ratio % wt	TETA/ GEP-OHs ratio % wt	Clay/GEP-OHs ratio % wt
T3GP-P	GEP-Pro-OHs	90	10	0
T3GP-P5	GEP-Pro-OHs	90	10	5
T4GP-P	GEP-But-OHs	90	10	0
T4GP-P5	GEP-But-OHs	90	10	5
T5GP-P	GEP-Pen-OHs	90	10	0
T5GP-P5	GEP-Pen-OHs	90	10	5

2.3 | Characterisation and analyses

Different techniques were used herein to elucidate and confirm the chemical structures of the synthesised polyols and polymers, to study their thermal stabilities and reaction to fire. The analyses for flame resistance of polymers were performed in collaboration with the PSGTECHS COE INDUTECH laboratory (Coimbatore), which is the center of excellence for industrial and home textiles in India.

2.3.1 | Spectroscopic characterisation

2.3.1.1 | Fourier transform infrared spectroscopy

Fourier transform infrared spectroscopy (FT-IR) is a technique which reveals the functional groups present in solid, liquid or gaseous samples. Its working principle is based on constructive and destructive interference phenomena. When radiated with infrared light, a sample absorbs a certain amount of incident radiations corresponding to different types on functional groups and their vibration modes (symmetric and asymmetric stretching, out-of and in-plane bending, and rocking). The reflected and unperturbed radiations are combined using instrumentation (like beam splitter, movable and stationary mirrors), and the interference is recorded to give interferogram (intensity vs. time spectrum). The Fourier transformation are applied to convert the time-domain spectrum into frequency-domain spectrum (transmittance or absorption modes). Each functional group has unique frequencies (just like a chemical fingerprint) which are used for its identification. The relative intensity of the bands is generally related to the concentration of the corresponding functional group in the sample. The change in the relative intensity of a band, and the presence of new band in a spectrum are used to study the chemical change in a sample and in new products.

FT-IR spectroscopic studies were performed to find the chemical structure of reactive precursors and verify the completion of the resin curing reaction. The FT-IR spectra of reactive precursors and polymeric materials were recorded on a Perkin Elmer spectrum TWO IR

spectrometer at room temperature without KBr pellets in the range 400 to 4000 cm^{-1} with 16 scans and 4 cm^{-1} of resolution. After performing the background, the sample was directly placed in the sample holder and pressed against the crystal.

2.3.1.2 | Nuclear magnetic resonance spectroscopy

Nuclear magnetic resonance (NMR) spectroscopy is a commonly used method for elucidating the structure of a molecule. It is a highly accurate and reproducible technique based on the interaction of a strong external magnetic field and energy from a second and weaker radio-frequency source with the nuclei of atoms (Patnaik, 2004). The nuclei of certain isotopes have an intrinsic spinning motion around their axes that generates a magnetic moment along the axis. Absorption occurs when these nuclei undergo transition from one alignment in the applied field to an opposite field. Excitation of the nuclei produces a spectrum of absorption intensity versus magnetic-field strength. The energy needed to excite these transitions can be measured. The resonance frequency ν that causes the transitions between energy levels is given by equation 2.1.

$$\Delta E = h\nu = \frac{\mu H_0}{I} \qquad \text{Equation 2.1}$$

where μ is the magnetic moment of the nucleus, H_0 the strong external magnetic field applied to the nuclei, h is the Planck's constant, and I the spin quantum number. Nuclei with I = 1/2 give the best resolved spectra because their electric quadrupole moment is zero. The most widely studied nuclei, ^{1}H, ^{13}C, ^{15}N, ^{31}P, and ^{19}F have a nuclear spin quantum number of 1/2. If the spin quantum number is larger, for instance equal to 1 in the case of deuteron (^{2}H), the nuclei have an electric quadrupole moment that interacts with an electric field gradient. The electric field gradient arises from the bond electrons, so that this nuclear quadrupole interaction also provides information on molecular structure.

In practice, modification of the local field at the nucleus due to the surrounding electrons causes the chemical shift which provides structural resolution. The chemical shift is defined as the nuclear shielding divided by the applied field, and thus it is only a function of the nucleus and its environment.

^{1}H-NMR, ^{13}C-NMR, and ^{31}P-NMR spectra of the reactive precursor samples were recorded on a Bruker Avance-III spectrometer at room temperature using the frequencies of 100 - 400 MHz. The samples were dissolved in a deuterated solvent ($CDCl_3$ or D_2O) at a concentration of 5-20% and tetramethyl silane was employed as an internal standard.

2.3.1.3 | X-ray diffraction analysis

Polymer materials are usually amorphous or semi-crystalline. The degree of crystallinity has a considerable impact on their properties and applications (Campo, 2008; Ebnesajjad, 2016). It is an important parameter for polymer characterisation which is determined by X-ray diffraction. X-ray diffraction (XRD) is a widely used technique to assess the crystallinity and structure of solid materials. It provides information on unit cells. The working principle of XRD is based on diffraction and constructive interference. A focused beam of monochromatic X-rays is incident on the sample. Interaction of the incident beam with the sample leads to constructive interference and a diffracted ray emerges only when Bragg's law conditions are satisfied (equation 2.2) (Patnaik, 2004). This law correlates the wavelength of electromagnetic radiation to the diffraction angle and the lattice spacing in a crystalline sample. Diffracted X-rays are then detected. As a result of random orientation in powder, scanning the sample through 2θ angles help detect all possible diffraction directions of the lattice.

$$n\lambda = 2d \times sin\theta \qquad \text{Equation 2.2}$$

where n gives the order of the diffraction, λ is the x-ray wavelength, d the spacing of the diffracting planes, and θ the angle between the incident rays and the diffracting planes.

The XRD patterns of the phosphorus and nitrogen-based polyurethane film were recorded by using a Rigaku Mini-fex diffractometer equipped with the $CuK_{\alpha 1}$ radiation (wavelength λ = 1.54056 Å) and operating voltage of 40 kV and current of 30 mA. The camera rotation speed employed was 2° min^{-1} over the 10° - 80° diffraction angle (2θ) range.

2.3.2 | Microscopic characterisation

2.3.2.1 | Optical microscopy

Light or optical microscopy is the oldest imaging technique that uses visible light and a system of lenses to magnify images of samples. The images from an optical microscope can be captured by normal light-sensitive cameras to generate a micrograph. Conventional optical microscopes have a resolution limited by the size of sub-micron particles approaching the wavelength of visible light (400-700 nm). This technique was used to observe and analyse the cell structure of the phosphorus-based polyurethane foams prepared in the study.

The physical appearance of the phosphorus-based polyurethane foams was determined with Carl Zeiss Axiocam MRC5 polarising optical microscope. The foam samples were placed

between 12-mm glass cover slips and transferred to observing the images. The photographs were taken using imager A2M digital camera.

2.3.2.2 | Scanning electron microscopy (SEM)

Scanning electron microscopy (SEM) is an imaging technique which produces images by scanning the sample surface with a focused high-energy electron beam. Interaction of electrons with atoms at sample surface generates a variety of signals revealing information about surface morphology/texture and chemical compositions. There are two modes for imaging, secondary electron imaging and back-scattered electron imaging based on depth of incident electron beam penetration into the surface it is illuminating. Secondary electrons are emitted by atoms near the surface of a specimen when bombarded with electron beam. Secondary electron imaging, being more surface sensitive, has greater resolution and provides more details regarding surface topography. As a result, secondary electron imaging mode was used to study polymer coated clay surfaces. On the other hand, back-scattered electrons are emitted from atom at much greater depth. As a result, they suffer in resolution.

The morphology of the phosphorus- and nitrogen- based polyurethane was assessed using scanning electron microscopy (SEM) on Phenom XL machine. In this experiment, a piece of polyurethane foam sample was first cut into 10×10 mm^2 and then mounted directly on to the SEM specimen slab using double-sided sticking tape. Each sample was coated at room temperature with thin layer of gold due to the non-conductivity of polyurethane (to avoid charging on exposure to the electron beam). Samples were placed into the outer vacuum chamber and vacuumed after coating with gold. They were then moved into the inner chamber and under an electron gun after the pressure was balanced between the two chambers. The surface and shape characteristics of the polyurethane samples were observed and recorded. The morphology of the cured epoxy resins at the surface of leather was assessed using scanning electron microscopy on the Hitachi (S-4500) machine by the same process.

2.3.2.3 | Atomic force microscopy

Atomic force microscopy (AFM) is a technique that enables the imaging of any type of surface, including biological samples, polymers, glass and ceramics. It is operated in two basic modes, which are the contact and tapping modes. In the contact mode, the AFM tip is in continuous contact with the surface. In contrast, in the tapping mode, the AFM cantilever is vibrated above the sample surface such that the tip is only in intermittent contact with the surface. This mode helps to reduce shear forces associated with the tip movement. The tapping

mode is the most commonly used for AFM imaging while the contact mode is usually reserved for force measurements and specific applications. The AFM is used to image and manipulate atoms and structures on a variety of surfaces. The atom at the apex of the tip senses individual atoms on the underlying surface when it forms incipient chemical bonds with each atom. Because these chemical interactions delicately alter the vibration frequency of tip, they can be detected and mapped. In addition, AFM provides a true three-dimensional surface profile.

AFM-imaging was carried out in the tapping mode under ambient conditions using a model NTEGRA Prima instrument from NT-MDT (Russia). The resonant frequency and force constant were set at 170 kHz and 5 N m^{-1}, respectively, at a scan rate of 0.5 Hz s^{-1}. The surface size of resulting square scans was in the range of 1 to 2500 μm^2.

2.3.3 | Mechanical testing

2.3.3.1 | Compressive Testing

The materials are usually subject to standards requirements regarding their mechanical performances and depending on the field of application. Compression is the most common test used to evaluate the performance of PU foams. Experimentally, an increasing compressive stress is applied to the material which is deformed. Therefore, this allows the determination the compressive strength, compressive yield strength, and modulus of elasticity. These parameters are important to estimate if the polymeric material is suited for specific applications or if it will fail under specific stress.

Compression tests of polyurethane foams were determined by using a universal testing machine from Instron model No.3369 / J 7257 (Figure 2.5). All the tests were conducted after foams were stored for 14 days at room temperature and the dimensions of the parallelepiped foam specimen were 65 mm ×18 mm ×18 mm. The force was applied in a direction parallel to the specimen and the crosshead speed was set 10 mm min^{-1} with a 1-N pre-load. Stress-strain curves were recorded, and the modulus of elasticity was determined from the slope of the linear portion of the stress–strain curve.

Figure 2.5 Universal machine for mechanical testing

2.3.3.2 | Tensile Testing

Tensile test is a destructive test process that provides information about the tensile strength, yield strength, and ductility of the material, among others. It is performed by applying a continuously increasing tensile force to the major axis of the sample until it breaks.

Tensile tests were used for coated leathers. The measures were carried out using the universal testing machine from Instron (model No.3369 / J 7257). Three dog-bone shaped samples were prepared for each composite and the force was applied in a direction parallel to the material as can be seen in the Figure 2.6. The crosshead speed was set 10 mm min^{-1} at ambient temperature with a 1-N pre-load as per ASTM D638 (Miller *et al.*, 2019). All the samples were prepared and conditioned for 24 hours before the test. The elastic modulus was determined from the slope of the linear portion the stress–strain curve. Three specimens of each sample were tested and the average reported.

Figure 2.6 Dumbbell-shaped leather specimen clamped with grips of the universal testing machine

2.3.4 | Thermal analysis

2.3.4.1 | Thermogravimetric analysis

Thermogravimetric analysis (TGA) is one of the simplest and widely used techniques to evaluate decomposition behaviour of polymeric materials. The sample is subjected to a controlled increase of temperature and the percentage mass loss as a function of temperature is measured. Decomposition under oxidative or inert conditions can be studied by selecting an appropriate purge gas i.e. air or nitrogen, respectively. TGA requires a small amount of sample between 5 and 50 mg, so it provides fundamental decomposition behaviour of polymers without bulk effects. Mass loss rate curves can be used to determine overall decomposition profiles, which can be related to decomposition kinetics, decomposition mechanism or both. TGA data is reproducible within ±1°C.

Thermogravimetric analyses (TGA) were carried out to study the thermal stability as well as the flame retardation properties of the cured formulations. The thermal degradation curves of all samples were obtained by using NETZSCH, STA 449 F3 Jupiter thermal analyser under a nitrogen atmosphere at a flow rate of 50 mL min^{-1}. The samples cut in small pieces of about 5 – 15 mg were heated in the alumina crucible from room temperature to 1000°C at the heating rate of 10 K min^{-1}. The recorded data were used to calculate some thermal parameters such as:

The ***integral procedural decomposition temperature*** (***IPDT***) yields semi-quantitative data regarding the relative thermal stabilities of the polymers. It is defined as a means of summing-up the entire shape of the normalised thermal data curve (Zohuriaan and Shokrolahi, 2004). The two major factors that influence the calculation results is the initial decomposition temperature and char yield. High values for these two factors indicate favorable thermal stability, heat resistance, and high IPDT, whereas low IPDT indicate poor overall thermal stability of polymers. The IPDT was calculated from the TGA curves obtained by using equation 2.3 (Liu *et al.*, 2019).

$$IPDT(°C) = \frac{(A_1 + A_2)^2}{A_1(A_1 + A_2 + A_3)}(T_f - T_i) + T_i \qquad \text{Equation 2.3}$$

where T_i is the initial experimental temperature and T_f the final experimental temperature. A_1, A_2 and A_3 are the areas delimited in Figure 2.7.

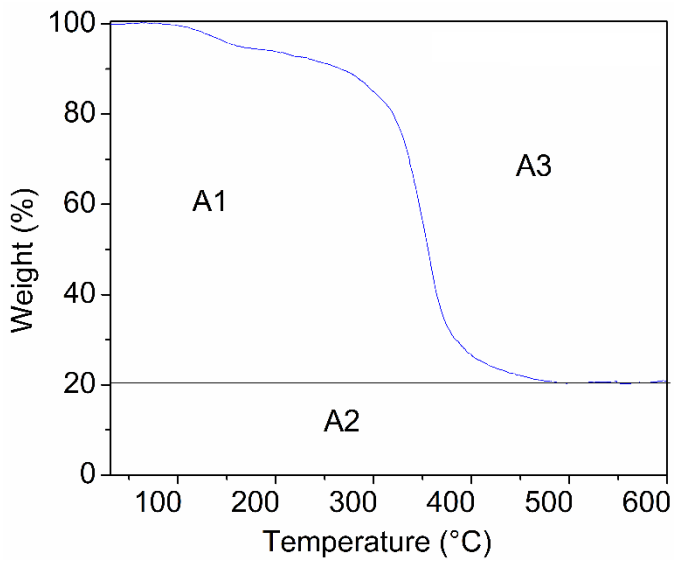

Figure 2.7 Schematic diagram of calculation of IPDT

The ***Statistic heat-resistant index temperature*** (T_s) is another parameter to assess the thermal stability of the cured polymer. It is defined as the temperature of polymer in the physical heat tolerance limit. This parameter was determined from TGA curves of the specimens using temperature at 5% mass loss (T_{d5}) and 30% mass loss (T_{d30}) in equation 2.4 (Benyahya *et al.*, 2014).

$$T_S(°C) = 0.49 \times [T_{d5} + 0.6 \times (T_{d30} - T_{d5})] \quad \text{Equation 2.4}$$

A theoretical ***limiting oxygen index*** (LOI) was calculated in accordance with the empirical formula established by Van Krevelen (1975). A numerical value represents the minimum concentration of oxygen required to just support combustion of a polymeric material in an oxygen-nitrogen mixture. Thus, higher LOI values represent better flame retardancy. LOI was deduced from TGA by the equation 2.5 (Venkatesh *et al.*, 2019).

$$LOI(\%) = 17.5 + 0.4 \times CR \quad \text{Equation 2.5}$$

where CR is the char residue in char yield mass percentage (%).

The correlation between TGA and LOI is not valid for halogen-containing polymers since halogen radicals inhibit combustion. Based on values of LOI, materials are generally considered:

- flammable for LOI < 20.95,
- marginally stable for 20.95 < LOI < 21, or
- slow burning for 21 < LOI < 28.

So, a high LOI value means generally safer material from the point of view of fire resistance (Nelson, 2001).

Kinetic parameters during the thermal degradation

TGA experiments were used to determine kinetic parameters of the thermal degradation of polymers. During isothermal decomposition the rate of decomposition of the materials is proportional to the concentration of non-degraded materials. Combining the rate of conversion (equation 2.6) and the Arrhenius equation (equation 2.7), a basic expression (equation 2.8) was obtained then integrated by using different approximation treatments.

$$\frac{d\alpha}{dt} = Q(\frac{d\alpha}{dT}) = K(T).f(\alpha) \qquad \text{Equation 2.6}$$

$$K(T) = A\exp(\frac{-E_a}{RT}) \qquad \text{Equation 2.7}$$

$$\frac{d\alpha}{dt} = f(\alpha)A\exp(\frac{-E_a}{RT}) \qquad \text{Equation 2.8}$$

where d(α)/dt is the rate of reaction; Q the heating rate; K(T) the rate constant; α is the reacted fraction at the time t; f(α) a function of α depending on the reaction mechanism; A the pre-exponential factor; E_a the activation energy; R the universal gas constant and T the temperature of decomposition.

The activation energy was predicted by different approaches by using the Broido model (Broido, 1969), Horowitz–Metzger model (Horowitz and Metzger, 1963), and Coats–Redfern model (Coats and Redfern, 1964).

(i) Based on the assumption that the thermal decomposition is a first order reaction, integrated expression from the Broido model is:

$$\ln(\ln(\alpha)) = \frac{-E_a}{RT} + Constant \qquad \text{Equation 2.9}$$

$$\text{with} \quad \alpha = \frac{W_i - W_f}{W_t - W_f} \qquad \text{Equation 2.10}$$

where W_i is the initial mass; W_t the mass at time t; and W_f is the final total mass after degradation.

The activation energy was obtained from the slope of the straight line $\ln(\ln(\alpha))$ versus $\frac{1}{T}$.

(ii) Horowitz–Metzger approximation method for the calculation of the activation energy of polymeric substances when the reaction order is equal to 1 is given by the following expression:

$$\ln(\ln(\alpha)) = \frac{E_a(T - T_{\max})}{RT_{\max}^2} \quad \text{Equation 2.11}$$

$$\text{with} \quad \alpha = \frac{W_i}{W_t} \quad \text{Equation 2.12}$$

where T_{max} is the peak temperature and T is the temperature at particular mass loss.

From the Horowitz–Metzger model, the activation energy was obtained from the slope of the straight line of $\ln(\ln(\alpha))\,\text{versus}(T - T_{\max})$.

(iii) Coats–Redfern integral method is used to express the decomposition process and can be better than other methods because it shows the best linearity of the data. If the reaction is a first order, the expression of the decomposition process is:

$$\ln\left[\frac{-\ln(1-\alpha)}{T^2}\right] = \ln\left[\frac{AR}{\beta E_a}\left(1 - \frac{2RT}{E_a}\right)\right] - \frac{E_a}{RT} \quad \text{Equation 2.13}$$

$$\text{with} \quad \alpha = \frac{W_i - W_t}{W_i - W_f} \quad \text{Equation 2.14}$$

where β is the heating rate (K min^{-1}).

The activation energy was obtained from the slope of the straight line of $\ln\left[\frac{-\ln(1-\alpha)}{T^2}\right]\text{versus}\frac{1}{T}$

2.3.4.2 | Differential scanning calorimetry

Differential scanning calorimetry (DSC) is a technique in which the heat flux of a specimen is monitored against temperature in a controlled atmosphere. In practice, the difference in heat flux between a pan containing the specimen and an empty pan is monitored. DSC is a common technique to measure the glass transition temperature (T_g) which is an important parameter for polymer characterisation. The glass transition represents the temperature region at which the amorphous phase of a polymer is transformed from a brittle, glassy material into a tough rubber-like liquid. In DSC, the glass transition appears as a step transition and not a peak such as might be seen with a melt transition (Saldivar and Vivaldo, 2013).

DSC analyses of polyurethane samples were carried out on NETZSCH DSC 214 Polyma instrument within the temperature range of 0°C to 220°C at a heating rate of 5 K min^{-1}. The sample (5 – 12 mg) was crimped in an aluminum pan and heated under nitrogen atmosphere at a purge rate of 50 mL min^{-1}. Meanwhile, DSC analyses of phosphorus-based epoxy samples

were performed with a calorimeter DSC1 from Mettler Toledo within the temperature range of 20°C to 150°C at a heating rate of 5 K min^{-1}.

2.3.5 | Flame retardancy tests

Flammability defines the ease of a material to ignite, the intensity with which it burns, and releases heat once ignited. Flammability tests can be classified into three groups (Kim, 2012):

- Official tests for official requirements: The most important official test is the cone calorimeter, which provides most of the combustion characteristics such as ease of ignition, rate of mass loss, rate of smoke release and yield of smoke, among others. Other official flammability tests are radiant heat panel test providing flame spread index, and smoke chamber test providing smoke density.
- Laboratory tests for product development: They are solicited to adjust formula or product design when the official tests are not feasible in terms of time and cost. The most common laboratory tests are the oxygen index analysis, the vertical burn test and horizontal burn test.
- Full scale tests for simulating actual use condition: They are used to determine the performance under actual combustion situation, which may be speculated based on the results from the official and laboratory tests.

In this work, laboratory tests were done to assess the flammability of different resulting polymeric materials by oxygen index analyses and vertical flammability tests.

2.3.5.1 | Oxygen index analysis

Oxygen index analysis describes the tendency of a material to sustain a flame. The technique is widely used to evaluate flammability of polymeric materials. Limiting oxygen index (LOI) is defined as the minimum concentration of oxygen in a mixture of oxygen and nitrogen that either maintains flame of a material for three minutes or consumes a length of 5 cm of a sample (Elbasuney, 2017). It is expressed as presented in equation 2.15.

$$LOI(\%) = 100 \times \frac{[O_2]}{[O_2]+[N_2]} \qquad \text{Equation 2.15}$$

where $[O_2]$ and $[N_2]$ are the concentrations of oxygen and nitrogen respectively. LOI value is suitable as a semi-qualitative indicator of the effectiveness of flame retardants during research and development stage, because the equipment is inexpensive and the sample size is small. It

is useful to ascribe materials into experimentally meaningful groups based on their LOI value. Since air contains about 20.95% oxygen and the LOI value of any material is less than this, it will burn easily in air. So, 20.95% is considered as a threshold value to classify materials. According to literature, classification of the materials based on LOI can be made as shown in Table 2.IV (Nelson, 2001).

Table 2.IV Classification based on LOI values

LOI value	Class
LOI < 20.95	Flammable
20.95 < LOI < 21	Marginally stable
21 < LOI < 28	Slow-burning
28 < LOI < 100	Self-extinguishing and intrinsically non-flammable

LOI measurements of all the samples were conducted on an oxygen index tester model CSI-178 (Figure 2.8(a)) from Custom Scientific Instruments Inc (India) according to ASTM D 2863 (Chang *et al*., 2011). Briefly, the sample was vertically placed in a transparent test column in a controlled atmosphere and its top inflamed with a burner. The oxygen concentration was adjusted until the sample supported sustained burning.

2.3.5.2 | Vertical flammability test

The vertical flammability test is designed to study and assess the flame retardation properties of polymeric materials. During the test, the vertical position of material allows the flame to spread faster due to hot air which rises. Depending of process, some parameters like ignition time, and char length can be measured.

In this study, the vertical flammability test was replicated four times for each sample. The flammability test device (Figure 2.8(b)) was equipped with a Bunsen burner fitted vertically, and the flame height was 38 mm. The test specimen measuring about 125 × 10 × 2 mm^3 was held vertical and the axis of the burner was kept below the edge of the specimen. The burner end was kept 40 mm away from the lower end of the specimen. A blue coloured flame from a liquefied petroleum gas (LPG) was made to ignite the specimen. The time taken for the specimen to be ignited was recorded.

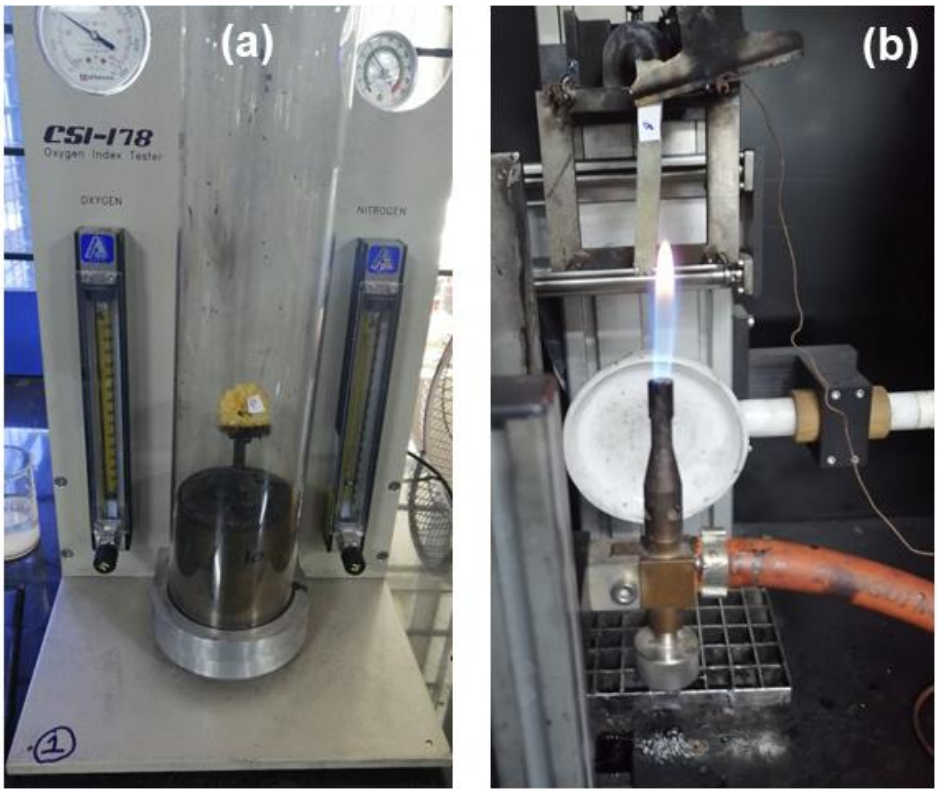

Figure 2.8 Oxygen index tester (a) and vertical flammability test device (b)

2.3.6 | Other characterisations

2.3.6.1 | Density measurement

The apparent density (ρ_a) of the phosphorus-based polyurethane foam was calculated according to equation 2.16 by determining the apparent volume from the cylindrical dimensions of foam and measuring the mass of the foam samples.

$$\rho_a = \frac{m_{foam}}{V_{foam}} \qquad \text{Equation 2.16}$$

where m_{foam} and V_{foam} are the mass and volume of flexible foam sample respectively. Four specimens were tested for each foam and the average density with standard deviation was reported.

The relative density (ρ_{rel}) is an expression of the solid fraction. It is defined by the ratio of the foam apparent density ρ_a to the solid density ρ_s (equation 2.17).

$$\rho_{rel} = \frac{\rho_a}{\rho_s} \qquad \text{Equation 2.17}$$

where ρ_a and ρ_s are the apparent density of flexible foam sample and solid density respectively. The solid density value was estimated by calculation, considering the density of the different

components of the flexible polyurethane foam and their proportions, which is in the density range of flexible foam density reported in the literature (Rampf *et al.*, 2012).

Porosity is defined as the pore fraction of the flexible foam and is usually expressed as a percentage. The percentage porosity was determined using equation 2.18.

$$\%Porosity = 100 \times \frac{\rho_s - \rho_a}{\rho_s} \qquad \text{Equation 2.18}$$

2.3.6.2 | Contact angle study

The contact angle measures the wettability of a material. If a water drop has a tendency to stick to itself more than it sticks to a given surface, then that surface is called hydrophobic and the water drop will bead up with a contact angle greater than 90°. Conversely, if a water drop tends to stick more to a given surface than it sticks to itself, that surface is called hydrophilic; the drop will have a contact angle of less than 90° (Simpson *et al.*, 2015). Figure 2.9 shows a water drop on a flat surface exhibiting different contact angle values.

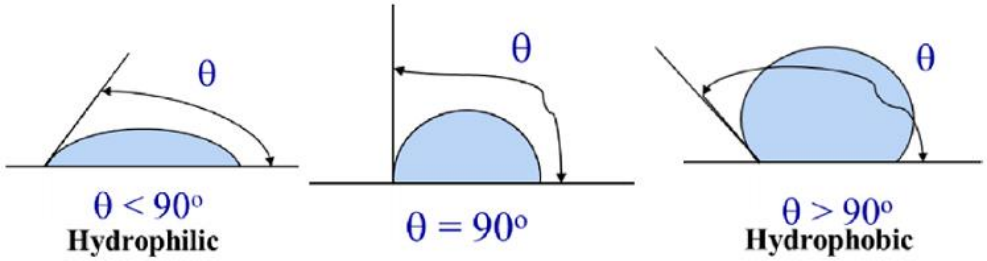

Figure 2.9 Contact angle of hydrophilic and hydrophobic surfaces (Simpson *et al.*, 2015)

A small amount of sample (10–15 mg) was dissolved in 500 µL of dimethyl formamide. Then, the mixture was poured on the glass plate 1 cm × 1 cm and dried at 80°C for 4 hours. Contact angle measurements were conducted at room temperature using the sessile drop method on a contact angle measuring system (Holmarc Model No. HO-IAD-Cam-01B). A droplet of distillated water (5 µL) was placed on the surface using a syringe, then digital images of the droplet silhouette were captured with a charge-coupled device camera. Water contact angles were evaluated using the measuring angle method. Reported values are an average of three values obtained for each sample.

Chapter 3: Results and Discussion

New organic-inorganic hybrid monomers were synthesised with the aim to produce polyurethane foams and epoxy products with improved resistance to fire and reduced ecological impact. The synthesised products were characterised to elucidate their physico-chemical and mechanical properties and fire performances according to the experimental methods described in the previous chapter. The results and discussions are herein presented. The chapter is sub-divided into four main sections: phosphorus-based polyurethane foams, phosphorus- and nitrogen-based polyurethanes, phosphorus-based epoxy/clay nanocomposites, and ecological aspects of resulting materials.

3.1 | Phosphorus-based polyurethane foams

This part of study assess the proprieties of the flexible polyurethane foams obtained from the dispersion of specific phosphorus-based flame retardants, displaying the role of phosphorus-containing polyols. In this section, a series of three reactive phosphorus-containing monomers, namely tris-(5-hydroxypentyl) phosphate, tris-(4-hydroxybutyl) phosphate, tris-(3-hydroxypropyl) phosphate, were synthesised and their chemical structure was studied by FT-IR and NMR (^{1}H, ^{13}C, and ^{31}P). These monomers were used for the synthesis of PU foams. The morphology, mechanical properties, thermal stability, and reaction to fire of the foams were evaluated by optical microscopy, compressive strength, thermogravimetric analysis, limiting oxygen index and vertical burning.

3.1.1 | Characterisation of phosphorus-containing monomers

The phosphorus-containing reactive monomers were synthesised according to the reaction scheme shown in Figure 2.1. The general chemical structures expected for the monomers are presented in Figure 3.1. Alcohols with various chain lengths from propyl to pentyl were tested.

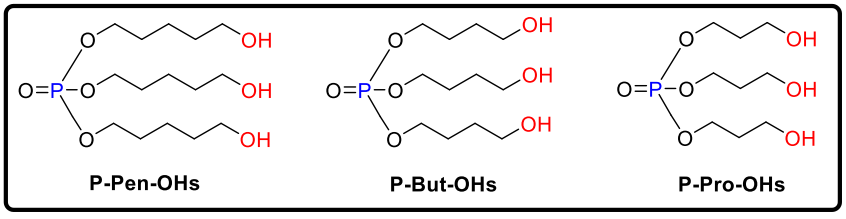

Figure 3.1 General chemical structures of the phosphorus-containing reactive monomers

3.1.1.1 | FT-IR characterisation

The phosphorus-containing monomers obtained for each synthesis P-Pro-OHs, P-But-OHs,

and P-Pen-OHs were characterised by FT-IR. The spectra are shown in Figure 3.2. The main functional groups in the structure of the synthesised monomers are directly identified on the spectra (Figure 3.2). The absorption band at around 3365 cm^{-1} was attributed to the stretching vibration of the hydroxyl (–OH) groups. This band has contribution of hydroxyl groups of the monomers, self-hydrogen bound-hydroxyl groups, water, and hydroxyl group hydrogen-bound with water. The high intensity of the band of hydroxyl groups revealed the presence of a considerable amount of hydroxyl groups and consequently, the polyol nature of the synthesised chemicals. The peak at 2950 cm^{-1} was assigned to symmetric and asymmetric stretching of aliphatic C–H and the peaks at 1470, 1392 and 804 cm^{-1} to the deformation vibrations C–H groups. The C-H groups belong to the methylene groups of propyl, butyl and pentyl fragments in the monomers. The absorption band at around 1015-1030 cm^{-1}, assigned to the asymmetric stretching vibration of the P–O–C group, revealed the formation of chemical bonds P–O during the reaction, as expected. The absorption band near 1230 cm^{-1}, attributed to the stretching vibration of the P=O group, also confirmed the presence of phosphorus (Gu *et al*., 2015).

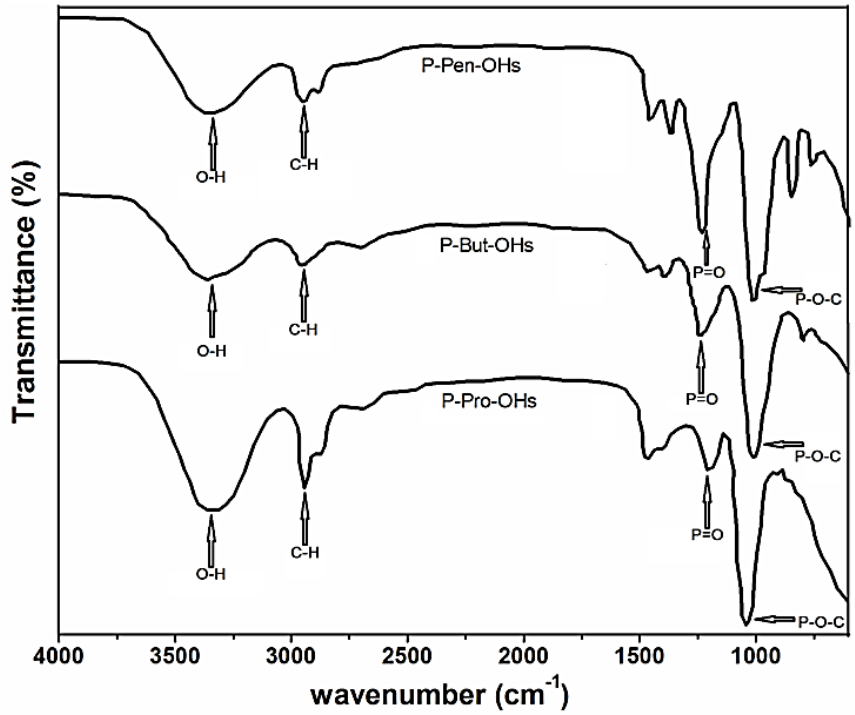

Figure 3.2 FT-IR spectra of different hydroxyl precursors (P-OHs)

3.1.1.2 | NMR characterisation

The chemical structures of phosphorus-containing monomers P-OHs were confirmed by ^{1}H-NMR, ^{13}C-NMR, and ^{31}P-NMR. ^{1}H-NMR spectra of the synthesised P-OHs are shown in Figure 3.3. The signal peak at 4.7 ppm was attributed to the protons of the alcohol group (-

OH), which confirmed that the P-OHs are phosphorus-containing (Rao *et al*., 2018a). The peaks at 4.2 ppm were assigned to the protons of the methylene group linked to phosphate group. The peaks at 3.7 ppm were assigned to protons of the methylene groups bearing the hydroxyl groups, while the peaks between 1 and 2 ppm corresponded to the methylene groups in the middle of the alkyl chains. The evidence of substitution of chlorine atoms is further visible in Figure 3.4. ^{13}C-NMR spectra show the resonance peaks around 64 ppm assigned to the carbon atom of methylene group linked to phosphate group. The assignment of all the chemical shifts observed on the ^{13}C-NMR spectra is shown in Figure 3.4(a). In addition, the peak at around -9.5 ppm was assigned to the phosphorus element in the ^{31}P-NMR spectra labelled for P-OHs in the Figure 3.4(b). The ^{1}H-NMR spectra agreed with the proposed chemical structures of the synthesised phosphorus compounds. The results indicate the successful syntheses of phosphorus-containing precursors by substituting chlorine atoms.

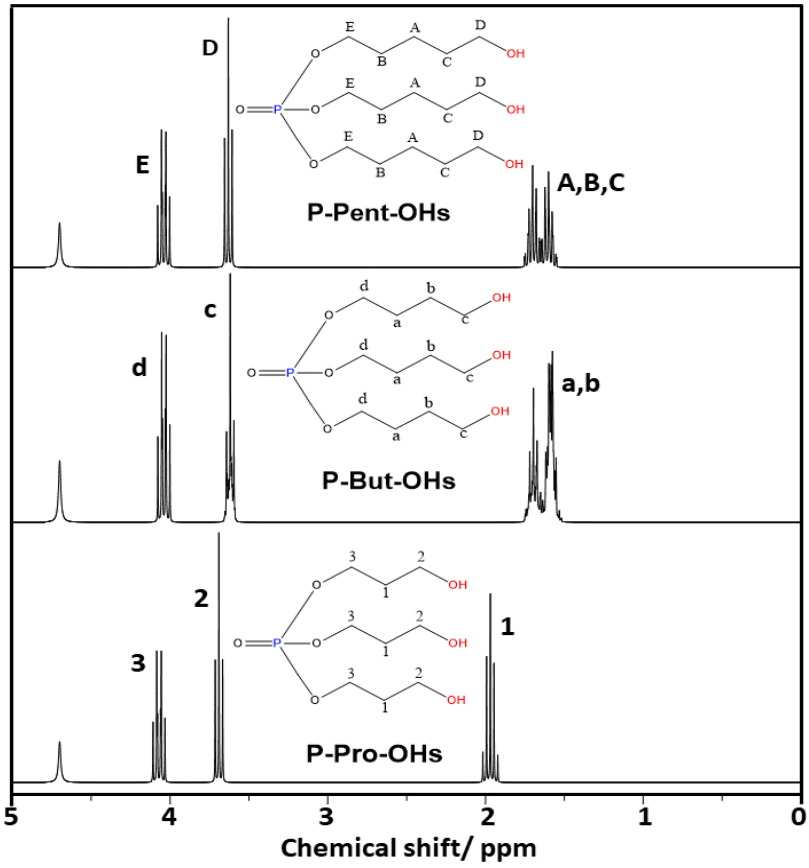

Figure 3.3 ^{1}H-NMR spectra of different phosphorus-containing polyols in $CDCl_3$

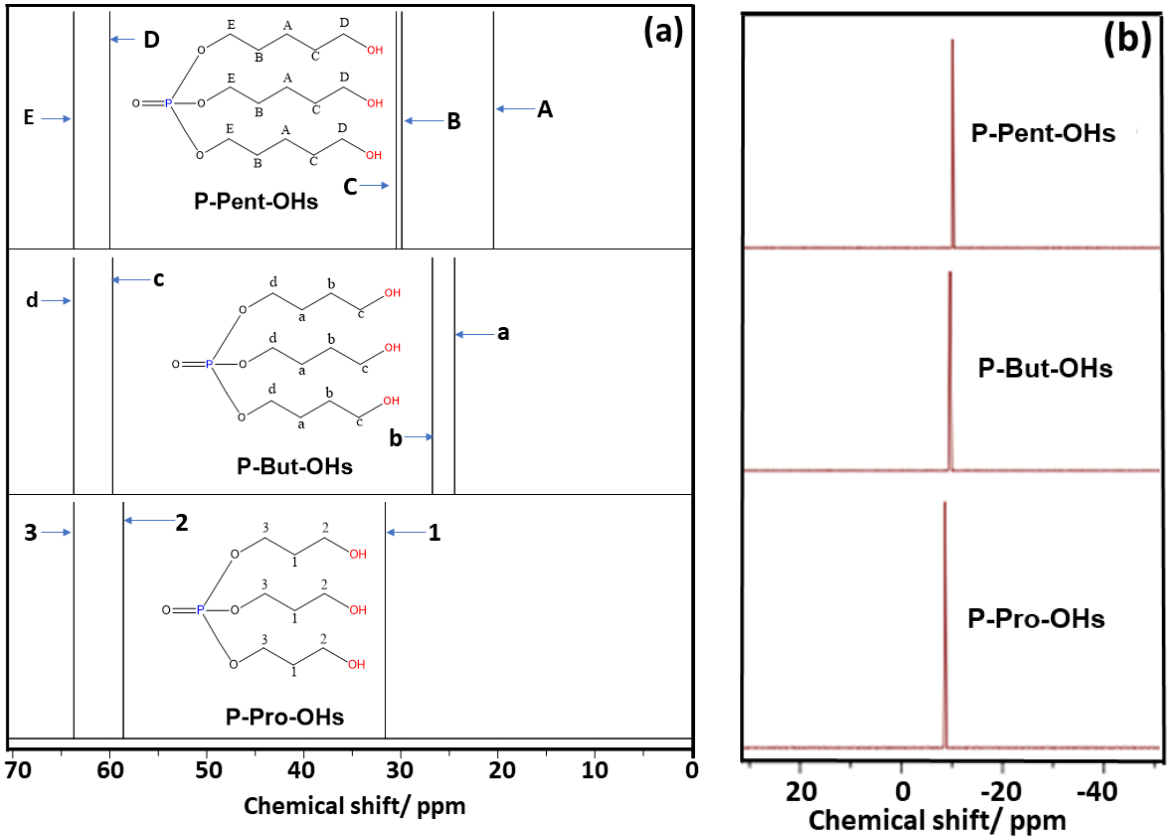

Figure 3.4 ^{13}C-NMR(a) and ^{31}P-NMR(b) spectra of phosphorus-containing polyols in $CDCl_3$

3.1.2 | Characterisation of phosphorus-based polyurethane foams

PU foams were synthesised using the phosphorus-containing polyol monomers, polyethylene glycol and toluene diisocyanate as the main ingredients.

3.1.2.1 | Visual appearance

Figure 3.5 shows the visual appearance of phosphorus-based polyurethane foam samples.

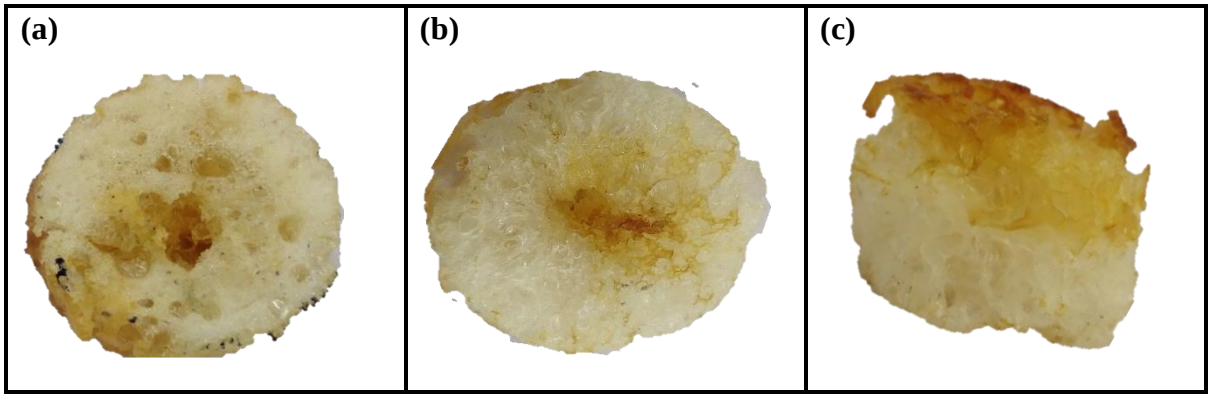

Figure 3.5 Photographs showing the appearance of the PU foams prepared with the phosphorus-containing monomers (a) P-Pen-OHs, (b) P-But-OHs and (c) P-Pro-OHs

The macrostructure of the products appeared porous with some surface defects. Foams usually consist of an arrangement of cells and cell voids with a honey-comb-like structure. Figure 3.6 shows the optical microscopic observation of the products. In this study, the morphology of phosphorus-based polyurethane foams was conserved by changing the polyol chemical structure. The cell structure of the polyurethane foam includes elements such as cell windows, struts, and strut joints (Gama *et al.*, 2018; Suhailuddin *et al.*, 2022).

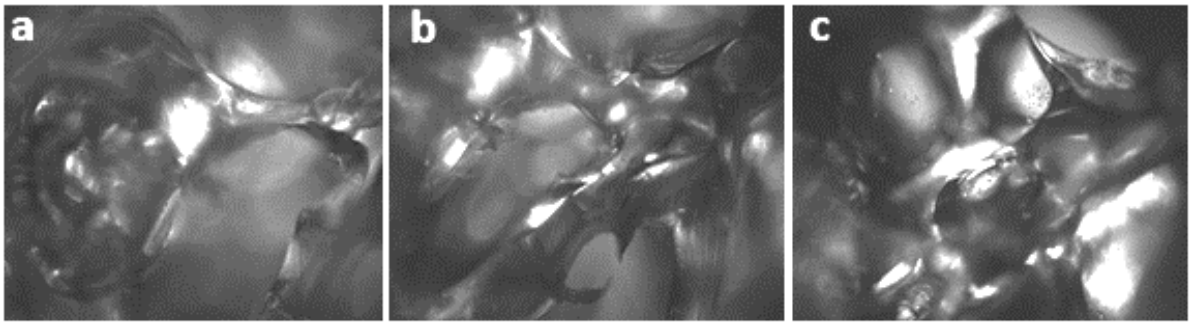

Figure 3.6 Optical microscopic images of phosphorus-based PU foams prepared with the phosphorus-containing monomers (a) P-Pen-OHs, (b) P-But-OHs and (c) P-Pen-OHs

3.1.2.2 | Density and morphology of flexible polyurethane foam

The polyurethane foam density is an essential factor that affects the flammability of polyurethane foams. It is considered that higher density foams perform better during contact with the flame (Chen *et al.*, 2014). Table 3.I shows the apparent and relative densities of different polyurethane foam samples. The densities are in the range of 0.23 - 0.43 g cm^{-3} and decrease when the chain length of the alkyl groups in the P-OHs monomers increases. The apparent density decreases in the order P-Pro-OHs, P-But-OHs and P-Pen-OHs. The shorter the chain length of the alkyl groups, the lower the density of the products. Meanwhile, the densities of commercial polyol based polyurethane foams were found in the range from 0.020 to 0.045 g cm^{-3} (Nikje *et al.*, 2011). These highest densities were influenced by the nature of hydroxyl precursors. P-Pro-OHs based polyurethane foam can be considered as microcellular elastomers due to the fact that their density values exceed 0.4 g cm^{-3} (Gama *et al.*, 2018).

The results of porosity are also summarised in Table 3.I. The porosity was high and decreased logically with the density of the foams. An increase of the density corresponds to a decrease of pore volume due to the reduction of voids in the foam. The density affects the properties of foams such as reaction to fire, sound absorption and mechanical performances. Nadafan *et al*. (2020) showed that the polyurethane foams with high porosity were good sound absorbers. P-Pen-OHs polyurethane foam is a better sound absorber than that P-But-OHs and

P-Pro-OHs foams due to the higher porosity (80%). Thus, it is clear that the carbon chain length of phosphorus-containing polyol affects the foaming system.

Table 3.I Densities and mechanical properties of polyurethane foams

P-OHs based polyurethane samples	Density of polyurethane foams			Compressive strength data	
	Apparent density /g cm^{-3}	Relative density	Porosity /%	Hardness /kPa	Young's modulus /kPa
P-Pen-OHs	0.24±0.04	0.20±0.04	80±4	74±25	84±30
P-but-OHs	0.37±0.03	0.32±0.03	68±2	97±33	167±70
P-Pro-OHs	0.43±0.03	0.36±0.03	64±3	114±49	125±50

In addition, polyurethane foam morphology is a critical parameter that influences the fire behaviour of polyurethane foam. The porous structure of the polyurethane foam allows the oxygen to diffuse easily into the polyurethane and speeds up the ignition process. Consequently, P-Pro-OHs based polyurethane foam could have better fire properties than P-But-OHs and P-Pen-OHs based polyurethane foam.

3.1.2.3 | Compressive strength

The mechanical properties of phosphorus-based polyurethane foams were evaluated by compression tests. The compressive stress-strain curves of phosphorus-based polyurethane foams are shown in Figure 3.7. The hardness value and Young's modulus are reported in Table 3.I. All foam samples were compressed up to 70% strain values which showed a flexible character of the resulting polymers. The stress-strain curves of the foams exhibit three main distinct regions including an elastic deformation region (stage I), a flattening region (stage II), and a densified region (stage III). This phenomenon is in agreement with the results reported by Li *et al.* (2019). These authors indicated that the initial linear zone primarily arises from the bending of cell struts. The elastic deformation stage occurred when the strain was 0–13%. In this stage, strain energy is stored in reversible bending and buckling of the struts, and it is followed by the flattening stage where the cell walls of the foam are deformed, and struts begin to impinge upon each other (Rampf *et al.*, 2012). The flattening region is one of the advantages of the flexible foam because the foam can absorb kinetic energy while limiting the stress transmitted to relatively low levels, which is important for crash protection (in helmets for example) (Esteves *et al*., 2017). The final densification zone begins at around 44% to 70% strain in which the cell walls are crushed. In this region, the polyurethane foam becomes a solid material for such the cells start hitting each other, causing a brusque increase in internal compression stiffness of the whole cellular network (Moghim *et al*., 2019).

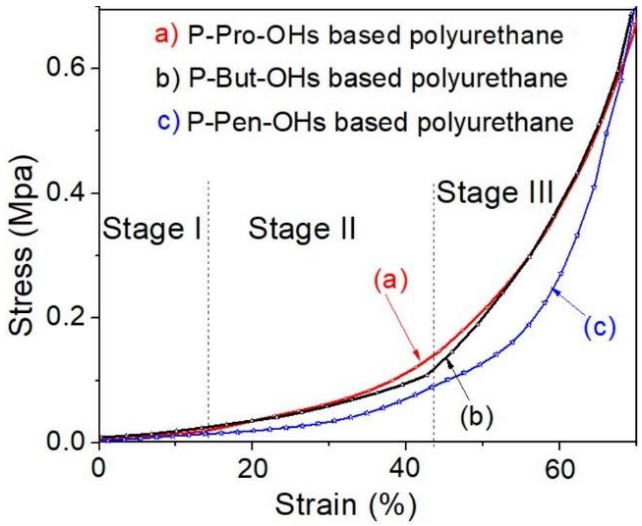

Figure 3.7 Stress–strain curves of different phosphorus-based polyurethane foams

The hardness values reported in Table 3.I correspond to the force required to compress the foam to 40% of its height (Prociak *et al.*, 2018). The hardness values decrease in the order P-Pro-OHs, P-But-OHs, and P-Pent-OHs for the polyurethane foams. Furthermore, the compressive properties of phosphorus-based polyurethane foams were proportional to their relative density. The hardness value increases with the relative density of the foam. However, it can be noted that the synthesised phosphorus-based polyurethane foams have compressive strengths lower than conventional commercial flexible polyurethane foams, which can have compressive strength at 10% strain around 100 kPa (Esteves *et al*., 2017).

The Young's moduli of foams correspond to the compression moduli of elasticity; they were measured in compression during the elastic deformation. The elastic region of deformation was found to be different for compression. Specifically, the use of P-But-OHs showed the best compressive properties of elastic phosphorus-based polyurethane foam. Its Young's modulus was found to be 167 kPa, which is double the value obtained with P-Pent-OHs. There is no direct identifiable relationship between Young's modulus and porosity/hardness. This result does not indicate a linear relationship between Young's moduli and density (Moghim *et al*., 2019).

3.1.2.3 | Thermogravimetric analyses

The thermal stability of the polyurethane foams was studied by TGA. The TGA curves are shown in Figure 3.8. The three materials showed comparable thermal behaviour. As can be seen from the differential thermogravimetric (DTG) curves of polyurethane foams (Figure 3.8(b)), the thermal degradation of foams proceeded via three main stages. The first stage,

appearing from 90° to 180°C with a DTG peak at 132.5°C was attributed to loss of moisture and small volatile compounds entrapped in closed cells. Polyurethane compounds contain polar urethane groups which can fix water through hydrogen bonding. Small molecules such as unreacted monomers and catalyst entrapped in the microstructure of the polymers can also be released. The second decomposition stage from 230° to 320°C and corresponding to peak with maximum 281°C was ascribed to the decomposition of hard segments composed of aromatic cycles deriving from toluene diisocyanate. This leads to depolymerisation reactions causing cleavage of urethane bonds (Chan *et al.*, 2022). Then, the third stage from 320° to 480°C with a DTG peak centralised at 352°C, was attributed to the degradation of soft segments and remaining polyol chains. The thermal degradation process of the polyurethane foams is in agreement with the previous work of Wei *et al*. (2017) who prepared polyurethane foams by modifying the quantity of water (used as a blowing agent). The authors showed that the thermal degradation process of the polyurethane foams occurred by decomposition because of the chain rupture at random points along the chain, giving a disperse mixture of fragments.

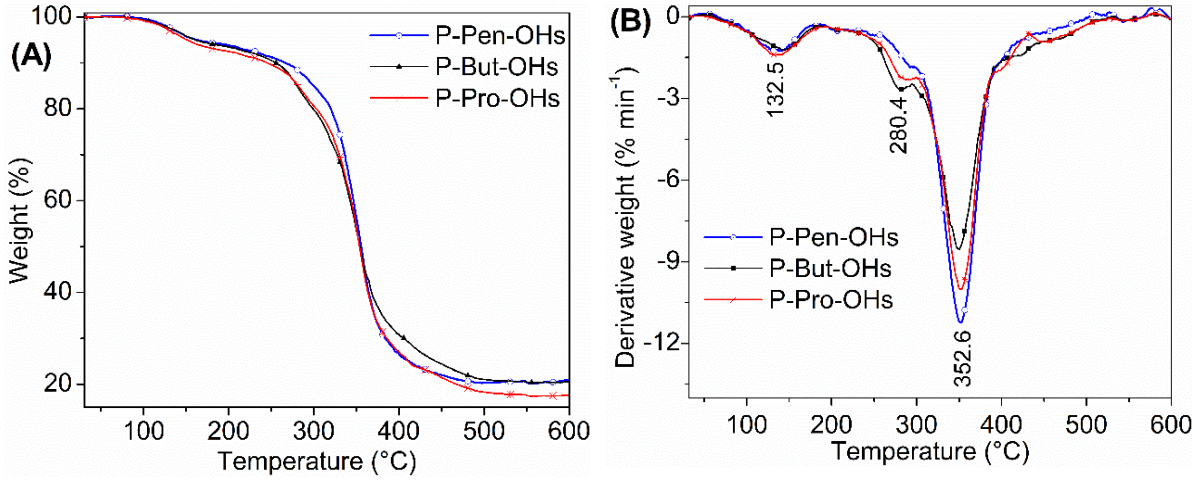

Figure 3.8 TGA (A) and DTG (B) curves of different phosphorus-based polyurethane foams under N_2 atmosphere

Table 3.II summarises the results of the selected parameters determined from Figure 3.8(A) during the thermal decomposition of different phosphorus-based polyurethane foams such as temperature at 5% mass loss (T_5), the temperature at 30% mass loss (T_{30}), char yield at 600°C, and maximum degradation temperature (T_{max}). T_{max} represents the temperature at which the highest thermal decomposition rate is recorded. The residue yield at 600°C varies from 17.06 to 20.9%, with the highest value corresponding to P-Pen-OHs-based polyurethane due to the highest carbon content. These residue yield values indicate that polyurethane foam samples

exhibit good thermal behaviour up to 600°C. The temperature corresponding to 5% mass loss is considered to be the initial temperature of the sample decomposition process (Yasmin *et al*., 2006; Liu *et al*., 2019). All the foams showed low T_5 values 151°-161°C, which are due to the high moisture content and volatile compounds entrapped in closed cells.

Table 3.II TGA data of thermal degradation of phosphorus-based polyurethane foams

Polyurethane samples	T_5 /°C	T_{30} /°C	T_s /°C	T_{max} /°C	IPDT /°C	Residue yield at 600°C / %	T_g /°C
P-Pen-OHs	161.3	336.1	130.4	352.6	276.5	20.9	70.8
P-But-OHs	160.3	328.3	127.9	349.6	286.2	20.5	58.8
P-Pro-OHs	151.2	330.6	126.8	352.6	255.1	17.6	65.9

T_g is the glass transition temperature; IPDT is the integral procedural decomposition temperature

The thermal stability was estimated by calculating the statistic heat-resistant index temperature (T_s) with equation 2.4 (Paraskar *et al*., 2020). This parameter was used to determine the thermal stability of the cured polymeric materials, and their value was determined from the temperatures at 5% mass loss and 30% mass loss of the sample obtained from the thermogravimetric analyses. The T_s values of the foams are listed in Table 3.II. The foams prepared from P-Pro-OHs and P-But-OHs displayed a lower statistic heat-resistant index than their homologue from P-Pen-OHs. P-Pen-OHs-based polyurethane foam was most thermally stable. Before any decomposition stage, the thermal stability of the foams is slightly linked to their porosity. Contrary to T_s, the integral procedural decomposition temperature (IPDT) takes into account the whole thermal degradation process and yield semi-quantitative data recording the relative thermal stabilities (Zohuriaan *et al*., 2004; Liu *et al*., 2019). As shown in Table 3.II, all the polyurethane foams exhibited IPDT values above 250°C, confirming the good thermal stability of foams. The IPDT values were in the temperature range of 30° to 600°C; polyurethane systems from P-But-OHs were most thermally stable. The foams exhibited the same behaviour attributable to the higher decomposition resistance of phosphorus-containing polyols at high temperatures (Lewin and Weil, 2001).

3.1.2.4 | Differential scanning calorimetry

DSC analyses were carried out to study the heat transition of the polyurethane foams. DSC curves of phosphorus-based polyurethane foams are presented in Figure 3.9. The curves showed that the glass transition temperature (T_g) of the foams obtained from P-Pen-OHs, P-But-OHs, P-Pro-OHs were 70.8°, 58.8°, 65.9°C respectively. These results agreed with the hypothesis of Hatakeyama *et al*. (2013), that the T_g of polyurethane foams is affected by such

factors as crosslinking density which is mainly expressed as NCO/OH ratio, monomer content, mixing time, reaction times and molecular mass of hard segments. Although the T_g of the polyurethane foams differed from each other, they were in agreement with the values reported in literature (Hatakeyama *et al.*, 2013; Wei *et al.*, 2017).

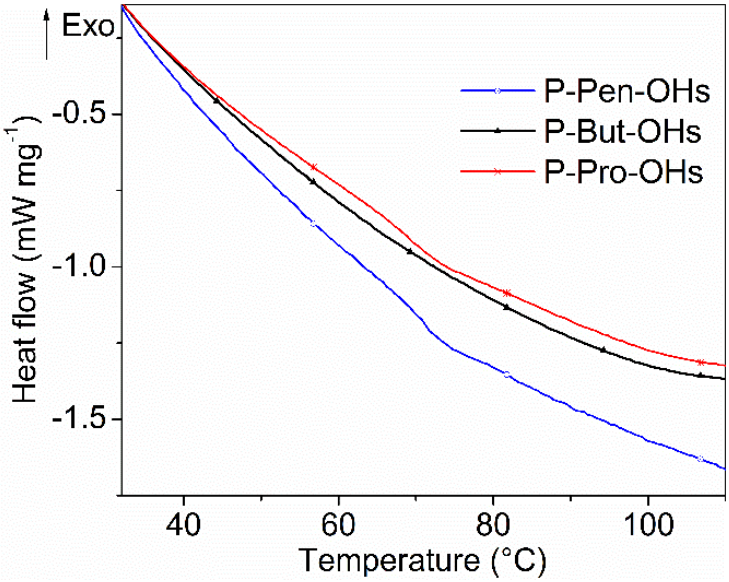

Figure 3.9 DSC curves of different phosphorus-based polyurethane foams under N_2 atmosphere

In this study, polyethylene glycol displayed a double role during the foaming process, namely, chain extender and plasticiser. The second role improved the mobility of the polymer chains, consequently influencing the T_g values of polyurethane foams (Pavličević *et al.*, 2013; Tai *et al.*, 2017).

3.1.2.5 | Limiting oxygen index tests

The reaction to fire of the polyurethane foams were studied by using the limiting oxygen index (LOI) test which is a commonly used method to study the flame-retardant properties of polymeric materials. Thus, higher LOI values illustrated better flame retardancy. Depending on LOI values, polymeric materials are generally considered as flammable (LOI < 20.95), slow-burning (LOI < 28.0), and self-extinguishing and intrinsically non-flammable (28 < LOI) (Nelson, 2001). Table 3.III lists the LOI values of the phosphorus-based polyurethane foam samples. Using P-Pen-OHs, or P-But-OHs as the flame retardant provided foams with LOI of 24.2; the use of P-Pro-OHs as flame retardants provided foam with LOI of 24.8. All the phosphorus-based polyurethane foams prepared in this section therefore fell into the category of slow-burning materials. Virgin polyurethane foam without flame retardants has an LOI value

below 20% (Yang *et al*., 2019; Zhou *et al*., 2020). The results showed that the phosphorus-containing polyols strengthened the combustion resistance of flexible polyurethane foam. During thermal degradation, the phosphorus flame retardant acted in the condensed phase by forming the poly(phosphoric acid), which promoted char formation. It covered the surface, further hindering the thermal oxidation of the char layer (Kausar *et al*., 2016).

There was no significant difference between the LOI values of the PU foams, which seemed to indicate little influence of density and porosity on fire performance. The use of reactive phosphorus-hydroxyl precursors for improving the flame retardation properties of the polyurethane foams is another proof confirming the high efficiency of the phosphorus-based flame retardants. As other illustrations of the high efficiency of the phosphorus-based flame retardants, Zhou *et al*. (2020) synthesised a liquid phosphorus-containing flame retardant named bis((dimethoxyphosphoryl)methyl) phenyl phosphate. When it has been incorporated into foam, the resulting polyurethane foam had a LOI with the maximum value of 23.0%. Rao *et al*. (2018a) synthesised a phosphorus-containing polyol by reacting with phenylphosphonic dichloride and ethylene glycol, and obtained LOI values of 23% for polyurethane foam filled with this compound. In addition, Chen *et al*. (2014) prepared phosphoryl trimethanol and showed that after their incorporation into polyurethane foams, the LOI value reached 22.5%.

3.1.2.6 | Vertical flammability

The ignition time of the PU foams was determined using vertical flammability tests. The ignition time can be defined as the time required to ignite a specimen subjected to a flame. It is an important flame retardant parameter for polymeric materials. A material with better flame resistance exhibits a longer ignition time (Rao *et al*. 2018b). Table 3.III summarises the ignition time of the different polyurethane foams.

Table 3.III Flame retardation parameters of phosphorus-based polyurethane foams

Polyurethane sample	LOI /%	Ignition time /s
P-Pen-OHs	24.2 ± 0.5	7.3 ± 0.5
P-But-OHs	24.2 ± 0.5	7.3 ± 0.5
P-Pro-OHs	24.8 ± 0.5	7.7 ± 0.5

The ignition time for each foam sample was in the range of 7-8 s. These values agree with results reported by Rao *et al*. (2018b), who studied the incorporation of a reactive liquid phosphorus-containing polyol into polyurethane foam and provided the foams with the ignition time values between 4-6 s. Because of the cellular structure of foams and the high flammability

of the soft segments, their ignition times were relatively short compared to monomeric diphenylmethane diisocyanate-based polyurethane foams with ignition times in the range of 7 to 16 s (Höhne *et al*., 2018). The phosphorus-based flexible polyurethane foams owe their performance to the excellent compatibility of all its components. In addition, the phosphorus present in the backbone structure acts by lowering decomposition temperature through dehydration reaction, which drastically inhibits the spreading of the flame from burner to polyurethane foam.

It is shown that the new phosphorus-based polyols can be efficiently used for the preparation of polyurethanes foams with improved flame retardancy. The polyurethane foams were flexible. Their reaction to fire shifted from flammable to slow-burning as seen from the LOI results. Further improvement can be obtained by integrating nitrogen and silicon in the polymer structures for a synergistic effect.

3.2 | Phosphorus- and nitrogen-based polyurethanes

In this section, a phosphorus- and nitrogen-based polyol was synthesised and blended with hydroxylated polydimethylsiloxane for the preparation of polyurethane foams to study the synergistic effect of these elements in the flame-retardant properties of polyurethane. The morphology, thermal stability, hydrophobicity and flame retardant properties of three-dimensional polyurethane networks were mainly evaluated by SEM, thermogravimetric analyses, water contact angle, limiting oxygen index and vertical burning. FT-IR, AFM, DSC, and XRD were performed to assess changes that occurred during the modification of polymerisation recipes.

3.2.1 | Characterisation of phosphorus- and nitrogen-containing polyol

The phosphorus- and nitrogen-containing reactive polyol (PN-OH) was synthesised by the reaction of triethanolamine and diethylchlorophosphate according to the reaction scheme presented in Figure 2.2. The yield of the reaction was 84%. The resulting white solid polyol was characterised by FT-IR and NMR (^{1}H, ^{13}C and ^{31}P) spectroscopies.

3.2.1.1 | FT-IR characterisation

The FT-IR spectrum of the polyol is shown in Figure 3.10. The spectrum shows absorption bands around 3394 associated to the stretching vibration of the hydroxyl (–OH) group. The peak appearing at 2981 and 2938 cm^{-1} were assigned to C–H aliphatic stretch of methylene groups of the compound. The peaks at 1470, 1392 and 804 cm^{-1} were related to the presence of C–H deformation. The absorption band at around 1045 cm^{-1}, assigned to asymmetric

stretching vibration of the P–O–C group (Höhne *et al.*, 2018); also the absorption band near 1218 cm^{-1} attributed to stretching vibration of the P=O group, showed the presence of phosphorus in the structure of the synthesised product as expected. The peak at 1172 cm^{-1} corresponded to C–N stretching vibration in the polyol. The peak at 962 cm^{-1} corresponded to C–O–H stretching vibration band.

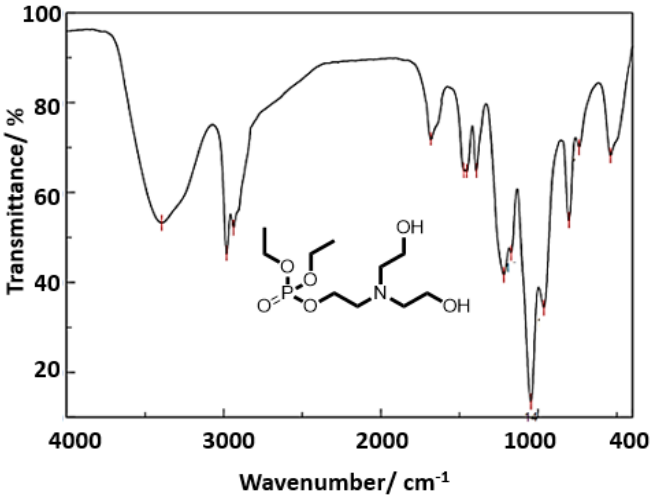

Figure 3.10 FT-IR spectrum of triethylaminodiethyl phosphate (PN-OH)

3.2.1.2 | NMR spectroscopy of PN-OH

The chemical structure of the monomer containing phosphorous and nitrogen (PN-OH) was studied using ^{1}H-NMR, ^{13}C-NMR, and ^{31}P-NMR spectroscopies. As shown by ^{1}H-NMR spectrum in Figure 3.11, the small signal peak at 4.3 ppm assigned to the protons of the alcohol group (-OH) proved that PN-OH is polyol product.

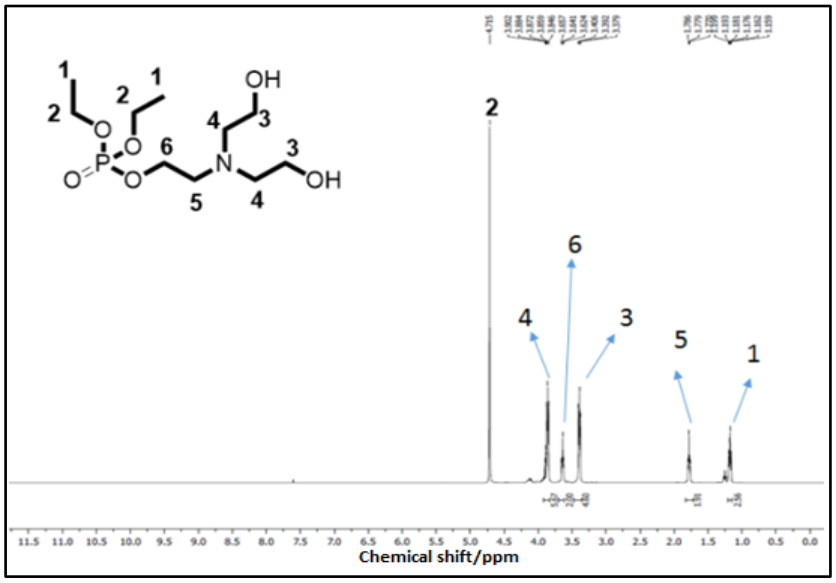

Figure 3.11 ^{1}H-NMR spectrum of PN-OH in D_2O

The resonance peaks at 1.2 ppm and 4.7 ppm were assigned to the protons of ethyl group linked to phosphate group in β-position (CH_3^*-CH_2-OP) and α-position (CH_3-CH_2^*-OP respectively. Signals of the protons in the bridge between phosphorous and nitrogen were found at 1.7 ppm for -N-CH_2^*-CH_2-OP- and 3.6 ppm for -N-CH_2-CH_2^*-OP- confirming the substitution of the chlorine atom in diethylchlorophosphate. Other signals of the branch protons on the nitrogen were observed at 3.4 ppm (-N-CH_2-CH_2^*-O-) and 3.9 ppm (-N-CH_2^*-CH_2-O-).

Further evidence of substitution of chlorine atom were the chemical shifts at 25.1 ppm and 46.7 ppm in ^{13}C-NMR spectrum assigned to the carbons between phosphorous and nitrogen as shown in Figure 3.12.

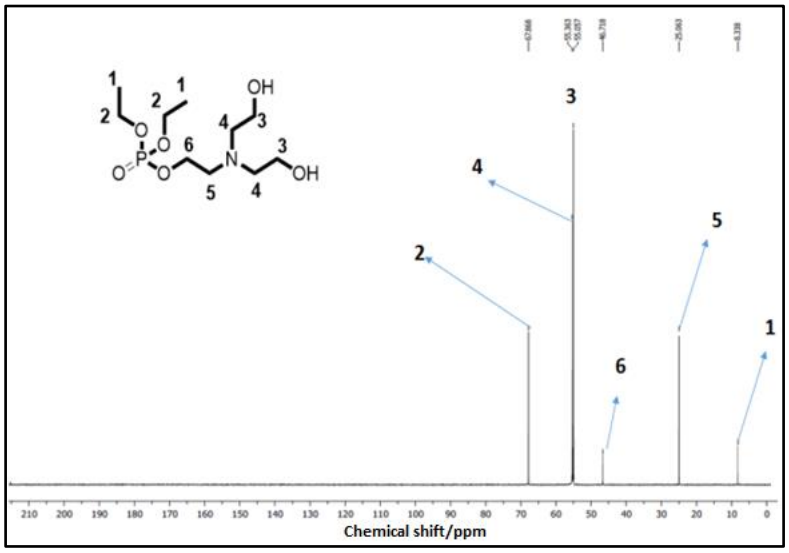

Figure 3.12 ^{13}C-NMR spectrum of PN-OH in D_2O

The ^{31}P-NMR spectrum of PN-OH is shown in Figure 3.13. Only one signal was observed in the spectrum as with P-OHs, which showed the existence of only one type of chemical environment for phosphorus in the compound.

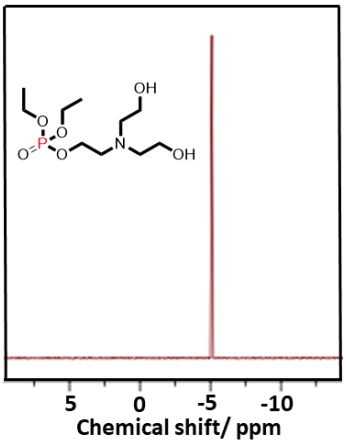

Figure 3.13 ^{31}P-NMR spectrum of PN-OH in D_2O

The higher chemical shift (-5.2 ppm) of phosphorus in the spectrum of PN-OH compared with the P-OH compounds previously shown (around -9.5 ppm), can be related to the new environment of phosphorus. The results above further confirm that PN-OH was successfully synthesised.

3.2.2 | Characterisation of PN-based polyurethane

Different formulations containing PN-OH, hydroxylated PDMS and PEG as polyol components and toluene diisocyanate as a diisocyanate crosslinking agents were prepared according the recipe summarised in Table 2.II (section 2.2.2.2). The visual appearance of phosphorus- and nitrogen- (PN-) based polyurethane sample is shown in Figure 3.14.

Figure 3.14 Film of PN-based polyurethane by Kanemoto, 2022.

3.2.2.1 | FT-IR

The FT-IR spectra of the polyurethane samples are shown in Figure 3.15. The peak at 3260 cm^{-1} attributed to N-H groups and the peak at 1715 cm^{-1} assigned to carbonyl (C=O) groups showed the formation of urethane bonds, while the very weak intensity or disappearance of the peak at 2200 cm^{-1} characteristic of isocyanate groups (-NCO) confirmed the occurrence of the polymerisation reaction (Liu *et al*., 2019). The peak of isocyanate groups at 2200 cm^{-1} was not observed for foam samples confirming an almost complete reaction. The FT-IR spectra support the proposed structure of the final polymer. Other important peaks appeared at 1514 cm^{-1}, 3500 cm^{-1} attributed to –NH deformation, and –OH groups respectively. Characteristic absorption peaks of $–Si–CH_3$ and Si–O–Si appearing at 780 cm^{-1} and 1080 cm^{-1} respectively, indicated that the PDMS polymer chain was successfully accessed (Du *et al*., 2016).

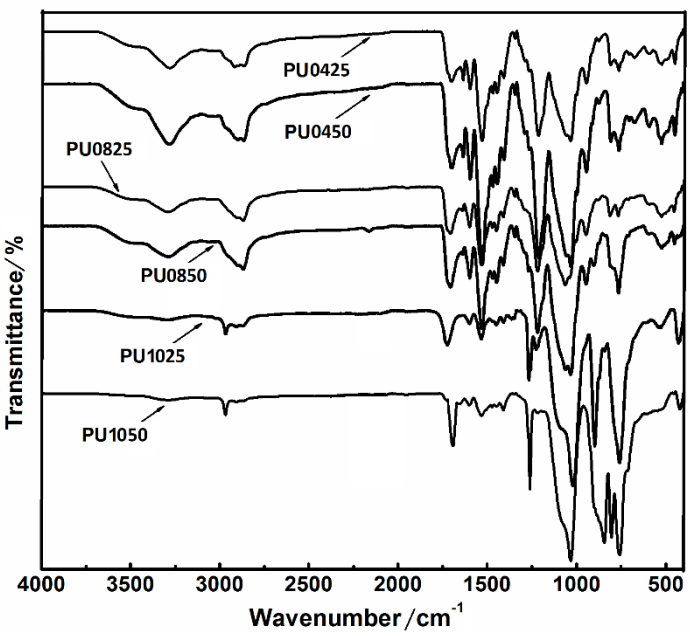

Figure 3.15 FT-IR spectra of different PU samples

3.2.2.2 | Scanning electron microscopy

The surface of PN-based polyurethane was examined by SEM (Figure 3.16) as shown, the major areas on the surface are hollow and conglomerate. In addition, hollow size increased with increasing quantity of polyethylene glycol in the polyurethane foam which could be attributed to improving of elasticity and decreasing of the initial solution density. The presence of conglomeration in the PN-based polyurethane structure seemed to indicate during the formation of film; PDMS domains tended to aggregate. The same phenomenon was also observed by Majumdar *et al.* (2007) when they prepared silicon-urethane films from PDMS, polycaprolactone polyol, and isophorone diisocyanate. It is evident that the conglomeration on the surface of polyurethane foams results in the aggregation of PDMS chains. In the SEM images of PU1025 and PU0825 (Figure 3.16), a break on the surface is clearly observed due to the miscibility issue and slow reaction rate that might have weakened the three-dimensional network of the polyurethane foam. This break disappeared in PU0425 and PU0450 samples with PEG 40% while the size of hollow decreased considerably.

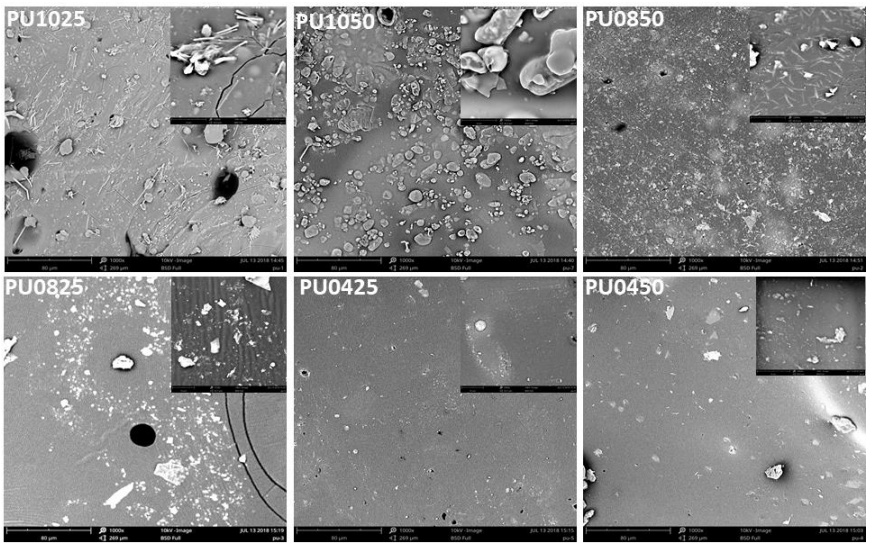

Figure 3.16 SEM images of different polyurethane foam samples

3.2.2.3 | AFM

AFM analysis was performed to follow and understand the influence of the PDMS and PEG (soft segment) content in the surface topography formation, and heterogeneity relief of PN-based polyurethane. AFM images of the surface topology were used for determination of average roughness. The different resulting AFM images are presented in Figure 3.17(a). The phase contrast in tapping mode AFM reflects the differences on the surfaces of polyurethane. The 3D nanometric - scale resolution images of the polyurethane show that the surface structure changes with increasing content of the PEG soft segments (Sundararajan *et al.*, 2017a; Sundararajan *et al*., 2017b). Average roughness (Ra) on the surface samples was determined from AFM. The Ra values for PU0850, PU0825, PU0425 and PU0450 samples were 20.63 nm, 33.78 nm, 19.67 nm, and 16.14 nm respectively. The samples have a different surface roughness. The roughness increased with increasing quantity of the PEG soft segments, but decreased with increasing quantity of the PDMS soft segments. The polyurethane nanocomposite samples are illustrated by the heterogeneous character. The samples had not a regular alternating between small soft and hard regions (Figure 3.17(b)), which indicated low degree of phase separation. It is known that immiscibility of PDMS with other polymers involves their predominance on the surface of block copolymers containing PDMS segments (Pergal *et al*., 2014).

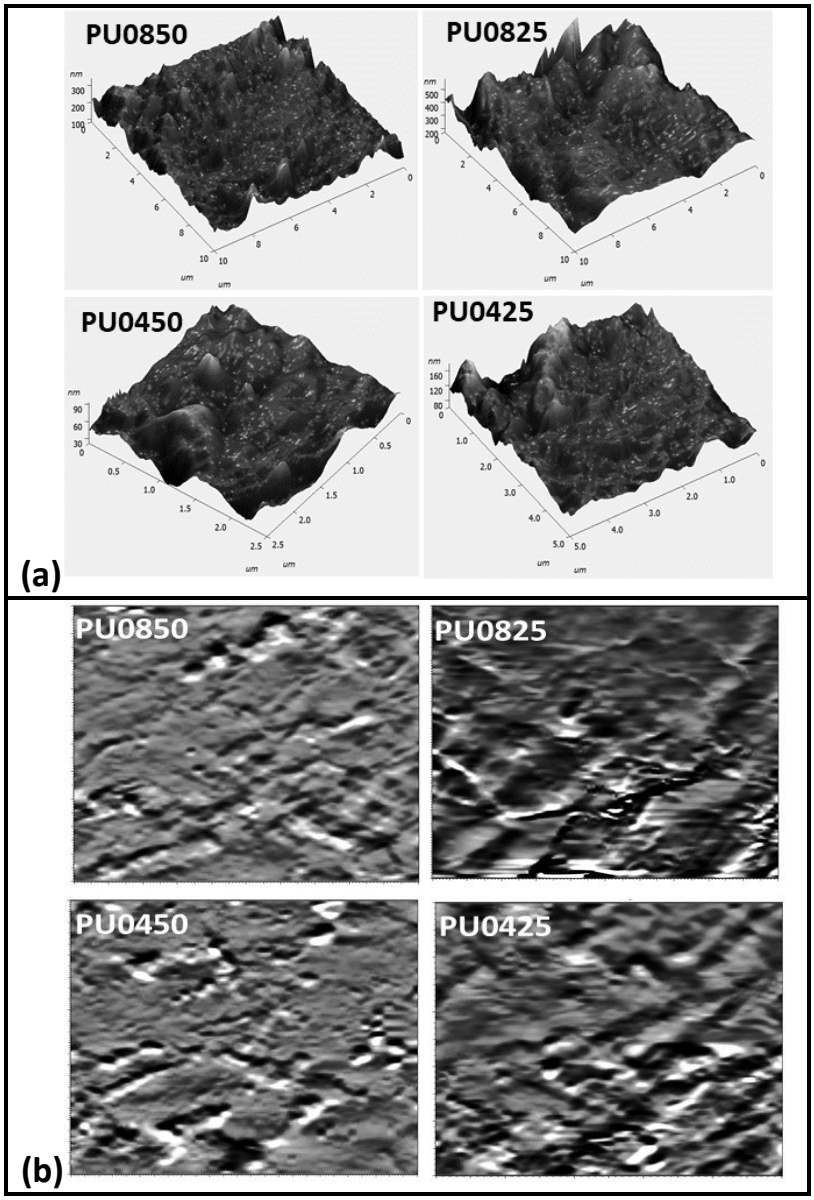

Figure 3.17 AFM images showing topology (a) and phase map (b) of polyurethane

3.2.2.4 | Water contact angle

The wettability of the polyurethane films was studied by measuring the static water contact angle at ambient temperature. Figure 3.18 presents the photographs of water-drop on the surface of the various PN-based polyurethane films. The values of water contact angle range from 92.0° to 71.6° and 138.7° to 90° for the samples with 25 and 50% of ratio PDMS/PEG (wt/wt) respectively. The surfaces with contact angle above 90°, i.e PU1025, PU0850, PU0450 and PU1050, were hydrophobic. The value of water contact angle increased with the amount PDMS in the polyurethane. The sample PU1050 with the highest PDMS is most hydrophobic. This property was conferred by the highest agglomeration of PDMS on the surface (Ji *et al.*, 2017).

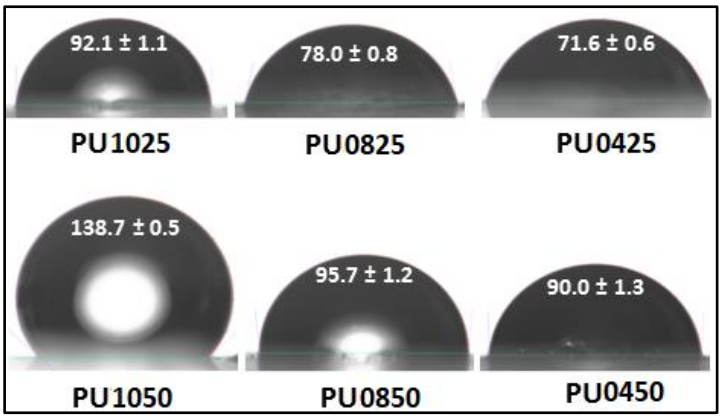

Figure 3.18 Water contact angles at the surface of PN-based polyurethane films

3.2.2.5 | X-ray diffraction

Figure 3.19 presents the X-ray diffraction patterns of PN-based polyurethane. The results exhibited characteristic features of amorphous and slightly crystalline materials. The XRD patterns of the PU1025, PU0850, and PU0825 showed a small hump at the 2θ value of 12.3°, which is the characteristic amorphous nature of PDMS, and was clearly distinguishable from the XRD patterns of other polyurethane formulations (Ferreira *et al*., 2013). The formation of crosslinking structure does not allow the hard region segments in the polyurethane to crystallise easily. The high intensity of the peak at 12.3° for PU1025 prepared with a high concentration of PDMS might imply a high deposition of PDMS layer on the surface (Bai *et al*., 2008). All the diffraction patterns presented a broad hump at the 2θ value of 23.1°. assigned to amorphous region of the polymers. This result indicates that the microstructure of the polyurethane composites was amorphous. The hard domain in PU0450, PU0425, and PU0850 samples contained fewer soft segments, and thus exhibited a thin peak at the 2θ values of 20.6° and 26.7°, which indicate that their microstructure was amorphous with a low crystallisation. This change for samples with 40 and 80% of ratio PEG/P-OH was likely caused by phase separation.

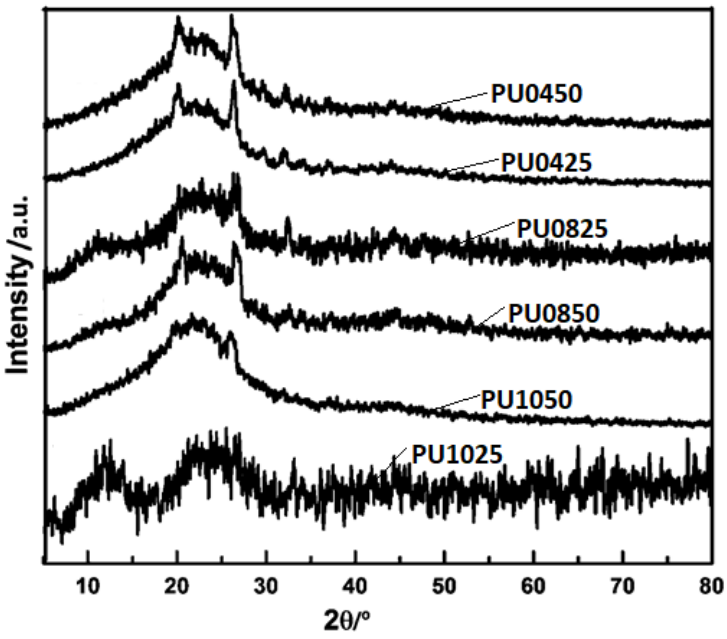

Figure 3.19 XRD patterns of PN-based polyurethane

3.2.2.6 | Thermogravimetric analyses

The thermal stability of foam materials and the integral procedural decomposition temperature (IPDT) were studied by TGA. The percentage mass loss with respect to change in temperature is shown in Table 3.IV. The compatibility of PDMS with polyurethane and the incorporation of phosphorus moieties leading to increased flame retardancy were already reported (Ji *et al.*, 2017; Wu *et al*., 2019).

Table 3.IV Thermal properties of PU composites

Samples	Initial decomposition temperature /°C	Final decomposition temperature /°C	T_g /°C	Residue yield at 600°C /%	IPDT /°C	Mass loss temperature /°C			
						5%	10%	40%	50%
PU1025	204	520.5	168.3	36.69	876	239	250	385	403
PU1050	192	533.7	176.3	28.04	687	241	269	394	408
PU0850	214	533.7	174.6	17.05	505	224	238	344	368
PU0825	217	563.9	177.3	19.42	536	228	239	354	372
PU0425	198	500.0	172.3	28.30	682	233	247	372	387
PU0450	203	510.0	170.9	28.55	689	235	248	380	395

T_g is the glass transition temperature; IPDT is the integral procedural decomposition temperature

Differential thermogravimetric curves of the polyurethane composites, shown on Figures 3.20(a) and 3.20(c), clearly exhibit three step degradation for PU1025, PU0850 and PU0825. The first stage from 80° to 150°C was attributed to removal of the water and volatile compounds in closed cells. The second degradation stage from 200° to 310°C was attributed to the decomposition of polyurethane structure and hard segments simultaneously. The third

degradation stage from 330° to 450°C was ascribed to the degradation of soft segment. While on the Figure 3.20(b) and 3.20(c), four step degradation was observed for PU1050, PU0450 and PU0425 (Gu *et al.*, 2015). The difference with the three first series of polyurethane is the separation from decomposition of flame retardant and degradation of hard segments appearing to 200° - 280 °C and 280° - 330°C respectively. The second and third decomposition processes of PU1050, PU0450 and PU0425 correspond to the second degradation process of the PU1025, PU0850 and PU0825.

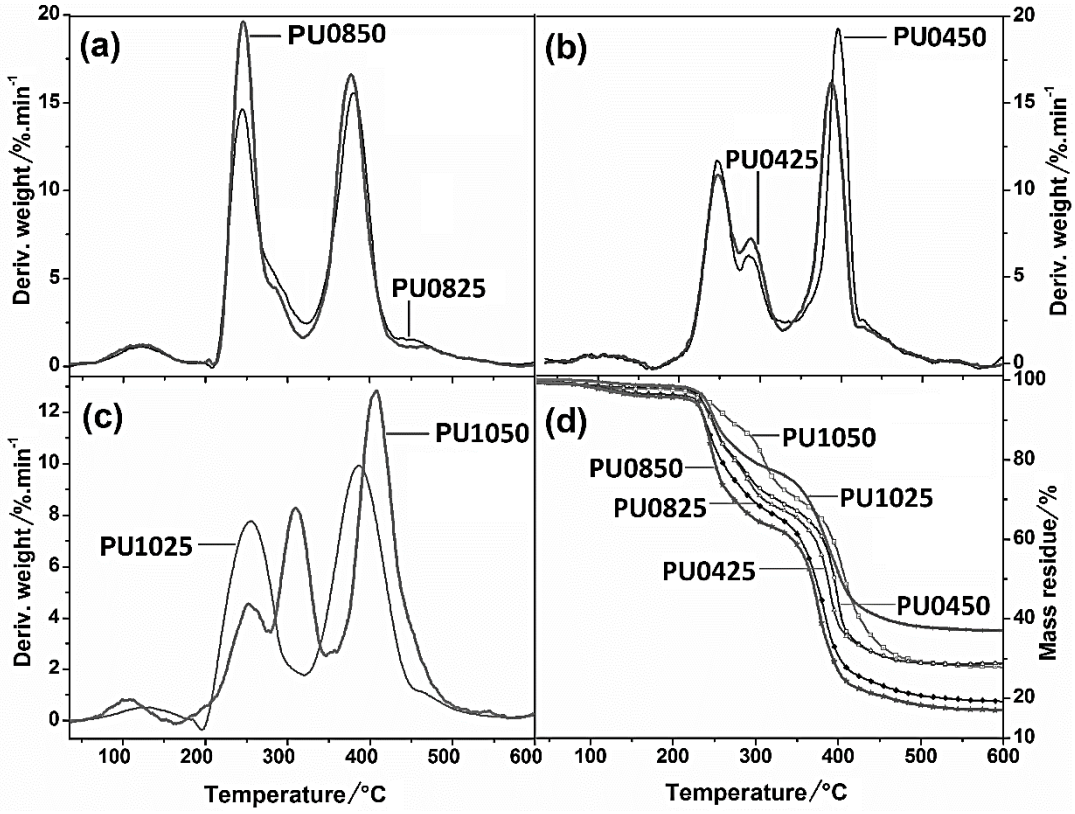

Figure 3.20 DTG (a, b, c) and TGA (d) curves of PN-based polyurethane in N_2

The residue yield at 600°C varied from 17.05 to 36.69% when PEG content increased from 40 to 100% equivalent in relation to PN-OH quantity. This can be attributed to the improved flame-retardant properties of the polyurethane foam structure. Table 3.IV shows the details of thermal decomposition temperatures of polyurethane determined from TGA. TGA curves of different samples are presented in Figure 3.20(d). All samples presented a 5% mass loss at 224° – 241°C. The values are similar to the results of the degradation of PDMS-modified polyurethane in argon (Zhang *et al.*, 2018). This result indicates that PN-based polyurethanes exhibit relatively good thermal behaviour in nitrogen up to 225°C (Höhne *et al*., 2018).

The IPDT value was in the order of PU0850 < PU0825 < PU0425 < PU1050< PU0450< PU1025. The polyurethanes with high quantity of PDMS have high IPDT values, i.e. of 876°C and 687°C for PU1025 and PU1050 respectively. Similar observations were made for PU0850 and PU0825 with IPDT value of 505°C and 536°C respectively. The thermal stability of the polyurethane composites increased with the PDMS content and could be attributed to the higher resistance to degradation of PDMS and PN-OH at high temperatures.

TGA data acquired from the experiments were used for the determination of the kinetic parameters of the thermal degradation of polymers. The kinetic investigation is one of the most important applications of thermal analysis, once the knowledge of the kinetic parameters, mechanisms and mathematical models associated to thermal decomposition process, can lead to the improvement of the current practices of polymeric material conversion in the products of interest. During isothermal decomposition, the rate of decomposition of the polyurethane composites is proportional to the concentration of non-degraded materials. The kinetic parameters of PN-based polyurethane samples by Broido, Coats–Redfern and Horowitz–Metzger methods were determined for each decomposition stage at the one heating rate of 10°C/min. The activation energy (E_a) and regression values (R^2) at the temperature range of the different stages of decomposition are presented in Table 3.V.

Table 3.V Activation energy of PN-based polyurethane samples

Sample	Temperature range /°C	Broido method		Horowitz–Metzger method		Coats–Redfern method	
		E_a /kJ mol^{-1}	R^2	E_a /kJ mol^{-1}	R^2	E_a /kJ mol^{-1}	R^2
PU1025	200 - 310	72.489	0.9440	69.077	0.9012	62.917	0.9280
	330 - 450	64.437	0.9775	49.969	0.9677	51.717	0.9684
PU1050	215 - 285	57.293	0.9902	64.498	0.9852	51.739	0.9865
	290 - 340	57.037	0.9685	53.693	0.9642	47.889	0.9558
	360 - 470	73.696	0.9833	48.124	0.9624	59.756	0.9766
PU0850	210 - 275	92.947	0,9539	93.935	0.9544	84.446	0.9451
	325 - 425	64.358	0.9560	51.363	0.9652	53.654	0.9400
PU0825	210 - 275	87.513	0.9608	87.457	0.9590	78.826	0.9526
	325 - 425	63.326	0.9592	51.798	0.9722	52.611	0.9440
PU0425	210 - 275	100.393	0.9816	102.345	0.9779	91.892	0.9783
	275 - 315	38.440	0.9779	34.741	0.9800	28.999	0.9660
	360 - 415	94.709	0.9662	66.736	0.9738	83.781	0.9589
PU0450	210 - 275	101.806	0.9792	102.721	0.9759	93.305	0.9755
	275 - 315	33.087	0.9776	30.039	0.9799	23.645	0.9624
	360 - 415	92.839	0.9188	68.187	0.9540	81.889	0.9001

E_a is the activation energy; and R^2, the regression value

The models of activation energy calculation have a regression value above 0.9. Thus, the simulations were valuable on the thermogravimetric results of the different polyurethane samples. The results obtained with the above models, showed that the second degradation stage (200° - 310°C) in the polyurethane samples has the higher activation energy when compared with the hard and soft segment degradation stages. This is due to higher crosslinking density of flame-retardant segment in the PN-based polyurethane. In the case of hard segment polyurethanes, the Table 3.V shows that the activation energy is lowest in the temperature range from 280° to 330°C allowing the identification of the fastest stage. The stability of the polyurethane depends on the breaking temperature of –CO-NH- bond. This breaking happens since the first stage from 200° to 280°C. The de-crosslinking of the long alkyl chain and the decomposition of polyurethane moiety occurs in the last decomposition stage from 330° to 450°C. Considering the activation energy in the different stages, the degradations of the flame retardant and soft segments are slower compared to the degradation of the hard segment where the breaking up of urethane linkages take place.

3.2.2.7 | Differential scanning calorimetry

Transitions in the PN-based polyurethanes were studied by DSC. The DSC curves are shown in Figure 3.21. The peak endotherm temperature appearing around 178°C was assigned to the melting temperature of the hard-segment microcrystalline structure (Ding *et al.*, 2015). Above 220°C, the decomposition of PN-based polyurethane samples starts with a significantly higher rate. Glass transition temperature (T_g) values were determined from Figure 3.21 and are listed in Table 3.IV. It can be seen that increasing the quantity of PEG decreases T_g values. PU1025 with 100 pph has the lowest Tg value of 168.3°C while PU0825 with 40 pph has the highest value of 177.3°C. This difference is attributed to aliphatic chain extender that makes the film softer (Gündüz and Kısakürek, 2004). The presence of aromatic groups in toluene diisocyanate - polyurethane may contribute to the higher packing ability of the hard segments, while the addition of PDMS increases the T_g value.

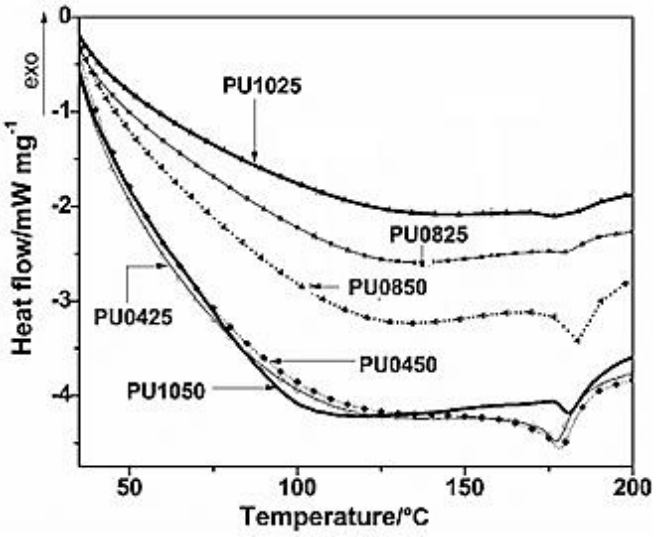

Figure 3.21 DSC curves of PN-based polyurethane under N_2 atmosphere

3.2.2.8 | Limiting oxygen index tests

The LOI values obtained from flammability tests was 25 ± 1% for all the samples. This parameter is higher than the values of LOI for polyurethane blended with hollow glass microsphere with values of 21- 23% (Jiao *et al*., 2019). Michałowski *et al.* (2017) found a low LOI value of 21 - 22% during the flammability tests of polyurethane foam blended with the polyhedral oligomeric silsesquioxanes. The formulation considerably increased the LOI value from 19% for virgin polyurethane to 25%. PN-OH/PDMS/PEG-based polyurethane samples owe their good flame resistance to the performance of three flame retardant elements such as phosphorus, nitrogen, and silicon present in the structure of resulting polyurethane, and to the excellent compatibility of the components. The nanocomposite systems were considered as being slow-burning with a level of UL-94 V-0 (burning stops within 10 s) (Nelson, 2001).

3.2.2.9 | Vertical flammability tests

Ignition occurs when volatile compounds reach critical concentration require to sustain combustion in the presence of external ignition source. Upon ignition, the fraction of the heat of combustion fed back to the condensed phase must be greater than its heat of gasification so as to maintain a pool of combustible volatiles for a sustained flame. For any given material, this condition can be related to the mass loss rate at ignition. The ignition time for each polyurethane sample is the same at 8.0 ± 0.5 s. Different combinations of PEG and PDMS did not significantly affect ignition time. Compared to the work of Modesti *et al*. (2002) who blended the polyurethane with expandable graphite, the reported ignition time was around 5 s. This significant difference finds an explanation in the high flammability of the blowing agent,

the high level of radiant flux and cellular structure of the samples. The soft segments of polyurethane foams are up of PEG as well as PDMS. The soft segment is recognised as the main cause of the low value of ignition time (Bai *et al*., 2008; Kirpluks *et al*., 2014). However, PDMS which has silicon in their structure, is a good flame retardant due to the low heat release, minimal sensitivity to external heat flux and low yields of carbon monoxide release. The high flammability of PEG is then inhibited by the reactive fragments of PN-OH and PDMS.

3.3 | Phosphorus-based epoxy/clays nanocomposites

Phosphorus-containing epoxy resins GEP-OHs were synthesised by glycidylation of the P-OH polyols prepared in section 3.1 and were used to blend commercial epoxy resin DGEBA for the preparation of epoxy coatings. The objective of adding GEP-OHs was to improve the reaction of the epoxy products to fire. Clay nanoparticles were also added as reinforcement and potentially for additional fire retardancy. The nanocomposite blended epoxy products were tested for surface finishing protection of leather.

3.3.1 | FT-IR spectroscopy of glycidylated P-OHs

Glycidylation of P-OHs was revealed by FT-IR analysis. The general chemical structures expected for the phosphorus-containing epoxy resins are presented in Figure 3.22.

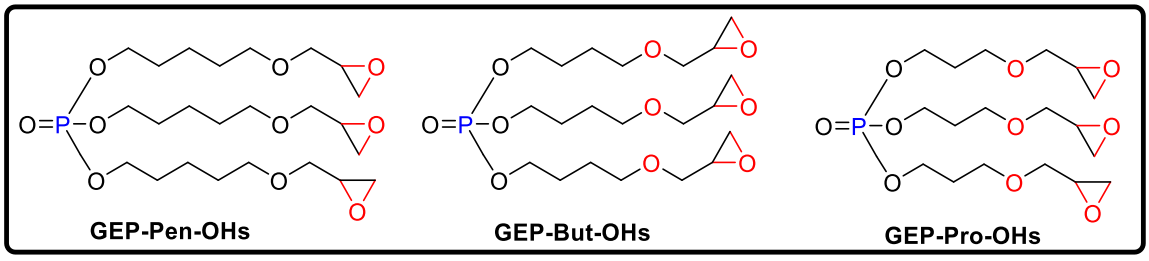

Figure 3.22 General chemical structures of the phosphorus-containing epoxy resins

Figure 3.23 shows the FT-IR spectra of the different GEP-OHs synthesised from P-OHs. The peaks appearing at 3369 cm^{-1} are assigned to OH stretching vibration of residual hydroxyl groups and moisture. By comparing the spectra of GEP-OHs and P-OHs (Figure 3.2), it appeared that the intensity of the band of hydroxyl groups considerably decreased but did not completely disappear. It seems that all the hydroxyl groups of the P-OHs were converted in the process. The peaks recorded at 2950 cm^{-1} and 2853 cm^{-1} were assigned to C-H stretching vibration. The peaks at 1470 cm^{-1} were ascribed to P=O stretch and peaks at 1020 cm^{-1} corresponded to P–O–C stretching vibration. The absorption band between 900 and 920 cm^{-1} showed the presence of epoxide function in GEP-OHs monomers [143,144]. The result

confirms that the glycidylation of P-OHs was effectively achieved. The hydroxyl terminated polyols were converted to oxirane rings.

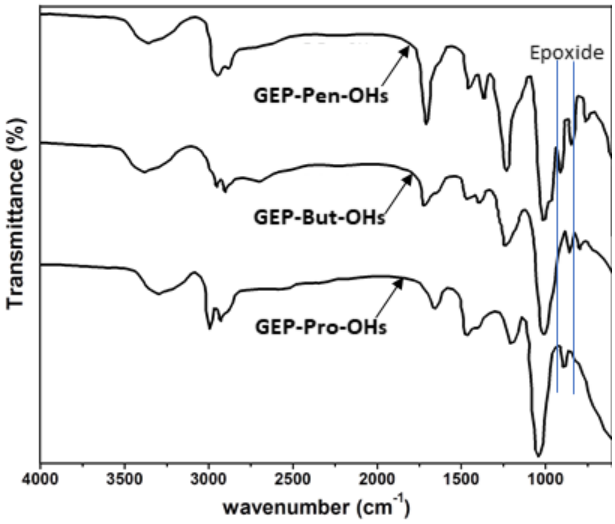

Figure 3.23 FT-IR spectra of GEP-OHs

3.3.2 | Characterisation of the cured resins

Epoxy resin systems were obtained by blend mixing of GEP-OHs, DGEBA and nanoclays, and cured with TETA. The cured films were characterised by FTIR, TG-DTG and DSC. Figure 3.24 shows cured epoxy network from GEP-Pen-OHs

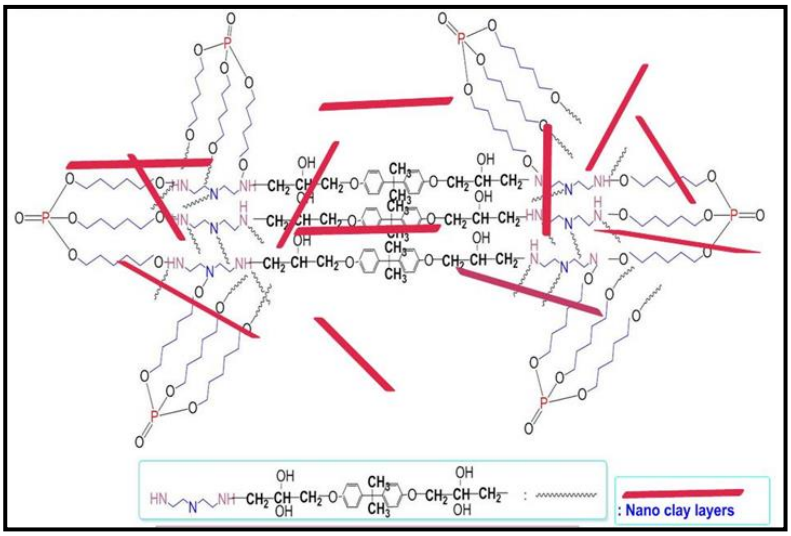

Figure 3.24 Cured epoxy network between GEP-Pent-OHs, DGEBA, TETA and clay

3.3.2.1 | FT-IR analyses of cured phosphorus-epoxy

FT-IR spectra of cured phosphorus-epoxy resins T5GP-P, T4GP-P and T3GP-P are shown in Figure 3.25. The Table 3.VI presents the principal functional groups in the cured phosphorus-epoxy resin. It provides the details of spectra interpretation and band assignments.

The epoxy resins were cured by chemical reaction between the resins and the curing agent forming new connecting chains and leading to a three-dimensional network. The peak at around 3330 cm^{-1} was assigned to N–H and O–H stretching vibrations. N-H stretching vibrations overlap with stretching vibration band of hydroxyl groups that are formed after the opening of the epoxide ring. Other important peaks at 1500 cm^{-1}, 1239 cm^{-1}, 1100 cm^{-1} and 1030 cm^{-1} were attributed to N–H deformation (scissoring), P=O stretching vibration, C–O–C stretching vibration and P–O–C stretching vibration respectively.

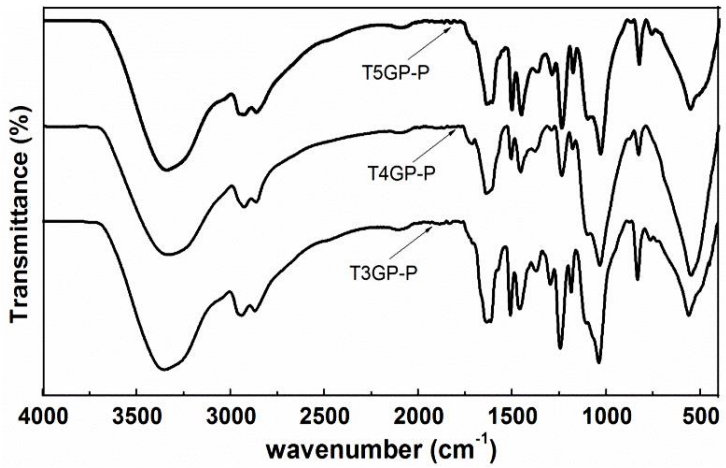

Figure 3.25 FT-IR spectra of the cured phosphorus-epoxy systems

The absence of the characteristic peak of the epoxy group at around 910 cm^{-1} revealed that the curing reaction between the epoxy group and the hardener was complete (Ferdosian *et al*., 2016).

Table 3.VI Assignment of peaks from FT-IR spectra of the cured epoxy systems

Samples	O-H & N-H Stretching vibration	$-CH_3$ aliphatic stretch	$-CH_2$ acyclic	C=C Stretching vibrations of aromatic ring	N-H deformation vibration	C-H (asymmetric) aliphatic deformation vibration	P=O Stretching vibration band	C-O-C Stretching vibration band	P-O-C Stretching vibration band	CH Deformation vibration	C-C vibration
T5GP-P	3334	2936	2845	1637	1507	1456	1239	1106	1038	832	558
T4GP-P	3320	2936	2865	1631	1507	1456	1239	1109	1032	832	532
T3GP-P	3328	2939	2859	1631	1501	1450	1239	1100	1032	832	552

3.3.2.2 | Thermogravimetric analyses of cured phosphorus-epoxy nanocomposites

TGA curves of cured phosphorus-epoxy and epoxy/clay composites are shown in Figure 3.26. The mass loss at 100°C was attributed to the removal of moisture. The onset of degradation observed at 200-250°C was due to the decomposition of the epoxy and the scission

of P=O linkages which confirmed that the material subjected to thermal degradation responded effectively to the flame retardant treatment.

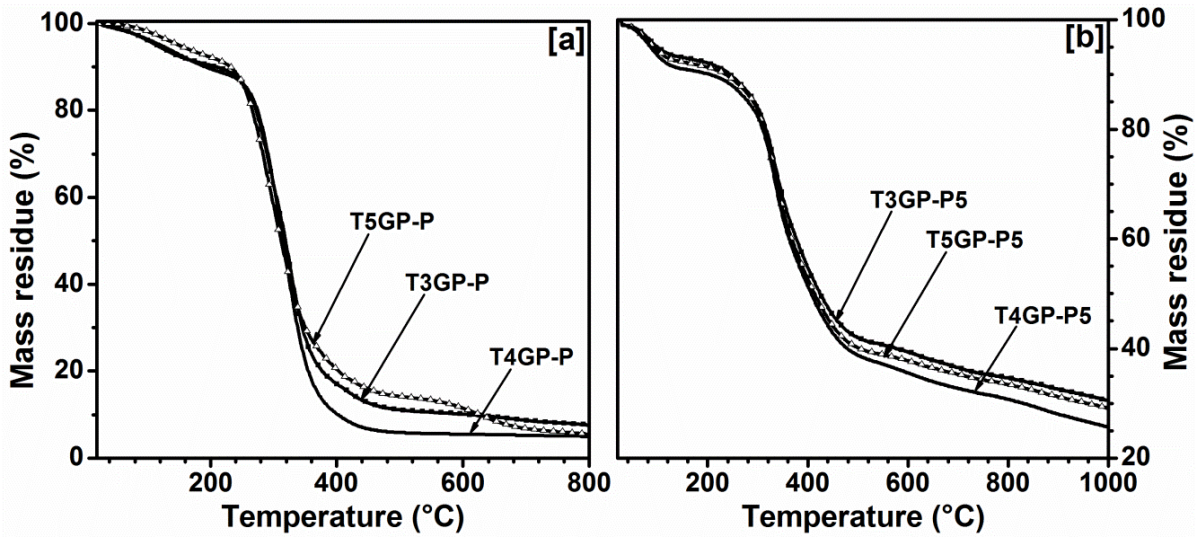

Figure 3.26 TGA curves of the cured phosphorus-epoxy (a) and epoxy/clay composites (b)

Table 3.VII summarises some parameters obtained during thermal degradation of the developed epoxy materials such as char yield, temperature at the maximum rate of degradation (T_{max}), the maximum rate of percentage mass loss (L_{max}), temperature at 5% mass loss (T_5) and temperature at 30% mass loss (T_{30}).

Thermal stability of the epoxy materials was estimated by determining the statistical heat-resistant index temperature (T_s). T5GP-P, T4GP-P and T3GP-P displayed lower statistical heat-resistant indices than their counterparts containing 5% of clay nanoparticles, T5GP-P5, T4GP-P5 and T3GP-P5. The addition of clay nanoparticles to the epoxy resins slightly increased the thermal stability of the cured epoxy system and decreased the maximal degradation rate (Table 3.VII). Residues significantly increased with the addition of clay. Considering that clay was added to a ratio of 5%, it appeared that the synergistic effect of clay and phosphorus in the resins was responsible for this performance. T3GP-P5 and T5GP-P5 showed the most thermally stable behaviour.

The integral procedural decomposition temperature (IPDT) of T4GP-P and T3GP-P increased by 5.4% and 17.9% respectively compared to T5GP-P. It is observed that the IPDT values decreased with the length of carbonated chain. The thermal stability of phosphorus epoxy composites increased with phosphorus content, proving their importance as a flame retardant in the epoxy system. At the same time, the incorporation of clay nanoparticles increased IPDT values substantially. These results demonstrate that adding clay nanoparticles

enhanced the thermal stability of epoxy resin and such high thermal stability could be attributed to the higher resistance of clay to degradation at high temperatures. The clay nanoparticles in the epoxy system acted as a barrier to the movement of the polymer segments.

Table 3.VII TGA data of thermal degradation of T5GP-P, T4GP-P and T3GP-P

Sample code	T_5 /°C	T_{30} /°C	T_s /°C	T_{max} /°C	IPDT /°C	L_{max} / % min^{-1}	T_g /°C	Residue / % wt	LOI / %
T5GP-P	120.9	290.9	109.22	298.4	373.7	6.67	98.0	5.48	19.69
T4GP-P	150.0	283.0	112.60	319.8	393.8	8.93	97.6	4.98	19.49
T3GP-P	114.5	289.5	107.56	317.7	440.5	7.05	97.3	7.63	20.55
T5GP-P5	90.9	337.5	117.04	337.2	1221.1	3.82	65.2	29.08	29.13
T4GP-P5	85.5	335.0	115.25	335.5	1047.4	3.85	67.4	25.71	27.78
T3GP-P5	99.5	343.0	120.34	337.0	1256.4	3.52	65.4	30.53	29.71

A correlation between char residue and limiting oxygen index (LOI) of the polymer was established by Van Krevelen (1975), who empirically demonstrated that polymer with higher char has lower flammability. Main properties of char are resistance to oxidation, density, continuity, coherence, permeability and thermal insulation (Gao *et al*., 2013). Char formation occurs when the decomposing polymer is highly crosslinked and possesses aromatic fragments or consists of conjugation prone to aromatisation during thermal decomposition (Van Krevelen, 1975). The formulated phosphorus-epoxy resins displayed a low char residue when the nano-clays were not incorporated. Without nano-clays, the char residue of T3GP-P, T4GP-P and T5GP-P samples was almost similar with values ranging between 6.35 and 6.85%. Those samples were considered as flammable because their theoretical LOI values were lower than 20.95 (Nelson, 2001). However, a significant increase of char residue was observed after the incorporation of nano-clays. Char residue values rose from 6.85% to 30.51%. The clay nanoparticles had a significant role in the thermal stability of epoxy composites. T3GP-P5, T4GP-P5 and T5GP-P5 could be considered as "self-extinguishable" and 'intrinsically non-flammable' considering their LOI values (Nguyen *et al*., 2012). Figure 3.26 shows that the incorporation of clay nanoparticles in the phosphorus-epoxy resin improved the thermal resistance of the composites. This improvement may be attributed to the excellent adhesion between the epoxy resin and the clay. The clay nanoparticles block the propagation of heat in the materials, thereby reducing the degradation rate (Yasmin *et al*., 2006).

The activation energy (E_a) for the main stage of thermal decomposition of the epoxy formulations were determined using Horowitz-Metzger kinetic model (Horowitz and Metzger, 1963). The activation energy values were calculated to estimate the correlation between the carbonated chain of phosphorous epoxy and the thermal decomposition rate. According to this model, the calculations were made where the main degradation occurred linearly, the temperature range of 270° – 340°C and 320 – 410°C for the epoxy system with and without clay nanoparticles. E_a values at the main stage of decomposition are presented in Figure 3.27. It is observed that the E_a value increase with the increase of carbonated chain. The highest E_a value was found for T5GP-P, followed by T4GP-P and T3GP-P, with the values equal to 20.19, 19.39 and 18.61 kJ mol^{-1} respectively. The activation energy during the thermal degradation reaction strongly depends on the molecular weight of phosphorous-epoxy resins (Funt *et al.*, 1974). The T3GP-P epoxy deteriorated faster than the T5GP-P epoxy. After the incorporation of clay nanoparticles in the epoxy system, the values of E_a drastically decreased. Its values ranged from 5.73 to 10.46 kJ.mol^{-1} for T5GP-P5 and T3GP-P5 respectively. The clay nanoparticles in the epoxy system acted as a barrier to the movement of the polymer segments because they need high activation energy for the translation and rotational motions.

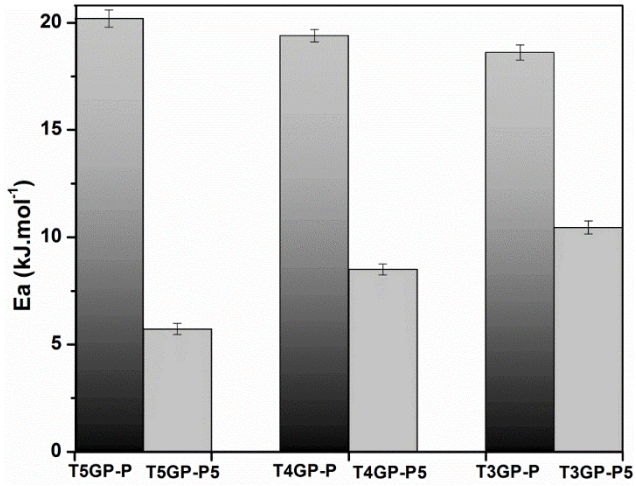

Figure 3.27 Activation energy of the hybrid epoxy samples during thermal decomposition

3.3.2.3 | Differential scanning calorimetry

The DSC of the different cured epoxy formulations revealed a slight increase in glass transition temperature (T_g) for T3GP-P, T4GP-P to T5GP-P with values of 97.3°, 97.6° and 98°C, respectively (Table 3.VII). The presence of –O–P=O groups linked to the methylene segments could increase the intermolecular interactions by hydrogen bonding with the epoxy hydroxyls. They have the propensity to increase the T_g by increasing the bond energy required

to attain chain mobility. The impact of T_g dependent on varying the number of methylene units was observed not to be so significant (Funt *et al*., 1974). Thus, decreasing methylene carbon numbers slightly decreased T_g values. The T_g of an epoxy depends on the concentration of elastic chains as well as backbone flexibility. This is attributed to the greater ability of the chains to undergo relaxation within the structure. An increase in the length of the methylene bridging unit improved backbone flexibility but lowered the density of hydroxyl groups along the backbone (Lakshmi *et al.*, 2003). The presence of clay nanoparticles in the epoxy system decreased the T_g values. Clay nanoparticles could act as plasticiser in the network.

3.3.3 | Application of phosphorus-based epoxy resins for leather protection

3.3.3.1 | Morphology of coated leathers

Figures 3.28(a) to (d) show the SEM images of uncoated and coated leather. Uncoated leather was the control sample. Leather was coated with different epoxy systems such as T5GP-P, T4GP-P and T3GP-P. SEM was performed on the grain interface of leather samples. The control specimen without any surface deposition (Figure 3.28) shows a compact fibre structure and hair pores on the surface. The fibre bundles were loosely and randomly interwoven with each other throughout the matrix. In leather specimens coated with the T5GP-P5 (Figure 3.28(b)), it can be observed that the top coating did not affect the structure and the fibre structure was dense. In the case of leather coated with T4GP-P5 (Figure 3.28), the fibre structure was homogeneous. For leather coated with T3GP-P5 (Figure 3.28(d)), the fibres were evenly dispersed.

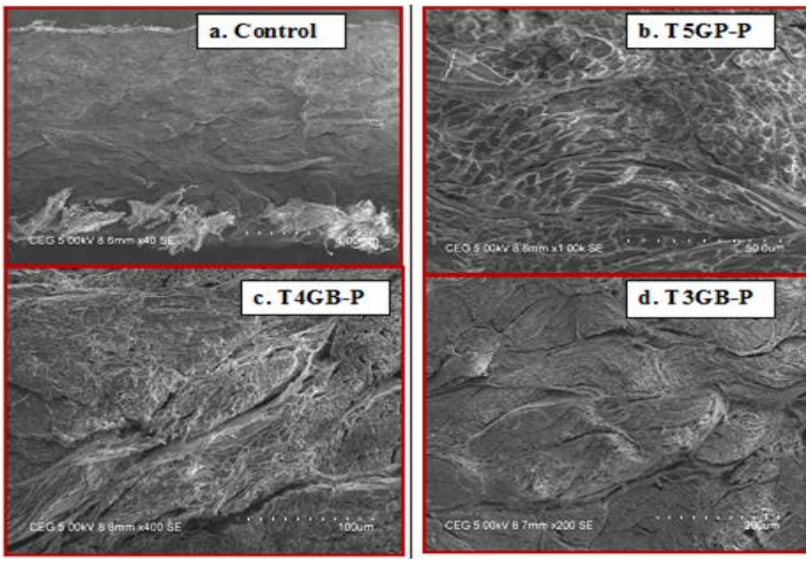

Figure 3.28 SEM images of uncoated leather(a); leather coated with T5GP-P5 (b), T4GP-P5 (c) and T3GP-P5 (d)

3.3.3.2 | Thermogravimetric analyses of coated leather

Thermal stability of coated leather samples was determined and compared to that of raw leather. The thermogravimetric and differential thermal analyses (DTG) curves of the raw leather and leather coated with T3GP-P5 and T5GP-P5 shown in Figure 3.29 present different behaviours. The thermal decomposition temperatures at different mass loss percentages and the char yields were listed in Table 3.VIII. DTG curves on Figure 3.29(b) show three main mass loss incidents for coated leather against two for raw leather. For all leather samples, the first mass loss at 110°C was attributed to the removal of water molecules adsorbed on the surface of the different samples. The mass loss in this step shows that uncoated leather contains much more adsorbed water than the coated samples. The second and the most important mass loss for the raw leather occurred at a maximum temperature of 350.3°C which was attributed to the combustion of leather [40]. The main degradation of coated leather samples (Figure 3.29(a)) occurred in two stages corresponding to one DTG peak between 270-350°C and a second peak at 350-450°C (Figure 3.29(b)). The results revealed a certain delay in the degradation of leather due to coating with the epoxy resins.

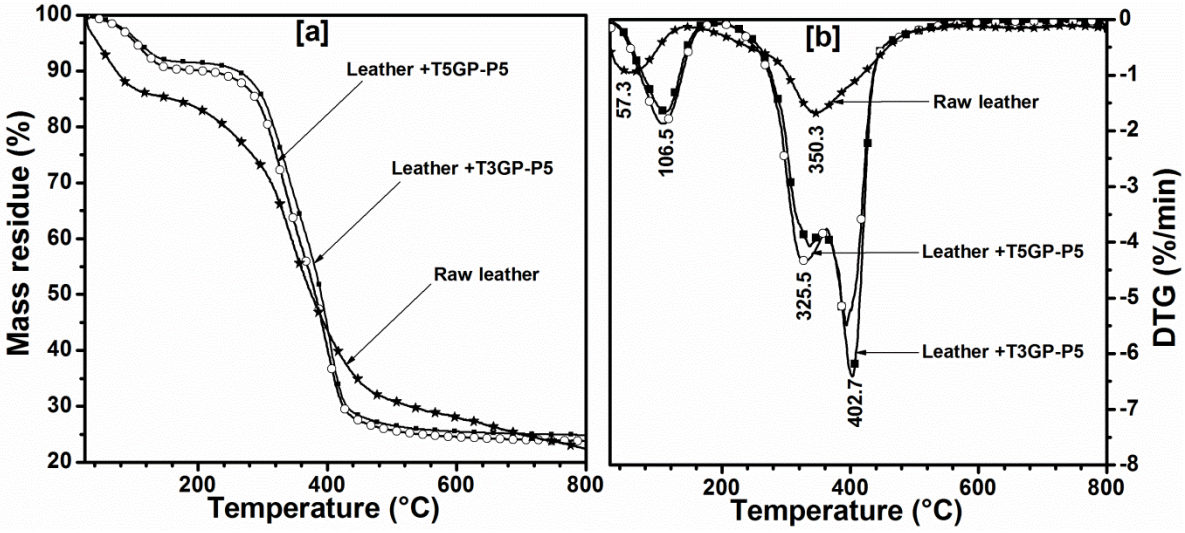

Figure 3.29 TGA (a) and DTG (b) curves of raw and coated leather

The T_s value for raw leather was lower compared to those of coated leathers. Coating with phosphorus-epoxy systems T5GP-P5 and T3GP-P5 slightly improved the thermal stability of the leather. Residual materials of leather at 800°C are presented in Table 3.VIII. The char values were higher for the coated leather compared to those of control leather. The presence of the epoxy system on the surface of leather increased the char values. These results indicate that the phosphorus-epoxy system had a positive effect on leather degradation.

3.3.3.3 | Tensile strength of coated leather

The tensile strengths of the raw uncoated leather and of coated leathers with T5GP-P5 and T3GP-P5 are shown in Table 3.VIII. These values are an average of three different replicates. This test was carried out to appreciate the coating effect on the properties of leather. The application of hybrid epoxy resin on leather modified the mechanical properties of leather considerably. The coating with hybrid epoxy decreases the tensile strengths of leather. The tensile strength was reduced from 14.40 N/mm² for uncoated leather to 8.59 N mm^{-2} for leather coated with the T3GP-P5 system. This effect can be explained by the swelling of the triple helical bundles of leather by the resins and the non-orientation of clay platelets. By implication, the orientation of the polymer chains to the loading direction contributes to a decrease in the reinforcing effect. The formation of crack initiation sites from epoxy coating decreases the tensile strength (Prabhu *et al*., 2013).

Table 3.VIII Recapitulative properties of coated and uncoated leather

Leather sample	Thermal behaviour				Tensile strength data	
	T_5 /°C	T_{30} /°C	T_S /°C	Residue /%	Tensile strength /N mm^{-2}	Stress /%
Uncoated leather	45.65	311.54	100.54	22.37	14.40	21.52
Leather/T5GP-P5	102.05	331.68	117.52	23.77	8.86	32.77
Leather/T3GP-P5	110.11	339.74	121.47	24.87	8.59	23.61

3.3.3.4 | Limiting oxygen index tests on coated leather samples

LOI measures were used to examine flame retardant performances of leather samples. Theoretical and experimental LOI values of the investigated leather samples are listed in Table 3.IX. There is a significant difference between the LOI values depending on the method of determination. The leather used as a control falls into the category of slow-burning materials. This characteristic of leather has been reported (Xu *et al*., 2017). When epoxy system was coated on leather, the LOI value increased from 26.7% of control leather to 28.6% of coated leather with T5GP-P5. Obviously, coated leather falls into the category of self-extinguishing materials. As a consequence, the leathers coated with 1% wt. of epoxy system showed better flame retardation properties. The LOI results indicate that epoxy systems, such as T3GP-P5 and T5GP-P5, promoted the formation of a compact char layer which isolated flammable gases and heat from the unburned leather and released non-combustible gases to dilute the concentration of dioxygen (Liu *et al.*, 2020). During the combustion especially, the phosphorus flame retardant acted in the condensed phase by forming the poly(phosphoric acid), which

promoted char formation (Vinay *et al.*, 2021). Meanwhile, the clays nanoparticles acted as a barrier and hindered the thermal oxidation of the char layer (Zabihi *et al.*, 2018). This means that phosphorus-based epoxy nanocomposite significantly reduced the flammability of leather and effectively improved the flame retardation properties of leather.

Table 3.IX LOI and vertical flammability test results of leather samples

Leather sample	LOI* /%	LOI /%	Ignition time /sec
Uncoated leather	26.5	26.7 ± 0.5	6.0 ± 0.5
Leather/T5GP-P5	27.0	28.6 ± 0.7	8.1 ± 0.9
Leather/T3GP-P5	27.5	28.4 ± 0.6	8.0 ± 1

*values determined from Van Krevelen's equation

3.3.3.5 | Vertical flammability tests on coated leather sample

Fire retardancy of phosphorus-containing epoxy nanocomposites was studied by vertical flammability tests of coated leather samples. The comparative study of ignition time of native (control) and coated leather samples permits an appreciation of the flame retardation properties of epoxy systems. Table 3.IX summarises the ignition times and standard deviations of control leather and coated leather. The ignition times after coating the leather increased from 6.0 s for control leather to 8.1 s for the coated leather with T5GP-P5. The presence of the phosphorus-epoxy nanocomposite on the leather surface hindered the transmission of the flame from the burner to leather. However, the synergetic effect between phosphorus and clay nanoparticles is the main reason for increasing of ignition time. There is an excellent compatibility between the system components. Migration of nanoparticles during combustion is a major physical factor which contributes to barrier formation in nanocomposites. Different driving forces such as thermal gradient, surface free energy difference between clay surface and the polymer matrix and rising bubbles of volatile decomposition products that carry filler were presumed to be responsible for this migration (Karak, 2021). The crosslinking reaction between the epoxy system and collagen fibres can form more compact intumescent foam layers when heated, helping to prevent air from entering into leather fibres and thereby slowing down the heat transfer (Xu *et al.*, 2017). This phenomenon inhibits the spread of the flame from burner to leather drastically. Vertical flammability tests are in agreement with the results from LOI, confirming that the leather samples burn slowly.

3.4 | Ecological aspects of resulting materials

To improve the fire reaction properties of polyurethane foams and leather while mitigating the potential environmental pollution of flame retardants from their synthesis, production and application, some aspects were investigated to follow the ecological impact of such materials. The ecological impact of different polymers developed in this work was assessed by the 12 principles of green chemistry established by Anastas and Warner (2000), and also by their reaction to fire in case of incineration or fire.

3.4.1 | Evaluation based on principles of green chemistry

There is not a universal approach for the conversion of polymer production into more sustainable ones, but rather a series of many steps can result in an environmentally friendly polymer production. However, an eco-friendly approach is guided by the 12 principles of green chemistry (Table 3.X).

Table 3.X Coordination of 12 principles of the green chemistry (Anastas and Warner, 2000)

Nº	**Principles**	**Observations**
1.	Prevent waste	Not applicable
2.	Design safer chemicals and products	Taken into account
3.	Design less hazardous chemical syntheses	Taken into account
4.	Use renewable feedstock	Not applicable
5.	Use catalysts not stoichiometric reagents	Taken into account
6.	Avoid chemical derivatives	Taken into account
7.	Maximise atom economy	Taken into account
8.	Use safer solvents and reaction conditions	Taken into account
9.	Increase energy efficiency	Not applicable
10.	Design for degradation after use	Not applicable
11.	Analyse in real time to prevent pollution	Taken into account
12.	Minimise the potential for accidents	Taken into account

Principles 1, 4, 9, and 10 were considered as being not applicable for this study.

Principles 5, 6, 7, 11, and 12 were achieved for the most part. For example, catalysts and atmospheric pressure were essentially used for the production of phosphorus-based polyurethane foam. During the syntheses, the yield was over 80%.

Principles 2, 3, and 8 were taken into account. For instance, additive flame retardants were replaced by reactive flame retardants, which are most efficient and solve the problem of the

homogeneity of polymeric materials. Water was used as a blowing agent. These principles seem to have the greatest potential for the environmental protection.

8 out of 12 green chemistry principles were taken into account for the production of polyurethane foam and epoxy. In this way, the ecological impact of polymeric materials presented in this thesis from the synthesis of flame retardant to the production of polymers was slightly improved. The 12 green chemistry principles should become standard guide for all polymer scientists and engineers (Dube *et al.*, 2014).

3.4.2 | Classification of ecologically friendly flame retardant polymers

All the polymers were free of halogen and heavy metal. These elements, during the combustion and incineration, produce the toxic compounds for the environment and human being.

The promotion of char formation can be viewed as the most important concept in fire retardancy of polymeric materials. Phosphorus-based polymers prepared in this work appear effective, to a certain extent where the phosphorus favoured the formation of carbonaceous char rather than carbon containing combustible gases. During the flammability tests, the materials burnt without emission of black smoke. However, one gram-mol of carbon produces 26.4 kcal of heat in burning to CO and 94 kcal of heat in burning to CO_2 (Lomakin and Zaikov, 1999). This heat is not produced if carbon is kept in the form of char. The greenhouse gas emissions produced by burning the polymeric materials have considerably decreased. Figure 3.30 shows the new types of ecologically friendly flame retardants.

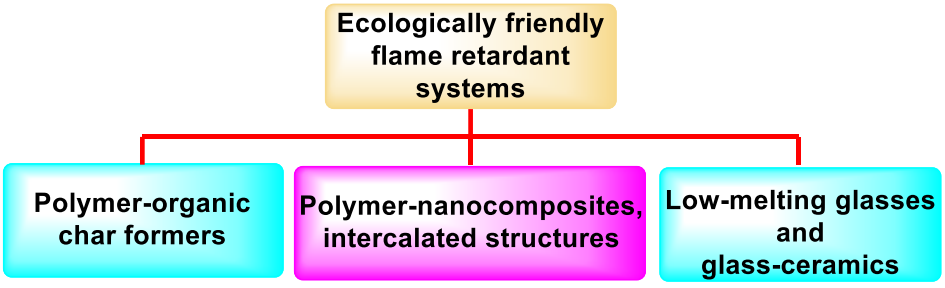

Figure 3.30 New types of ecologically friendly flame retardant systems

The resulting polyurethane foams and coated leather showed during the flammability tests:

- reduction in the ease of ignition,
- suppression of black smoke,
- reduction of toxic gas evolution, particularly carbon monoxide.

As consequence, the ecological impact of flame retardant polymers was slightly reduced.

Conclusion

This thesis aimed to design the phosphorus- and nitrogen-based polymer precursors and study their action on such common thermoset materials as polyurethane and epoxy, especially on thermal stability and reaction to fire, while taking into account their ecological impact. Phosphorus-containing polyols (P-OHs) were successfully prepared by reacting phosphoryl chloride with various aliphatic diols. The phosphorus-based compounds were used as the polyol components in the preparation polyurethane foams. It was shown that polyurethane foams obtained were flexible with similar global behaviour and had good thermal stability as observed by thermal analyses. There was no direct relationship established between the Young's modulus, hardness and porosity. Limiting oxygen index tests indicated that the polyurethane foams were slow-burning materials. In addition, the ignition time of foams was found to be in the range 7-8 s, confirming an improvement of fire resistance. The flexible polyurethane foams owe their fire resistance to the high compatibility of foam components and the presence of phosphorus, which can act in the condensed phase during ignition.

Other phosphorus-nitrogen containing monomers were successfully synthesised via reaction of diethylchlorophosphate and triethanolamine and blended with PEG and hydroxylated PDMS for the preparation of polyurethanes with toluene diisocyanate. TGA and DSC analyses of resulting polyurethanes indicated a decrease in glass transition and integral procedural decomposition temperatures due to increasing PDMS content. The hydrophobicity of polyurethane samples increased when the quantity of PDMS in the matrix increased. However, different combinations of PEG and PDMS affected the polyurethane microstructure. Still, they did not affect the ignition time because all the formulations had an ignition time of 8 s. This type of polyurethane can be used for energy-saving buildings and thermal energy storage.

Three different epoxy pre-polymers such as tris(propyl glycidyl ether) phosphate, tris(butyl glycidyl ether) phosphate and tris(pentyl glycidyl ether) phosphate were synthesised from the P-OHs polyols, blended with DGEBA and clay nanoparticles, then successfully cured with TETA as the hardener. The cured epoxy resins containing nano-clays exhibited higher thermal stability. The thermal stability, thermal decomposition and flame retardation of the phosphorus-based epoxy/clay nanocomposites were dependent on the length of carbon chains in epoxy pre-polymer. This epoxy system containing 5% wt. clay coated on leather.

significantly improved the thermal and flame retardation properties. However, the tensile strength of coated leather decreased compared to that of native leather. These results show that hybrid epoxy systems are promising for leather finishing applications.

The results have shown that addition of phosphorus-containing chemicals as halogen-free flame retardants in the preparation of polyurethane or epoxy polymer products provides a slight improvement on thermal stability and flame retardancy. The addition of silicon-based compounds or clay nanoparticles can significantly enhance the thermal stability and fire properties of the materials. Further fire tests using some standard tests for reaction to fire, such as cone calorimetry and radiant heat panel test, are planned to fully understand the contribution of the addition of the phosphorus-nitrogen monomers in polymer fire performances. The fire classification of a material is dependent to the application and the method used for evaluation. Large scale test simulating fire scenarios can better provide information on the fire behaviour of the synthesised materials.

Based on the 12 principles of green chemistry and flammability findings, the ecological impact of all the flame retardant polymers reported in this doctoral thesis has been slightly reduced. However, a life cycle assessment of these polymeric materials should be conducted in future work to estimate greenhouse gas emissions, water consumption, biodegradability, and toxic emissions.

References

Akindoyo, J. O., Beg, M. D. H., Ghazali, S., Islam, M. R., Jeyaratnama, N., Yuvaraj, A. R. Polyurethane types, synthesis and applications – a review, *RSC Advances*, 2016, *6*, 114453-114482.

Alongi, J., Han, Z., Bourbigot, S. Intumescence: tradition versus novelty. A comprehensive review, *Progress in Polymer Science*, 2015, *51*, 28-73.

Ambrogi, V., Carfana, C., Cerruti, P., Marturano, V. Additives in polymers. In Jaso-Gastinel, C. F., Kenny, J. M. (Eds.), Modification of polymer properties. Elsevier, Norwich, 2017, 87-108.

Anastas, P. T., Warner, J. C. Green chemistry: theory and practice. Oxford University Press, New York, 2000, 135p.

Ashida, K. Polyurethane and related foams chemistry and technology. Taylor & Francis, Boca Raton, 2006, 154p.

Bai, C., Zhang, X., Dai, J., Wang, J. Synthesis of UV crosslinkable waterborne siloxane–polyurethane dispersion PDMS-PEDA-PU and the properties of the films. *Journal of Coatings Technology and Research*, 2008, *5*(2), 251-257.

Balani, K., Verma, V., Agarwal, A., Narayan, R. Physical, thermal, and mechanical properties of polymers. In Balani, K., Verma, V., Agarwal, A., Narayan, R. (Eds.), Biosurfaces: a materials science and engineering perspective. John Wiley & Sons, Hoboken, 2015, 329-344.

Bandzierz, K., Reuvekamp, L., Dryzek, J., Dierkes, W., Blume, A., Bielinski, D. Influence of network structure on glass transition temperature of elastomers. *Materials*, 2016, *9*(7), 607-623.

Barabanova, A. I., Lokshin, B. V., Kharitonova, E. P., Afanasyev, E. S., Askadskii, A. A., Philippova, O. E. Curing cycloaliphatic epoxy resin with 4-methylhexahydrophthalic anhydride: Catalyzed vs. uncatalyzed reaction. *Polymers*, 2019, *178*, 121590.

Benyahya, S., Aouf, C., Caillol, S., Boutevin, B., Pascault, J. P., Fulcrand, H. Functionalized green tea tannins as phenolic prepolymers for bio-based epoxy resins. *Industrial Crops and Products*, 2014, *53*, 296-307.

Bhuvaneswari, C. M., Kale, S. S., Gouda, G., Jayapal, P., Tamilmani, K. Elastomers and adhesives for aerospace applications. In Prasad, N. E., Wanhill, R. J. H. (Eds.), Aerospace materials and material technologies. Springer, Singapore, 2017, 563-586.

Brandsch, J., Piringer O. Characteristics of plastic materials. In Piringer, O.G., Baner, A.L. (Eds.), Plastic packaging. WILEY-VCH, Weinheim, 2008, 15-61.

Brocas, A. L., Mantzaridis, C., Tunc, D., Carlotti, S. Polyether synthesis: From activated or metal-free anionic ring-opening polymerization of epoxides to functionalization. *Progress in Polymer Science*, 2013, *38*(6), 845-873.

Broido, A. A simple, sensitive graphical method of treating thermogravimetric analysis data. *Journal of Polymer Science Part A-2: Polymer Physics*, 1969, *7*(10), 1761-1773.

Campo, E. A. Thermal properties of polymeric materials. In Campo, E. A. (Ed.), Selection of polymeric materials. William Andrew, Norwich, 2008, 103-140.

Çelebi, F., Polat, O., Aras, L., Gündüz, G., Akhmedov, I. M. Synthesis and characterization of water-dispersed flame-retardant polyurethane resin using phosphorus-containing chain extender. *Journal of Applied Polymer Science*, 2004, *91*(2), 1314-1321.

Chan, Y. Y., Ma, C., Zhou, F., Hu, Y., Schartel, B. A liquid phosphorous flame retardant combined with expandable graphite or melamine in flexible polyurethane foam. *Polymers for Advanced Technologies*, 2022, *33*(1), 326-339.

Chang, S., Condon, B., Graves, E., Uchimiya, M., Fortier, C., Easson, M., Wakelyn, P. Flame retardant properties of triazine phosphonates derivative with cotton fabric. *Fibers and Polymers*, 2011, *12*(3), 334-339.

Chen, M. J., Chen, C. R., Tan, Y., Huang, J. Q., Wang, X. L., Chen, L., Wang, Y. Z. Inherently flame-retardant flexible polyurethane foam with low content of phosphorus-containing cross-linking agent. *Industrial & Engineering Chemistry Research*, 2014, *53*(3), 1160-1171.

Chen, M. J., Lin, Y. C., Wang, X. N., Zhong, L., Li, Q. L., Liu, Z. G. Influence of cuprous oxide on enhancing the flame retardancy and smoke suppression of epoxy resins containing microencapsulated ammonium polyphosphate. *Industrial & Engineering Chemistry Research*, 2015, *54*(51), 12705-12713.

Claeys, B., Vervaeck, A., Hillewaere, X.K., Possemiers, S., Hansen, L., De Beer, T., Remon, J.P., Vervaet, C. Thermoplastic polyurethanes for the manufacturing of highly dosed oral sustained release matrices via hot melt extrusion and injection molding. *European Journal of Pharmaceutics and Biopharmaceutics*, 2015, *90*, 44-52.

Coats, A. W., Redfern, J. P. Kinetic parameters from thermogravimetric data. *Nature*, 1964, *201*(4914), 68-69.

Covaci, A., Harrad, S., Abdallah, M. A. E., Ali, N., Law, R. J., Herzke, D., Wit, C. A. Novel brominated flame retardants: a review of their analysis, environmental fate and behaviour. *Environment International*, 2011, *37*(2), 532-556.

Cui, Z., Lü, C., Yang, B., Shen, J., Su, X., Yang, H. The research on syntheses and properties of novel epoxy/polymercaptan curing optical resins with high refractive indices. *Polymer*, 2001, *42*(26), 10095-10100.

Das, A., Mahanwar, P. A brief discussion on advances in polyurethane applications. *Advanced Industrial and Engineering Polymer Research*, 2020, *3*(3), 93-101.

Dasari, A., Yu, Z. Z., Cai, G. P., Mai, Y. W. Recent developments in the fire retardancy of polymeric materials, *Progress in Polymer Science*, 2013, *38*(3), 1357-1387.

Davesne, A. L., Jimenez, M., Samyn, F., Bourbigot, S. Thin coatings for fire protection: An overview of the existing strategies, with an emphasis on layer-by-layer surface treatments and promising new solutions. *Progress in Organic Coatings*, 2021, *154*, 106217.

Ding, H., Wang, J., Liu, J., Xu, Y., Chen, R., Wang, C., Chu, F. Preparation and properties of a novel flame retardant polyurethane quasi-prepolymer for toughening phenolic foam. *Journal of Applied Polymer Science*, 2015, *132*(35), 42424.

Du, Y., Zhang, J., Zhou, C. Synthesis and properties of waterborne polyurethane-based PTMG and PDMS as soft segment. *Polymer Bulletin*, 2016, *73*(1), 293-308.

Dube, M. A., Salehpour, S. Applying the principles of green chemistry to polymer production technology. *Macromolecular Reaction Engineering*, 2014, *8*(1), 7-28.

Ebnesajjad, S. Introduction to plastics. In Baur, E., Ruhrberg, K., Woishnis, W. (Eds.), Chemical resistance of commodity thermoplastics. Elsevier, Norwich, 2016, 13-25.

Elbasuney, S. Novel multi-component flame retardant system based on nanoscopic aluminium-trihydroxide (ATH). *Powder Technology*, 2017, *305*, 538-545.

Elizalde, L. E., Santos-Villarreal, G., Santiago-Garcia, J. L., Aguilar-Vega. Step-growth polymerization. In Saldivar-Guerra, E., Vivaldo-Lima E. (Eds.), Handbook of polymer synthesis, characterization, and processing. John Wiley & Sons, Hoboken, 2013, 41-64.

Engels, H. W., Pirkl, H. G., Albers, R., Albach, R. W., Krause, J., Hoffmann, A., Casselmann, H., Dormish, J. Polyurethanes: versatile materials and sustainable problem solvers for today's challenges. *Angewandte Chemie International Edition*, 2013, *52*(36), 9422-9441.

España, J. M., Sánchez-Nacher, L., Boronat, T., Fombuena, V., Balart, R. Properties of biobased epoxy resins from epoxidized soybean oil (ESBO) cured with maleic anhydride (MA). *Journal of the American Oil Chemists' Society*, 2012, *89*(11), 2067-2075.

Esteves, B., Dulyanska, Y., Costa, C., Ferreira, J.V., Domingos, I., Pereira, H., de Lemos, L.T., Cruz-Lopes, L.V. Cork liquefaction for polyurethane foam production. *BioResources*, 2017, *12*(2), 2339-2353.

Ferdosian, F., Zhang, Y., Yuan, Z., Anderson, M., Xu, C. C. Curing kinetics and mechanical properties of bio-based epoxy composites comprising lignin-based epoxy resins. *European Polymer Journal*, 2016, *82*, 153-165.

Ferreira, P., Carvalho, Á., Correia, T. R., Antunes, B. P., Correia, I. J., Alves, P. Functionalization of polydimethylsiloxane membranes to be used in the production of voice prostheses. *Science and Technology of Advanced Materials*, 2013, *14*(5), 055006-055013.

Funt, J. M., Magill, J. H. Thermal decomposition of polystyrene: effect of molecular weight. *Journal of Polymer Science: Polymer Physics Edition*, 1974, *12*(1), 217-220.

Gama, N. V., Ferreira, A., Barros-Timmons, A. Polyurethane foams: past, present and future. *Materials*, 2018, *11*(10), 1841.

Gao, M., Wu, W., Xu, Z. Q. Thermal degradation behaviors and flame retardancy of epoxy resins with novel silicon-containing flame retardant. *Journal of Applied Polymer Science*, 2013, *127*(3), 1842-1847.

Gu, L., Ge, Z., Huang, M., Luo, Y. Halogen-free flame-retardant waterborne polyurethane with a novel cyclic structure of phosphorus-nitrogen synergistic flame retardant. *Journal of Applied Polymer Science*, 2015, *132*(3), 41288-41296.

Gündüz, G., Kısakürek, R. R. Structure–property study of waterborne polyurethane coatings with different hydrophilic contents and polyols. *Journal of Dispersion Science and Technology*, 2004, *25*(2), 217-228.

Hatakeyama, H., Hirogaki, A., Matsumura, H., Hatakeyama, T. Glass transition temperature of polyurethane foams derived from lignin by controlled reaction rate. *Journal of Thermal Analysis and Calorimetry*, 2013, *114*(3), 1075-1082.

Hayashi, M., Katayama, A. Preparation of colorless, highly transparent, epoxy-based vitrimers by the thiol-epoxy click reaction and evaluation of their shape-memory properties. *ACS Applied Polymer Materials*, 2020, *2*(6), 2452-2457.

Hearle, J. W. S. Fibre structure: its formation and relation to performance. In Eichhorn, S. J., Hearle, J. W. S., Jaffe, M., Kikutani, T. (Eds.), Handbook of textile fibre structure. CRC Press, Boca Raton, 2009, 3-21.

Höhne, C. C., Hanich, R., Kroke, E. Intrinsic flame resistance of polyurethane flexible foams: unexpectedly low flammability without any flame retardant. *Fire and Materials*, 2018, *42*(4), 394-402.

Horowitz, H. H., Metzger, G. A new analysis of thermogravimetric traces. *Analytical Chemistry*, 1963, *35*(10), 1464-1468.

Hosier, I. L., Vaughan, A. S., Mitchell, G. R., Siripitayananon, J., Davis, F. J. Polymer characterization. In Davis, F. J. (Ed.), Polymer chemistry. Oxford University Press, New York, 2004, 1-42.

Hull, T. R., Law, R. J., Bergman, A. Environmental drivers for replacement of halogenated flame retardants. In Papaspyrides, C. D., Kiliaris, P. (Eds.), Polymer green flame retardants. Elsevier, Oxford, 2014, 119-179.

Jaudouin, O., Robin, J. J., Lopez-Cuesta, J. M., Perrin, D., Imbert, C. Ionomer-based polyurethanes: a comparative study of properties and applications. *Polymer International*, 2012, *61*(4), 495-510.

Jeong, J. O., Park, J. S., Lim, Y. M. Development of styrene-grafted polyurethane by radiation-based techniques. *Materials*, 2016, *9*(6), 441.

Ji, X., Wang, H., Ma, X., Hou, C., Ma, G. Progress in polydimethylsiloxane-modified waterborne polyurethanes. *RSC Advances*, 2017, *7*(54), 34086-34095.

Jiao, C., Wang, H., Chen, X., Tang, G. Flame retardant and thermal degradation properties of flame retardant thermoplastic polyurethane based on HGM@[EOOEMIm][BF4]. *Journal of Thermal Analysis and Calorimetry*, 2019, *135*(6), 3141-3152.

Joost, T. V., Roesyanto, I., Satyawan, I. Occupational sensitization to epichlorohydrin (ECH) and bisphenol-A during the manufacture of epoxy resin. *Contact Dermatitis*, 1990, *22*(2), 125-126.

Kahlerras, Z., Irinislimane, R., Bruzaud, S., Bensemra, N. B. Elaboration and characterization of polyurethane foams based on renewably sourced polyols. *Journal of Polymers and the Environment*, 2020, *28*(11), 3003-3018.

Karak, N. Overview of epoxies and their thermosets. In Karak, N. (Ed.), Sustainable epoxy thermosets and nanocomposites. American Chemical Society, Washington, 2021, *1385*, 1-36.

Kausar, A., Rafique, I., Anwar, Z., Muhammad, B. Recent developments in different types of flame retardants and effect on fire retardancy of epoxy composite, *Polymer-Plastics Technology and Engineering*, 2016, *55*(14), 1512-1535.

Khatoon, H., Iqbal, S., Irfan, M., Darda, A., Rawat, N. K. A review on the production, properties and applications of non-isocyanate polyurethane: A greener perspective. *Progress in Organic Coatings*, 2021, *154*, 106124.

Kim, Y. K. Natural fibre composites (NFCs) for construction and automotive industries. In Kozłowski, R. M. (Ed.), Handbook of natural fibres. Woodhead Publishing, Philadelphia, 2012, 254-279.

Kirpluks, M., Cabulis, U., Zeltins, V., Stiebra, L., Avots, A. Rigid polyurethane foam thermal insulation protected with mineral intumescent mat. *AUTEX Research Journal*, 2014, *14*(4), 259-269.

Klampfl, C. W., Himmelsbach, M. Advances in the determination of hindered amine light stabilizers - a review. *Analytica Chimica Acta*, 2016, *933*, 10-22.

Lakshmi, M. S., Reddy, B. S. R. Synthesis and characterization of new epoxy and cyanate ester resins. *European Polymer Journal*. 2002, *38*(4), 795-801.

Lakshmi, M. S., Srividhya, M., Reddy, B. S. R. New epoxy resins containing hard-soft segments: synthesis, characterization and modification studies for high performance applications. *Journal of Polymer Research*, 2003, *10*(4), 259-266.

Lee, S. K., Bai, B. C., Jisun, I., Sejin, I., Lee, Y. S. Flame retardant epoxy complex produced by addition of montmorillonite and carbon nanotube. *Journal of Industrial and Engineering Chemistry*, 2010, *16*(6), 891-895.

Lei, L., Xia, Z., Ou, C., Zhang, L., Zhong, L. Effects of crosslinking on adhesion behavior of waterborne polyurethane ink binder. *Progress in Organic Coatings*, 2015, *88*, 155-163.

Lei, L., Zhong, L., Lin, X., Li, Y., Xia, Z. Synthesis and characterization of waterborne polyurethane dispersions with different chain extenders for potential application in waterborne ink. *Chemical Engineering Journal*, 2014, *253*, 518-525.

Lewin, M., Weil, E. D. Mechanisms and modes of action in flame retardancy of polymers. In Horrocks, A. R., Price, D. (Eds.), Fire retardant materials. CRC Press, Boca Raton, 2001, 31-68.

Li, C., Strachan, A. Molecular scale simulations on thermoset polymers: A review. *Journal of Polymer Science Part B: Polymer Physics*, 2015, *53*(2), 103-122.

Li, T. T., Xing, M., Wang, H., Huang, S. Y., Fu, C., Lou, C. W., Lin, J. H. Nitrogen/phosphorus synergistic flame retardant-filled flexible polyurethane foams: microstructure, compressive stress, sound absorption, and combustion resistance. *RSC Advances*, 2019, *9*(37), 21192-21201.

Liu, Q., Wang, D., Li, Z., Li, Z., Peng, X., Liu, C., Zhang, Y., Zheng, P. Recent developments in the flame-retardant system of epoxy resin. *Materials.* 2020, *13*, 2145.

Liu, S. H., Shen, M. Y., Kuan, C. F., Kuan, H. C., Ke, C. Y., Chiang, C. L. Improving thermal stability of polyurethane through the addition of hyperbranched polysiloxane. *Polymers*, 2019, *11*(4), 697-712.

Liu, S., Chevali, V. S., Xu, Z., Hui, D., Wang, H. A review of extending performance of epoxy resins using carbon nanomaterials. *Composites Part B: Engineering*, 2018, *136*, 197-214.

Lochner, U., Chin, H., Yamaguchi, Y. Polyurethane foams- chemical economics handbook. IHS Markit, Englewood, 2022, p121.

Lomakin, S. M., Zaikov, G. E. Ecological aspects of polymer flame retardancy. Taylor & Francis, Zeist, 1999, p162.

Lu, S. Y., Hamerton, I. Recent developments in the chemistry of halogen-free flame retardant polymers. *Progress in Polymer Science*, 2002, *27*(8), 1661-1712.

Lu, S., Feng, Y., Zhang, P., Hong, W., Chen, Y., Fan, H., Yu, D., Chen, X. Preparation of Flame-Retardant Polyurethane and Its Applications in the Leather Industry, *Polymers*, 2021, *13*, 1730.

Majumdar, P., Stafslien, S., Daniels, J., Webster, D. C. High throughput combinatorial characterization of thermosetting siloxane–urethane coatings having spontaneously formed microtopographical surfaces. *Journal of Coatings Technology and Research*, 2007, *4*(2), 131-138.

Mantzaridis, C., Brocas, A.L., Llevot, A., Cendejas, G., Auvergne, R., Caillol, S., Carlotti, S., Cramail, H. Rosin acid oligomers as precursors of DGEBA-free epoxy resins. *Green Chemistry*, 2013, *15*(11), 3091-3098.

Marosi, G., Szolnoki, B., Bocz, K., Toldy, A. Reactive and additive phosphorus-based flame retardants of reduced environmental impact. In Papaspyrides, C. D., Kiliaris, P. (Eds.), Polymer green flame retardants. Elsevier, Oxford, 2014, 181-219.

Martín-Alfonso, J. E., Valencia, C., Sánchez, M. C., Franco, J. M., Gallegos, C. Development of new lubricating grease formulations using recycled LDPE as rheology modifier additive. *European Polymer Journal*, 2007, *43*(1), 139-149.

Marzec, M., Kucinska-Lipka, J., Kalaszczynska, I., Janik, H. Development of polyurethanes for bone repair. *Materials Science and Engineering: C*, 2017, *80*, 736–747.

Maso, F. D., Halary, J. L., Barrere-Tricca, C. Relationship between epoxy resin properties and weepage of glass-reinforced filament-wound pipes. *Oil & Gas Science and Technology*, 2002, *57*(2), 169-175.

Michałowski, S., Hebda, E., Pielichowski, K. Thermal stability and flammability of polyurethane foams chemically reinforced with POSS. *Journal of Thermal Analysis and Calorimetry*, 2017, *130*(1), 155-163.

Miller, A., Brown, C., Warner, G. Guidance on the use of existing ASTM polymer testing standards for ABS parts fabricated using FFF. *Smart and Sustainable Manufacturing Systems*, 2019, *3*(1), 1-17.

Modesti, M., Lorenzetti, A., Simioni, F., Camino, G. Expandable graphite as an intumescent flame retardant in polyisocyanurate–polyurethane foams. *Polymer Degradation and Stability*, 2002, *77*(2), 195-202.

Moghim, M. H., Keshavarz, M., Zebarjad, S. M. Effect of SiO_2 nanoparticles on compression behavior of flexible polyurethane foam. *Polymer Bulletin*, 2019, *76*(1), 227-239.

Mohanty, S. R., Mohanty, S., Nayak, S. K. Synthesis and evaluation of novel acrylic and ester-based polyols for transparent polyurethane coating applications. *Materials Today Communications*, 2021, *27*, 102228.

Montané, X., Dinu, R., Mija, A. Synthesis of resins using epoxies and humins as building blocks: a mechanistic study based on in-situ FT-IR and NMR spectroscopies. *Molecules*, 2019, *24*(22), 4110.

Muuronen, M., Deglmann, P., Tomović, Z. Design principles for rational polyurethane catalyst development. *The Journal of Organic Chemistry*, 2019, *84*(12), 8202-8209.

Nadafan, M., Anvari, J. Z. Evaluation of structural, optical and physical properties of polyurethane composites doped with metal alkoxides. *Materials Science-Poland*, 2020, *38*(3), 416-423.

Nelson, M. I. A dynamical systems model of the limiting oxygen index test: II. Retardancy due to char formation and addition of inert fillers. *Combustion Theory and Modelling*, 2001, *5*(1), 59-83.

Nguyen, T. M. D., Chang, S., Condon, B., Slopek, R. Synthesis of a novel flame retardant containing phosphorus-nitrogen and its comparison for cotton fabric. *Fibers and Polymers*, 2012, *13*(8), 963-970.

Nikje, M. M. A., Garmarudi, A. B., Idris, A. B. Polyurethane waste reduction and recycling: From bench to pilot scales. *Designed Monomers and Polymers*, 2011, *14*(5), 395-421.

Oertel, G., Abele, L. Polyurethane handbook: chemistry, raw materials, processing, application, properties. Hanser, New York, 1994, p688.

Ousaka, N., Endo, T. One-pot non-isocyanate synthesis of sequence-controlled poly (hydroxy urethane) s from a bis (six-membered cyclic carbonate) and two different diamines. *Macromolecules*, 2021, *54*(5), 2059-2067.

Pack, S., Si, M., Koo, J., Sokolov, J. C., Koga, T., Kashiwagi, T., Rafailovich, M. H. Mode-of-action of self-extinguishing polymer blends containing organoclays. *Polymer Degradation and Stability*, 2009, *94*(3), 306-326.

Paraskar, P. M., Prabhudesai, M. S., Deshpande, P. S., Kulkarni, R. D. Utilization of oleic acid in synthesis of epoxidized soybean oil based green polyurethane coating and its comparative study with petrochemical based polyurethane. *Journal of Polymer Research*, 2020, *27*(8), 1-10.

Patnaik, P. Dean's analytical chemistry handbook. McGraw-Hill, New York, 2004, p1280.

Pavličević, J., Špírková, M., Bera, O., Jovičić, M., Szécsényi, K. M., Budinski-Simendić, J. The influence of bentonite and montmorillonite addition on thermal decomposition of novel polyurethane/organoclay nanocomposites. *Macedonian Journal of Chemistry and Chemical Engineering*, 2013, *32*(2), 319-330.

Pergal, M. V., Nestorov, J., Tovilović, G., Ostojić, S., Gođevac, D., Vasiljević-Radović, D., Djonlagić, J. Structure and properties of thermoplastic polyurethanes based on poly (dimethylsiloxane): assessment of biocompatibility. *Journal of Biomedical Materials Research Part A*, 2014, *102*(11), 3951-3964.

Pfaendner, R. Polymer additives. In Saldivar-Guerra, E., Vivaldo-Lima E. (Eds.), Handbook of polymer synthesis, characterization, and processing. John Wiley & Sons, Hoboken, 2013, 225-248.

Prabhu, T. N., Demappa, T., Harish, V., Prashantha, K. Mechanical, thermal and flame-retardant properties of epoxy–nylon fabric–clay hybrid laminates. *High Performance Polymers*, 2013, *25*(5), 559-565.

Pradhan, S., Pandey, P., Mohanty, S., Nayak, S. K. Insight on the chemistry of epoxy and its curing for coating applications: A detailed investigation and future perspectives. *Polymer-Plastics Technology and Engineering*, 2016, *55*(8), 862-877.

Prociak, A., Malewska, E., Kurańska, M., Bąk, S., Budny, P. Flexible polyurethane foams synthesized with palm oil-based bio-polyols obtained with the use of different oxirane ring opener. *Industrial Crops and Products*, 2018, *115*, 69-77.

Raasch, J., Ivey, M., Aldrich, D., Nobes, D. S., Ayranci, C. Characterization of polyurethane shape memory polymer processed by material extrusion additive manufacturing. *Additive Manufacturing*, 2015, *8*, 132–141.

Rampf, M., Speck, O., Speck, T., Luchsinger, R. H. Structural and mechanical properties of flexible polyurethane foams cured under pressure. *Journal of cellular plastics*, 2012, *48*(1), 53-69.

Rao, W. H., Xu, H. X., Xu, Y. J., Qi, M., Liao, W., Xu, S., Wang, Y. Z. Persistently flame-retardant flexible polyurethane foams by a novel phosphorus-containing polyol. *Chemical Engineering Journal*, 2018a, *343*, 198-206.

Rao, W. H., Zhu, Z. M., Wang, S. X., Wang, T., Tan, Y., Liao, W., Zhao, H. B., Wang, Y. Z. A reactive phosphorus-containing polyol incorporated into flexible polyurethane foam: Self-extinguishing behavior and mechanism. *Polymer Degradation and Stability*, 2018b, *153*, 192-200.

Ren, H., Sun, J., Wu, B., Zhou, Q. Synthesis and properties of a phosphorus-containing flame retardant epoxy resin based on bis-phenoxy (3-hydroxy) phenyl phosphine oxide. *Polymer Degradation and Stability*, 2007, *92*(6), 956-961.

Saldivar, G. E., Vivaldo L. E. Introduction to polymers and polymer types. In Saldivar, G. E., Vivaldo, L. E. (Eds.), Handbook of polymer synthesis, characterization, and processing. John Wiley & Sons, Hoboken, 2013, 3-14.

Salmeia, K. A., Fage, J., Liang, S., Gaan, S. An overview of mode of action and analytical methods for evaluation of gas phase activities of flame retardants, *Polymers*, 2015, *7*, 504-526.

Sharmin, E., Zafar, F. Polyurethane: an introduction. In Zafar, F., Sharmin, E. (Eds.), Polyurethane. IntechOpen, Rijeka, 2012, 3-16.

Shen, D., Xu, Y. J., Long, J. W., Shi, X. H., Chen, L., Wang, Y. Z. Epoxy resin flame-retarded via a novel melamine-organophosphinic acid salt: Thermal stability, flame retardance and pyrolysis behavior. *Journal of Analytical and Applied Pyrolysis*, 2017, *128*, 54-63.

Silva, A. L., Bordado, J. C. Recent developments in polyurethane catalysis: catalytic mechanisms review. *Catalysis Reviews*, 2004, *46*(1), 31-51.

Simpson, J. T., Hunter, S. R., Aytug, T. Superhydrophobic materials and coatings: a review. *Reports on Progress in Physics*, 2015, *78*(8), 086501.

Singh, H., Jain, A. K. Ignition, combustion, toxicity, and fire retardancy of polyurethane foams: a comprehensive review. *Journal of Applied Polymer Science*, 2009, *111*(2), 1115-1143.

Spontón, M., Ronda, J. C., Galià, M., Cádiz, V. Flame retardant epoxy resins based on diglycidyl ether of (2, 5-dihydroxyphenyl) diphenyl phosphine oxide. *Journal of Polymer Science Part A: Polymer Chemistry*, 2007, *45*(11), 2142-2151.

Srividhya, M., Lakshmi, M. S., Reddy, B. S. R. Chemistry of siloxane amide as a new curing agent for epoxy resins: Mate rial characterization and properties. *Macromolecular Chemistry and Physics*, 2005, *206*(24), 2501-2511.

Suhailuddin, S. H., Aprajith, K., Sanjay, B., Shabeeruddin, S. H., Begum, S. S. Development and characterization of flame retardant property in flexible polyurethane foam. *Materials Today: Proceedings*, 2022, *59*, 819-826.

Sun, Z., Hou, Y., Hu, Y., Hu, W. Effect of additive phosphorus-nitrogen containing flame retardant on char formation and flame retardancy of epoxy resin. *Materials Chemistry and Physics*, 2018, *214*, 154-164.

Sundararajan, S., Samui, A. B., Kulkarni, P. S. Versatility of polyethylene glycol (PEG) in designing solid-solid phase change materials for thermal management and their application to innovative technologies. *Journal of materials chemistry A*, 2017a, *5*(35),18379-18396.

Sundararajan, S., Samui, A. B., Kulkarni, P. S. Synthesis and characterization of poly (ethylene glycol) (PEG) based hyperbranched polyurethanes as thermal energy storage materials. *Thermochimica Acta*, 2017b, *650*, 114-122.

Sut, A., Metzsch-Zilligen, E., Großhauser, M., Pfaendner, R., Schartel, B. Synergy between melamine cyanurate, melamine polyphosphate and aluminum diethylphosphinate in flame retarded thermoplastic polyurethane. *Polymer Testing*, 2019, *74*, 196-204.

Szycher, M. Structure-property relations in polyurethanes. In Szycher, M. (Ed.), Szycher's handbook of polyurethanes. CRC Press, London, 2012, 37–88.

Tai, N. L., Adhikari, R., Shanks, R., Adhikari, B. Starch-polyurethane films synthesized using polyethylene glycol-isocyanate (PEG-iso): Effects of molecular weight, crystallinity, and composition of PEG-iso on physiochemical characteristics and hydrophobicity of the films. *Food Packaging and Shelf Life*, 2017, *14*, 116-127.

Tang, S., Wachtendorf, V., Klack, P., Qian, L., Dong, Y., Schartel, B. Enhanced flame-retardant effect of a montmorillonite/phosphaphenanthrene compound in an epoxy thermoset. *RSC Advances*, 2017, *7*(2), 720-728.

Thorstensen, T. C. Practical leather technology. Krieger Publishing Company, Huntington, 1993, p340.

Van Krevelen, D. W. Some basic aspects of flame resistance of polymeric materials. *Polymer*, 1975, *16*(8), 615-620.

Vinay, J., Rahul, P., Siddhesh, M., Mhaske, S. T. P- and Si-modified shellac for flame-retardant epoxy-based coatings. *Iranian Polymer Journal*, 2021, *30*, 907-916.

Wang, D., Wen, P., Wang, J., Song, L., Hu, Y. The effect of defect-rich molybdenum disulfide nanosheets with phosphorus, nitrogen and silicon elements on mechanical, thermal, and fire behaviours of unsaturated polyester composites. *Chemical Engineering Journal*, 2017a, *313*, 238-249.

Wang, Y., Wang, F., Dong, Q., Xie, M., Liu, P., Ding, Y., Zhang, S., Yang, M., Zheng, G. Core-shell expandable graphite@ aluminum hydroxide as a flame-retardant for rigid polyurethane foams. *Polymer degradation and stab*ility, 2017b, *146*, 267-276.

Wei S., Lee, C. S., Chuah, C. H., Cheng, S. F. Preparation and modification of water-blown porous biodegradable polyurethane foams with palm oil-based polyester polyol. *Industrial Crops and Products*, 2017, *97*, 65-78.

Witkowski, A., Stec, A. A., Hull, T. R. Thermal decomposition of polymeric materials. In Hurley, M. J., Gottuk, D. T., Hall, J. R. (Eds.), SFPE handbook of fire protection engineering. Springer, Berlin, 2016, 167-254.

Wolfgang, J. D., White, B. T., Long, T. E. Non-isocyanate polyurethanes from 1, 1′-carbonyldiimidazole: a polycondensation approach. *Macromolecular Rapid Communications*, 2021, *42*(13), 2100163.

Wu, Y., Guo, P., Zhao, Y., Liu, X., Du, Z. Hydrophobic, transparent waterborne polyurethane-polydimethylsiloxane composites prepared from aqueous sol-gel process and applied in corrosion, *Progress in Organic Coatings*, 2019, *127*, 231–238.

Xu, W., Li, J., Liu, F., Jiang, Y., Li, Z., Li, L. Study on the thermal decomposition kinetics and flammability performance of a flame-retardant leather. *Journal of Thermal Analysis and Calorimetry*, 2017, *128*(2), 1107-1116.

Yan, Z., Ma, Z., Deng, J., Luo, G. Mechanism and kinetics of epoxide ring-opening with carboxylic acids catalyzed by the corresponding carboxylates. *Chemical Engineering Science*, 2021, *242*, 116746.

Yang, H., Yu, B., Song, P., Maluk, C., Wang, H. Surface-coating engineering for flame retardant flexible polyurethane foams: a critical review. *Composites Part B: Engineering*, 2019, *176*, 107185.

Yang, L., Liu, Y., Wu, Y., Deng, L., Liu, W., Ma, C., Li, L. Thermal degradation kinetics of leather fibers treated with fire-retardant melamine resin. *Journal of Thermal Analysis and Calorimetry*, 2016, *123*(1), 413-420.

Yasmin, A., Luo, J. J., Abot, J. L., Daniel, I. M. Mechanical and thermal behavior of clay/epoxy nanocomposites. *Composites Science and Technology*, 2006, *66*(14), 2415-22.

Yin, B., Hakkarainen, M. Oligomeric isosorbide esters as alternative renewable resource plasticizers for PVC. *Journal of Applied Polymer Science*, 2011, *119*(4), 2400-2407.

Yuan, Y., Yang, H., Yu, B., Shi, Y., Wang, W., Song, L., Hu, Y., Zhang, Y. Phosphorus and nitrogen-containing polyols: synergistic effect on the thermal property and flame retardancy of rigid polyurethane foam composites. *Industrial & Engineering Chemistry Research*, 2016, *55*(41), 10813-10822.

Zabihi, O., Ahmadi, M., Nikafshar, S., Preyeswary, K. C., Naebe, M. A technical review on epoxy-clay nanocomposites: structure, properties, and their applications in fiber reinforced composites. *Composites Part B-Engineering*. 2018, *135*, 1-24.

Zhang, J., Zhang, X. Y., Dai, J. B., Li, W. H. Synthesis and characterization of yellow water-borne polyurethane using a diol colorant as extender. *Chinese Chemical Letters*, 2010, *21*(2), 143-145.

Zhang, L., Brostowitz, N. R., Cavicchi, K. A., Weiss, R. A. Perspective: Ionomer research and applications. *Macromolecular Reaction Engineering*, 2014, *8*(2), 81-99.

Zhang, Q., Wang, J., Yang, S., Cheng, J., Ding, G., Hu, Y., Huo, S. Synthesis of a P/N/S-based flame retardant and its flame retardant effect on epoxy resin. *Fire Safety Journal*, 2020, *113*, 102994.

Zhang, Z. P., Song, X. F., Cui, L. Y., Qi, Y. H. Synthesis of polydimethylsiloxane-modified polyurethane and the structure and properties of its antifouling coatings. *Coatings*, 2018, *8*(5), 157-174.

Zhou, F., Zhang, T., Zou, B., Hu, W., Wang, B., Zhan, J., Ma, C., Hu, Y. Synthesis of a novel liquid phosphorus-containing flame retardant for flexible polyurethane foam: combustion behaviors and thermal properties. *Polymer Degradation and Stability*, 2020, *171*, 109029.

Zohuriaan, M. J., Shokrolahi, F. Thermal studies on natural and modified gums. *Polymer Testing*, 2004, *23*(5), 575-579.

Zuber, M., Tabasum, S., Hussain, R., Khan, M. B., Bukhari, I. H. Blends of polyurethane-polymethyl methacrylate/TiO2-based composites. *Korean Journal of Chemical Engineering*, 2013, *30*(8), 1652-1658.

Appendix

The following papers are included in this thesis

1. **Kanemoto, S. O**., Gouthaman, S., Venkatesh, M., Cheumani, A. M., Ndikontar, M. K., Lakshmi, M. S. Thermal stability of phosphorus-based epoxy/clay composites and their effect on the flame retardation properties of leather. *Iranian Polymer Journal*, 2022, *31*(12), 1583-1594.
2. **Kanemoto, S. O**., Gouthaman, S., Venkatesh, M., Cheumani, A. M., Ndikontar, M. K., Lakshmi, M. S. Thermal performance of polyurethane nanocomposite from phosphorus and nitrogen-containing monomer, polyethylene glycol and polydimethylsiloxane for thermal energy storage applications. *Journal of Thermal Analysis and Calorimetry*, 2021, *146*(6), 2435-2444.
3. Venkatesh, M., Gouthaman, S., **Kanemoto, S. O**., Lakshmi, M. S., Hamerton, I. Development of epoxy-cyanate ester-clay nanocomposites offering enhanced thermally stability. *Journal of Applied Polymer Science*, 2019, *136*(28), 47754.
4. **Kanemoto, S. O**., Cheumani, A. M., Ndikontar, M. K., Lakshmi, M. S. Reactive flame-retardation of flexible polyurethane foams based on phosphorus-hydroxyl precursors dispersed in polyethylene glycol. *Iranian Polymer Journal*, (*Under review*)